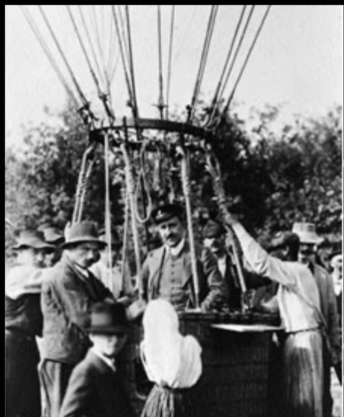

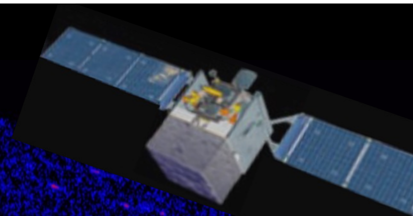

100 лет

ПРОГРЕСС В АСТРОФИЗИКЕ ВЫСОКИХ ЭНЕРГИЙ

Игорь Москаленко – Станфорд

Амбициозная задача – за час рассказать о наиболее интересных результатах в астрофизике космических лучей и гамма-астрономии

Благодаря беспрецендентным усилиям и достижениям экспериментаторов – задача трудновыполнимая

Многое останется за кадром…

(См. доклад Андрея Быкова по источникам γ-излучения)

Атлант Фарнезе. II век н. э.

The discovery of cosmic rays

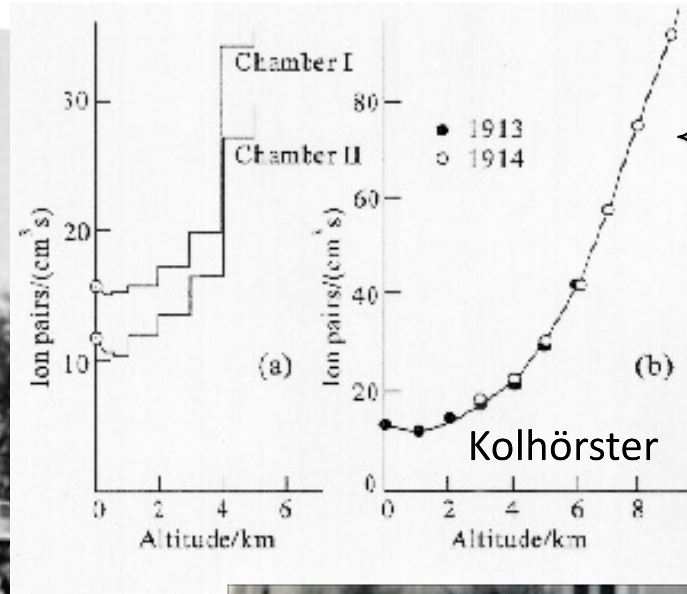

- ✧ Victor Hess, an Austrian scientist, took a radiation counter (a simple electroscope) on a balloon flight
- ✧ He rose to 5200 m (without oxygen) and found that the amount of radiation increases as the balloon climbed. Hess correctly concluded that the ionization was caused by highly penetrating radiation coming from outside the atmosphere

- ✧ Domenico Pacini, an Italian scientist, measured ionization on mountains, on the shoreline and at sea between 1906 and 1910; came to the same conclusion

Spectrum of Cosmic Rays – 20th century

~32 orders of mag

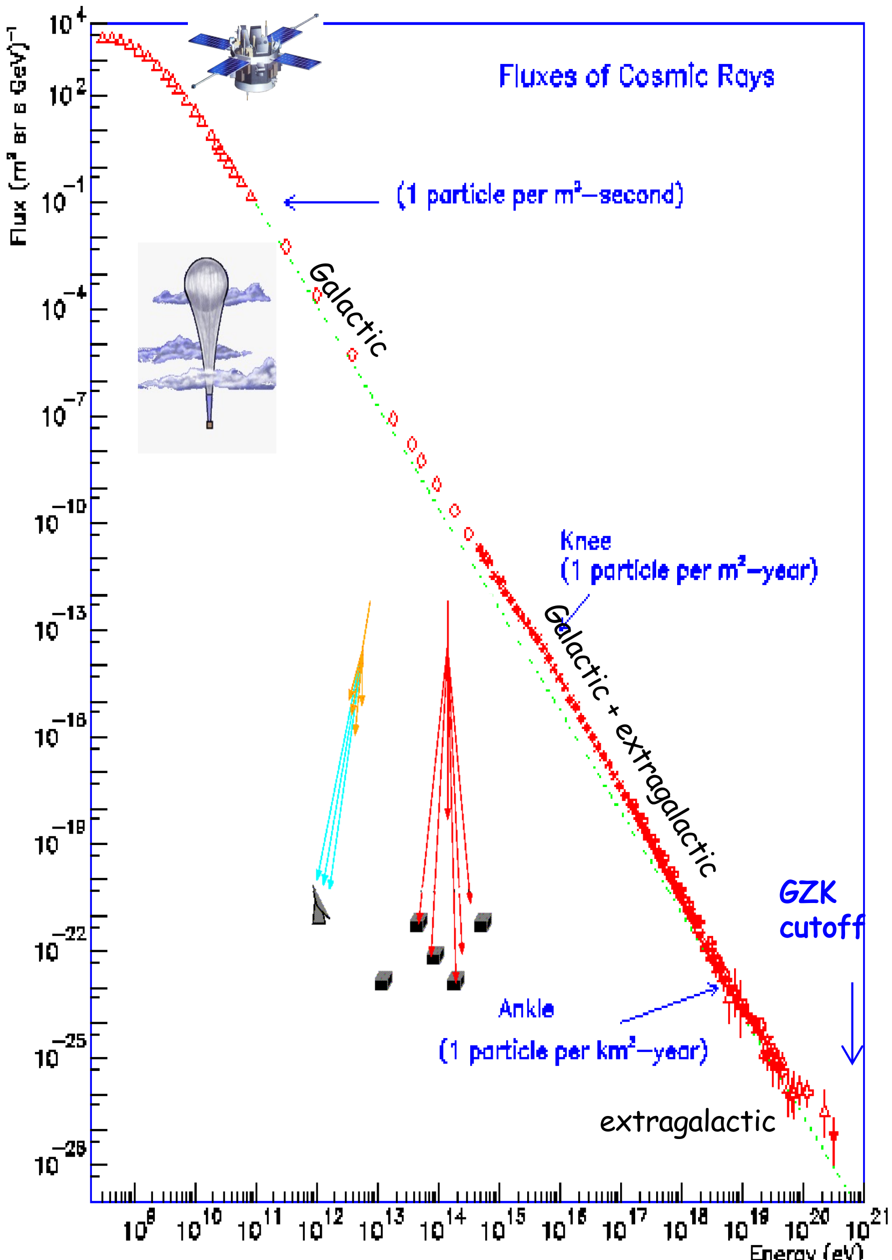

>12 orders of mag

- ✧ All particle CR spectrum:
  - ✦ The knee (Kulikov & Christiansen 1958)
  - ✦ The ankle (Linsley 1963, Fly's eye 1990s)
  - ✦ GZK cutoff (predicted Greisen-Zatsepin-Kuzmin 1966)

GZK cutoff:

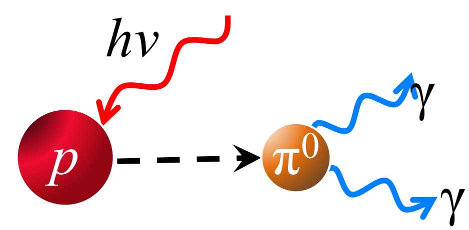

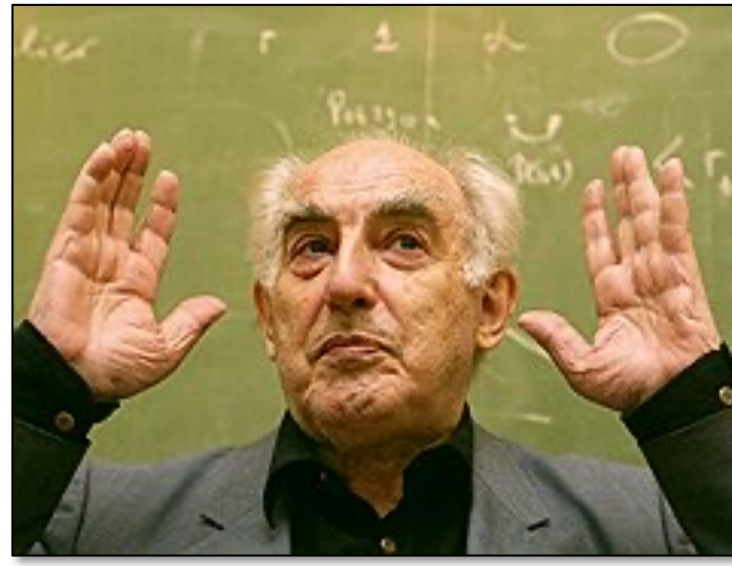

Основные книги в астрофизике КЛ на многие годы

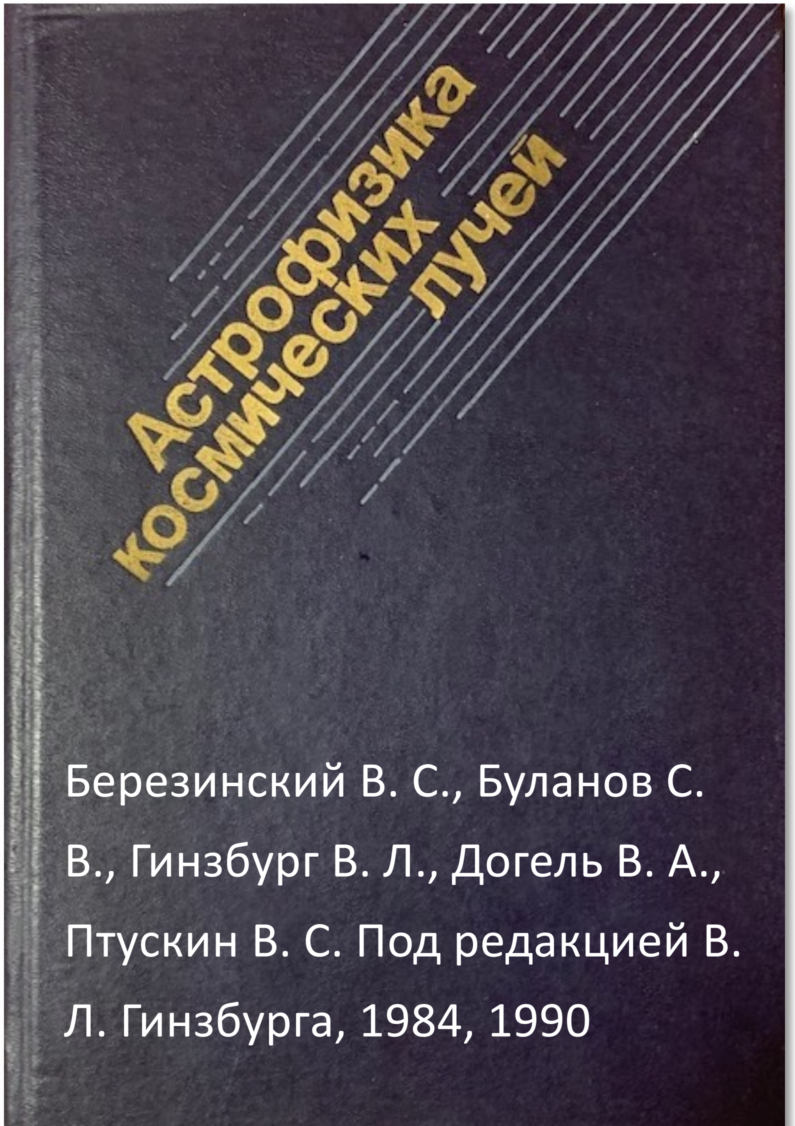
Астрофизика космических лучей
Березинский В. С., Буланов С. В., Гинзбург В. Л., Догель В. А., Птускин В. С. Под редакцией В. Л. Гинзбурга, 1984, 1990

НИИЯФ МГУ является лидирующим институтом в РФ в области КЛ; 3 из 5 директоров НИИЯФ внесли выдающийся вклад в астрофизику КЛ

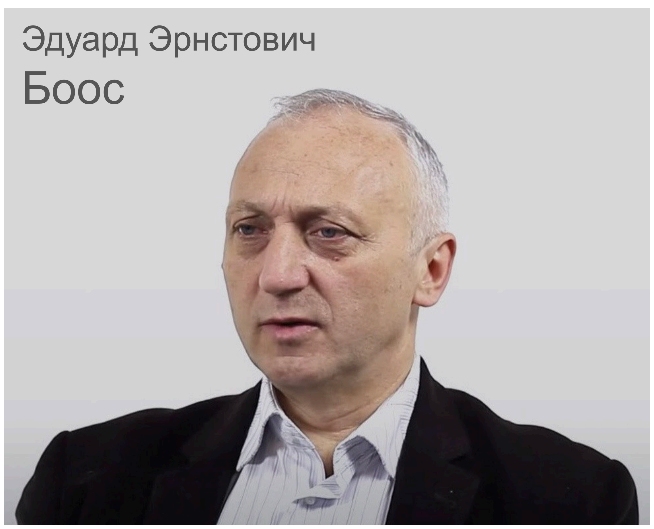

Spectrum of Cosmic Rays – about now

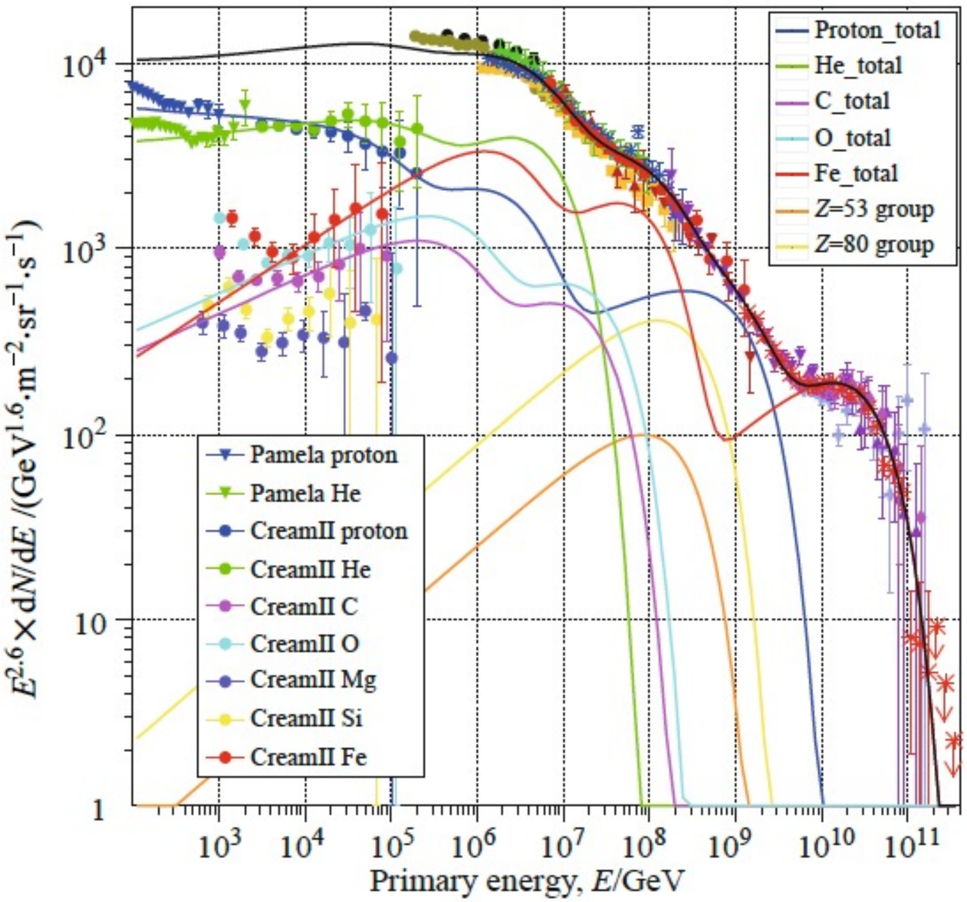

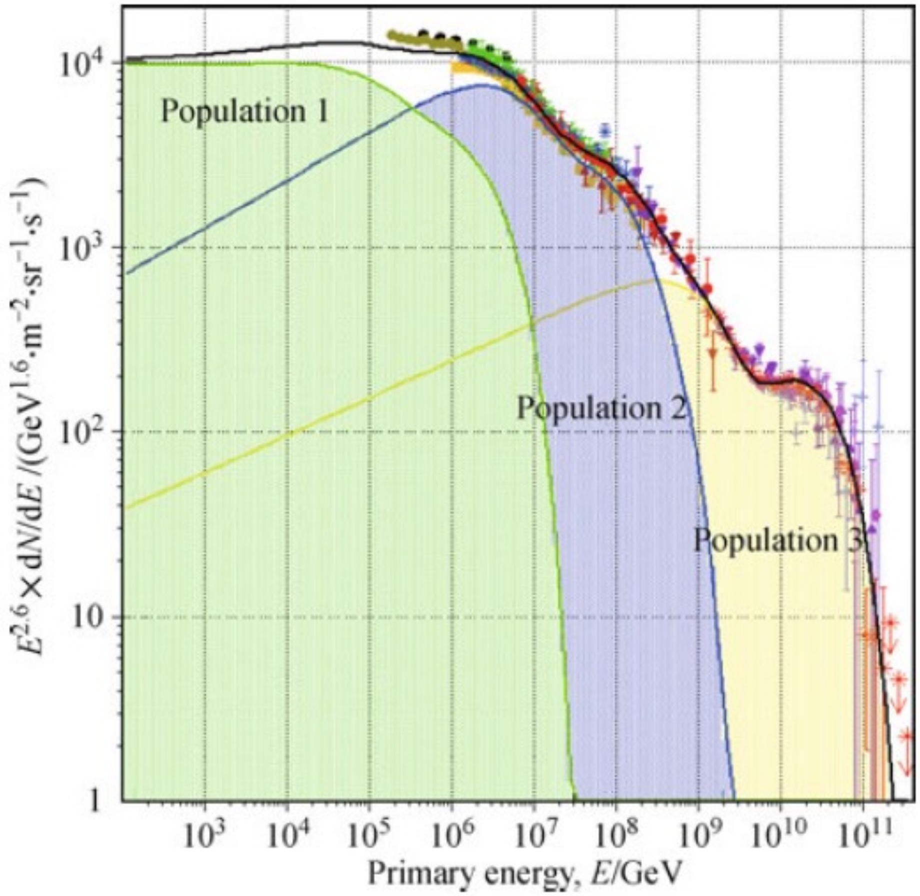

Gaisser, Stanev, Tilav 2013

- Are these features transient?
- Which type of sources are producing them?
- Are they typical for the whole Galaxy?
- What are the consequences if they do or they do not?

Notice also a shift in our understanding of the subject of CRs!

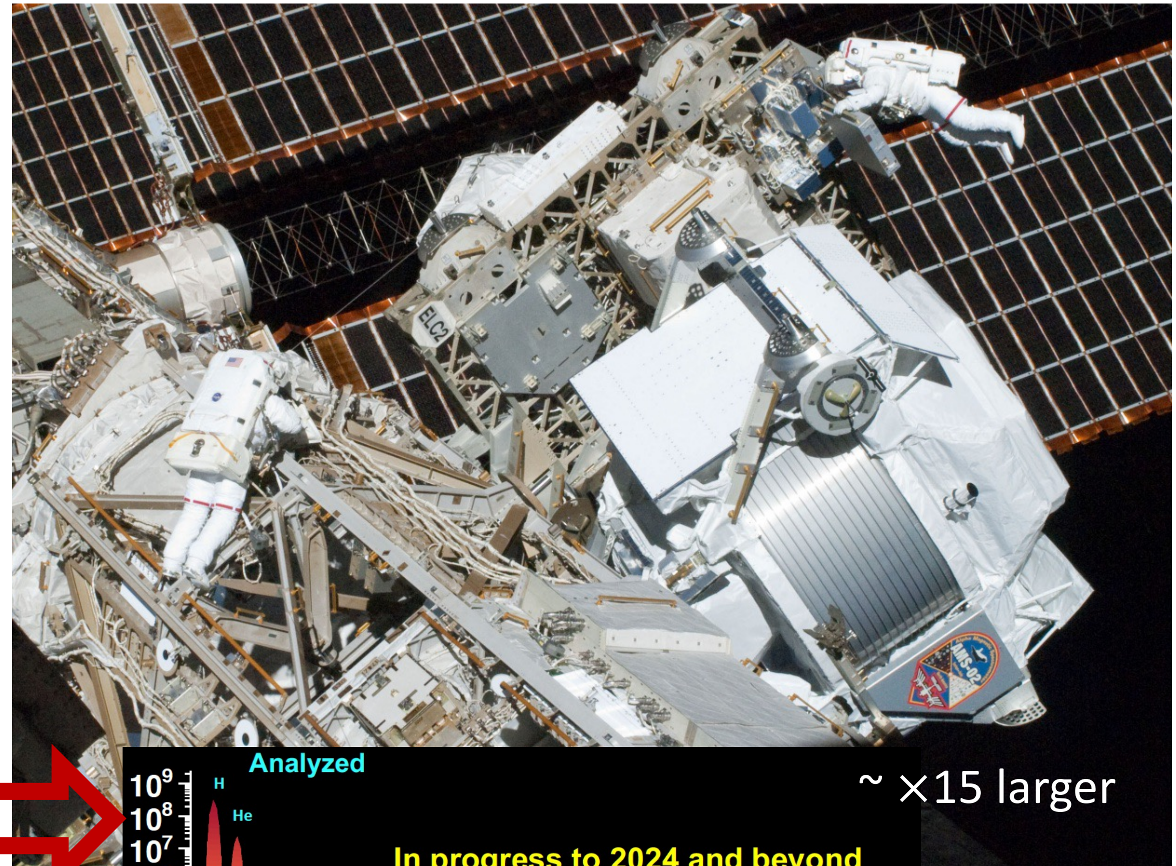

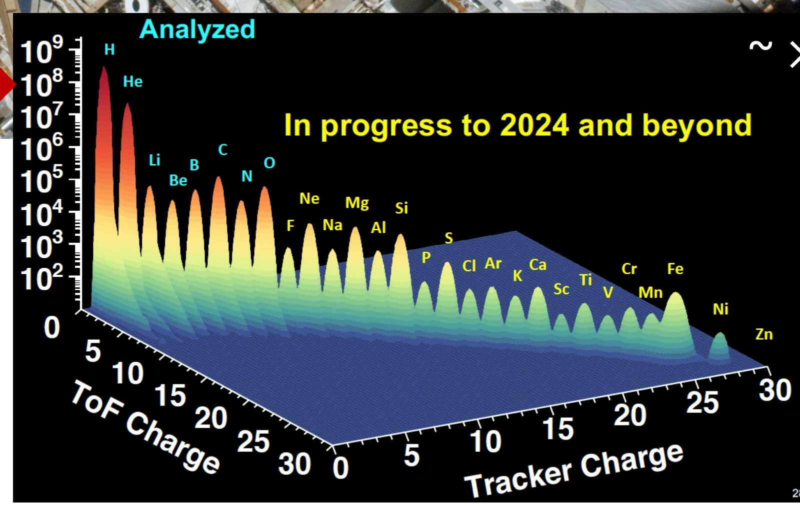

"…this ionization might be attributed to the penetration of the earth's atmosphere from outer space by hitherto unknown radiation of exceptionally high penetrating capacity…" – V. Hess

Fluxes of CR species

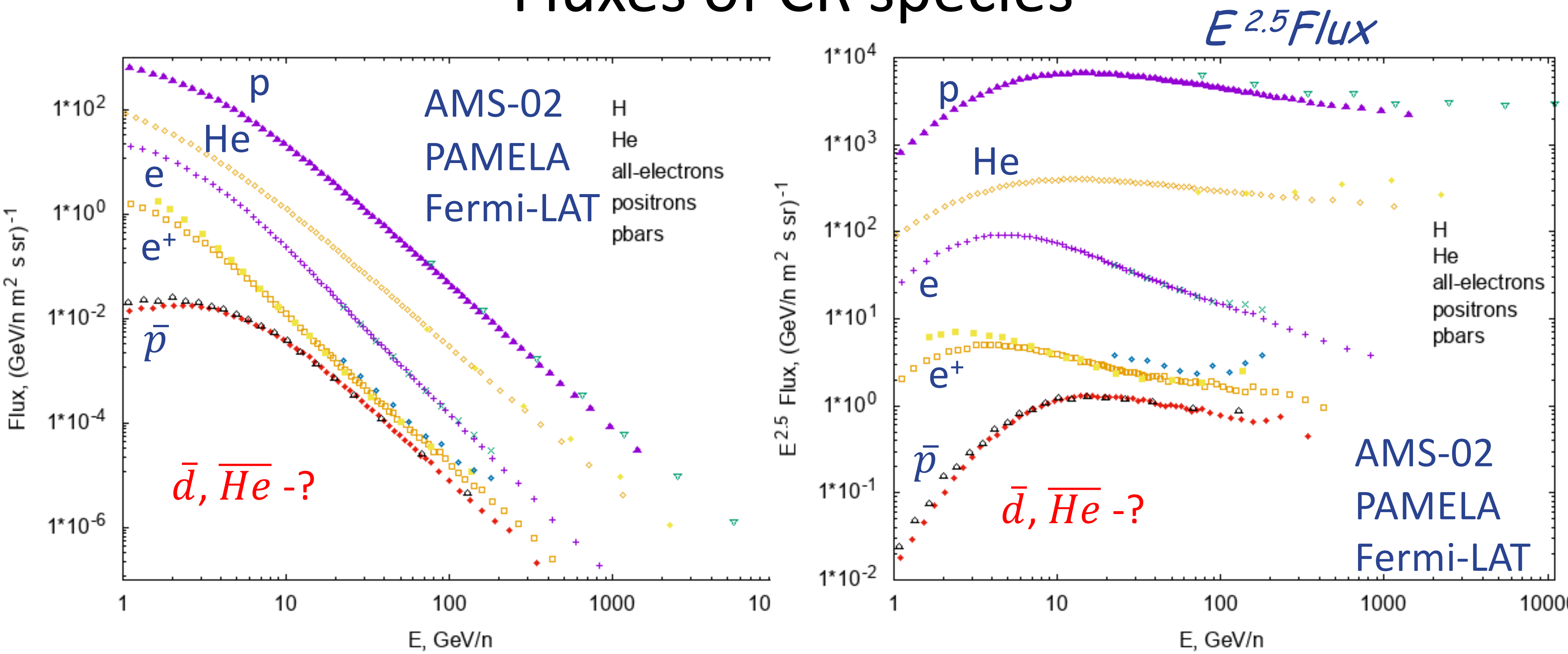

- ✧ Positrons and antiprotons are 10^4-10^6 *less abundant* then protons – discriminating them especially at very high energies is a challenge
- ✧ Expect first reports about anti-deuterons and anti-He in CRs (AMS-02 talks in E1.3 section at COSPAR-2022)

PAMELA discovery: Rising positron fraction

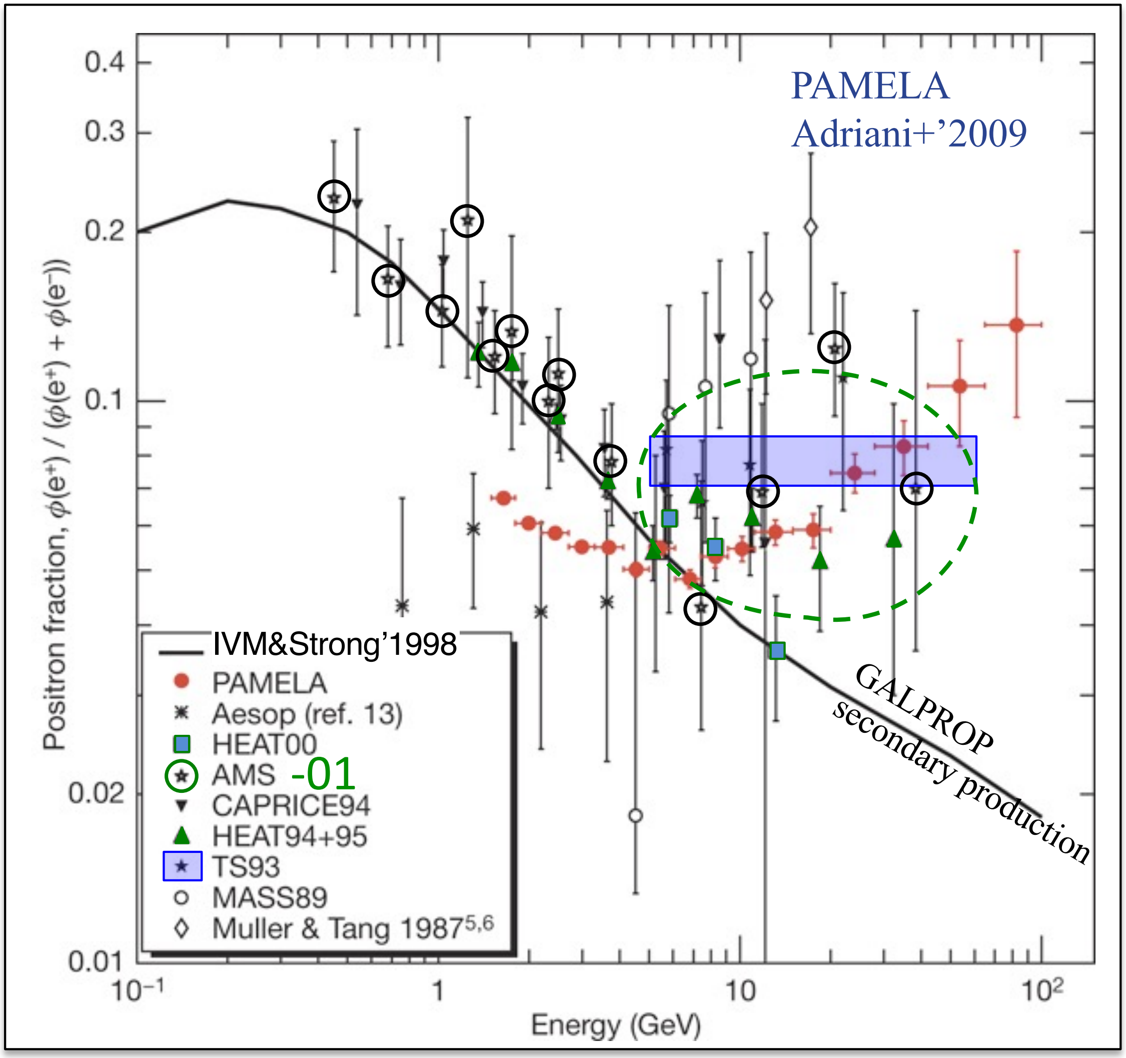

✧TS93 (Golden+'96): flat positron fraction 0.078±0.016 in the range 5-60 GeV

✧HEAT-94,95,00 (Beatty+'04): "a small positron flux of nonstandard origin"

✧AMS-01 (Aguilar+'07, 1998 flight) confirmed HEAT results

✧PAMELA team reported a clear and very significant rise in the positron fraction compared to the "standard" model predictions

✧"Standard" model:

- Secondary production in the ISM
- Steady state
- Smooth CR source distribution

Take home:

✧ New physics may appear early (at the current exp. limits)

✧ Need a model to compare

The positron flux is the sum of low-energy part from cosmic ray collisions plus a high-energy part from a new source or dark matter both with a cutoff energy E_s.

$$\Phi_{e^+}(E) = \frac{E^2}{\hat{E}^2}\Big[\underbrace{C_d(\hat{E}/E_1)^{\gamma_d}}_{\text{Collisions}} + \underbrace{C_s(\hat{E}/E_2)^{\gamma_s}\exp(-\hat{E}/E_s)}_{\text{New Source or Dark Matter}}\Big]$$

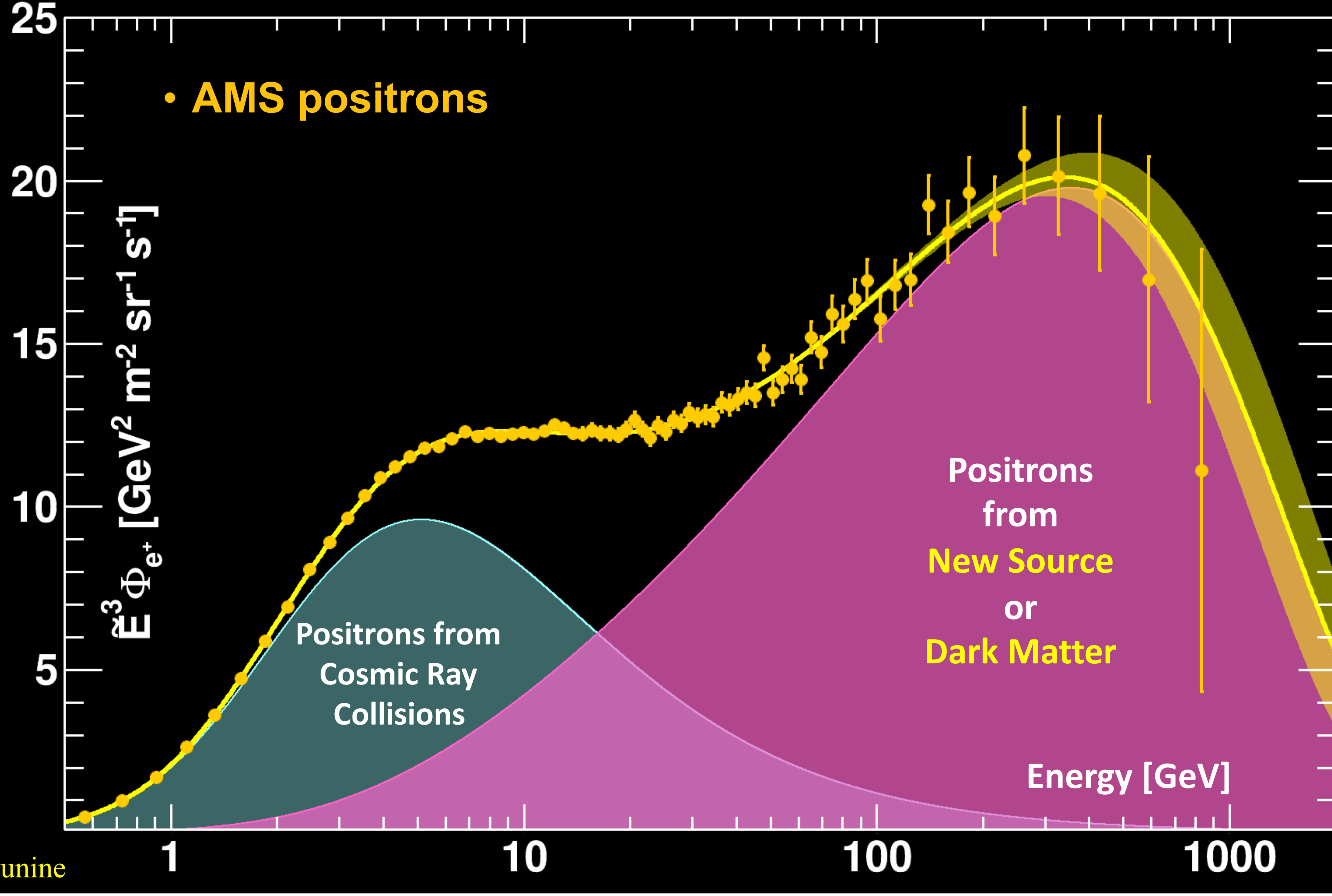

A.Kounine

Secondary production in a SNR shock

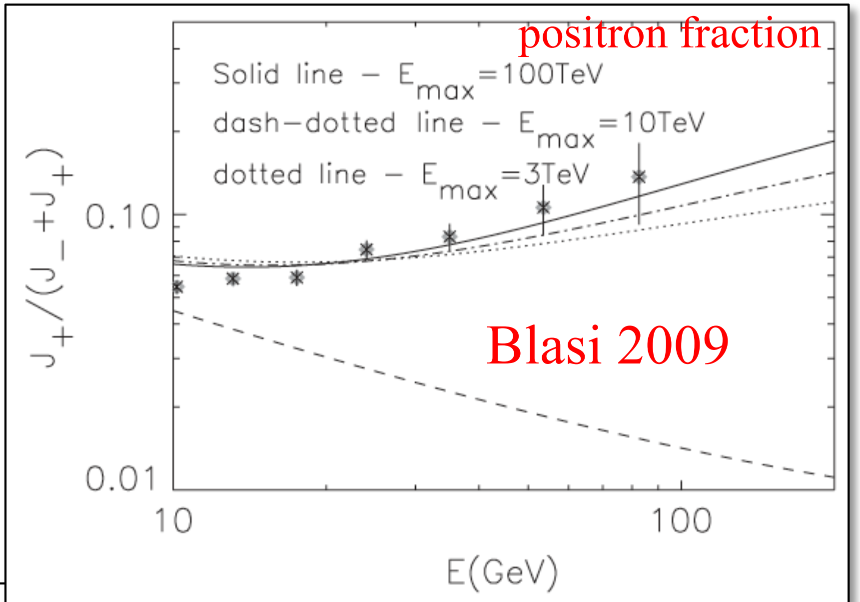

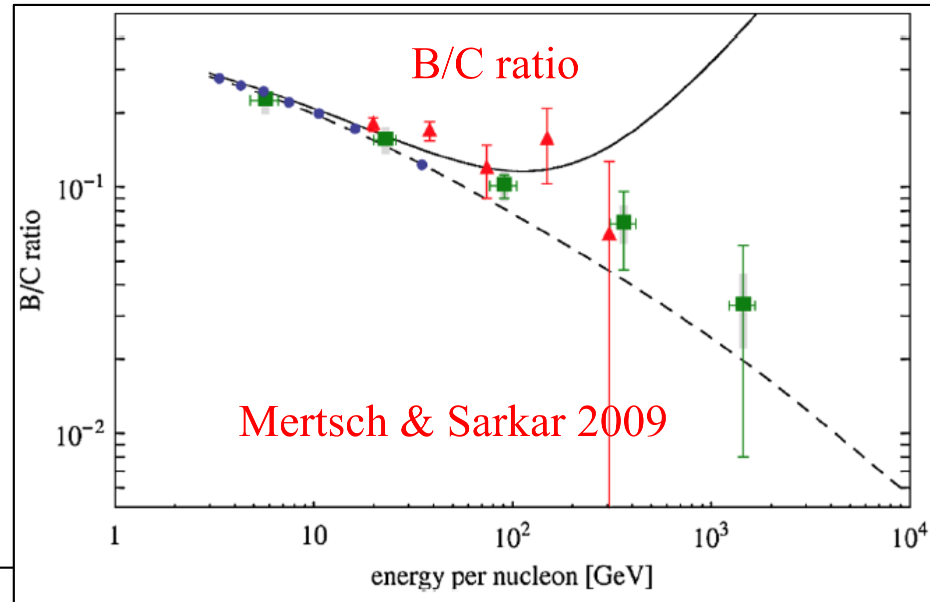

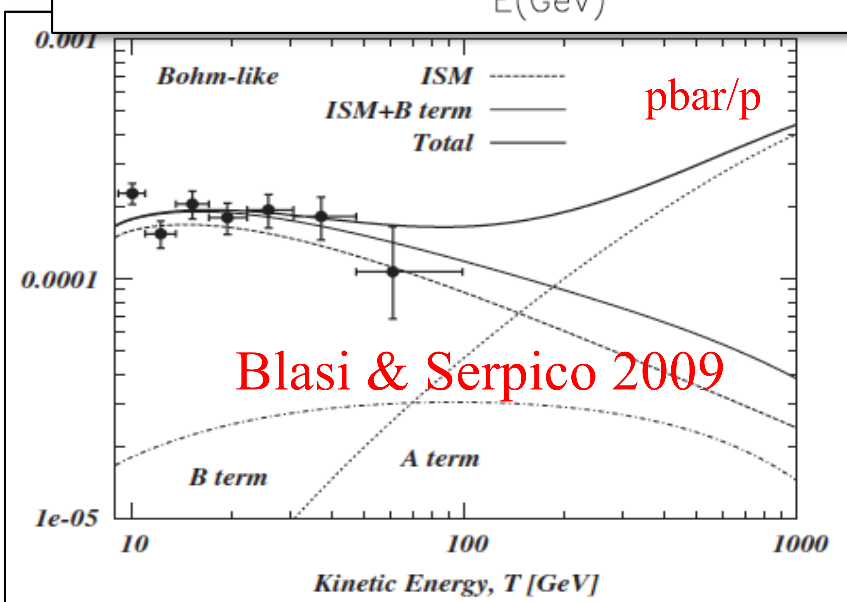

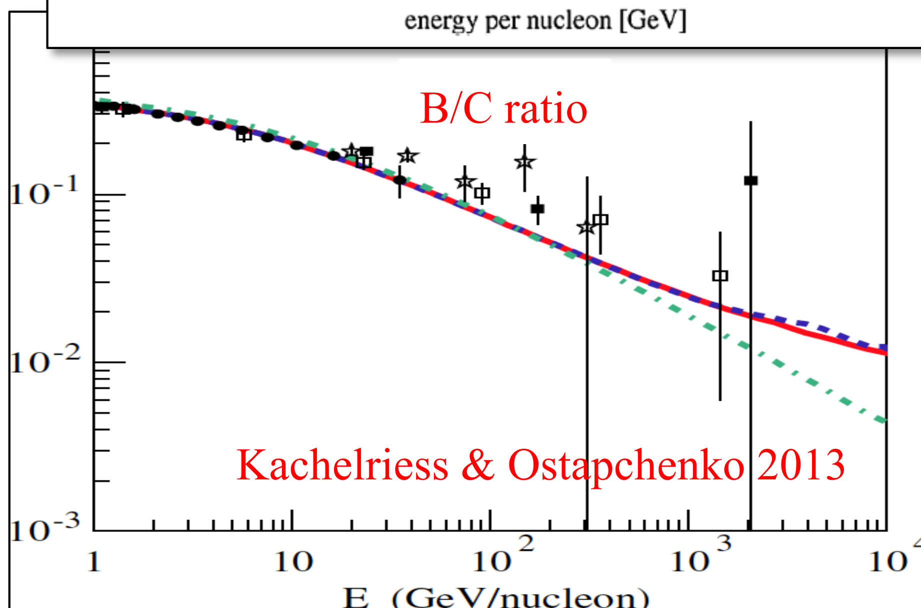

- ✧ A rise in all secondary products
- ✧ Time- and spatially-dependent (?)

B/C ratio in reality

- ✧ The B/C ratio as measured by AMS-02 (2018) agrees pretty well with the model calculations
- ✧ Does not exhibit any significant excess

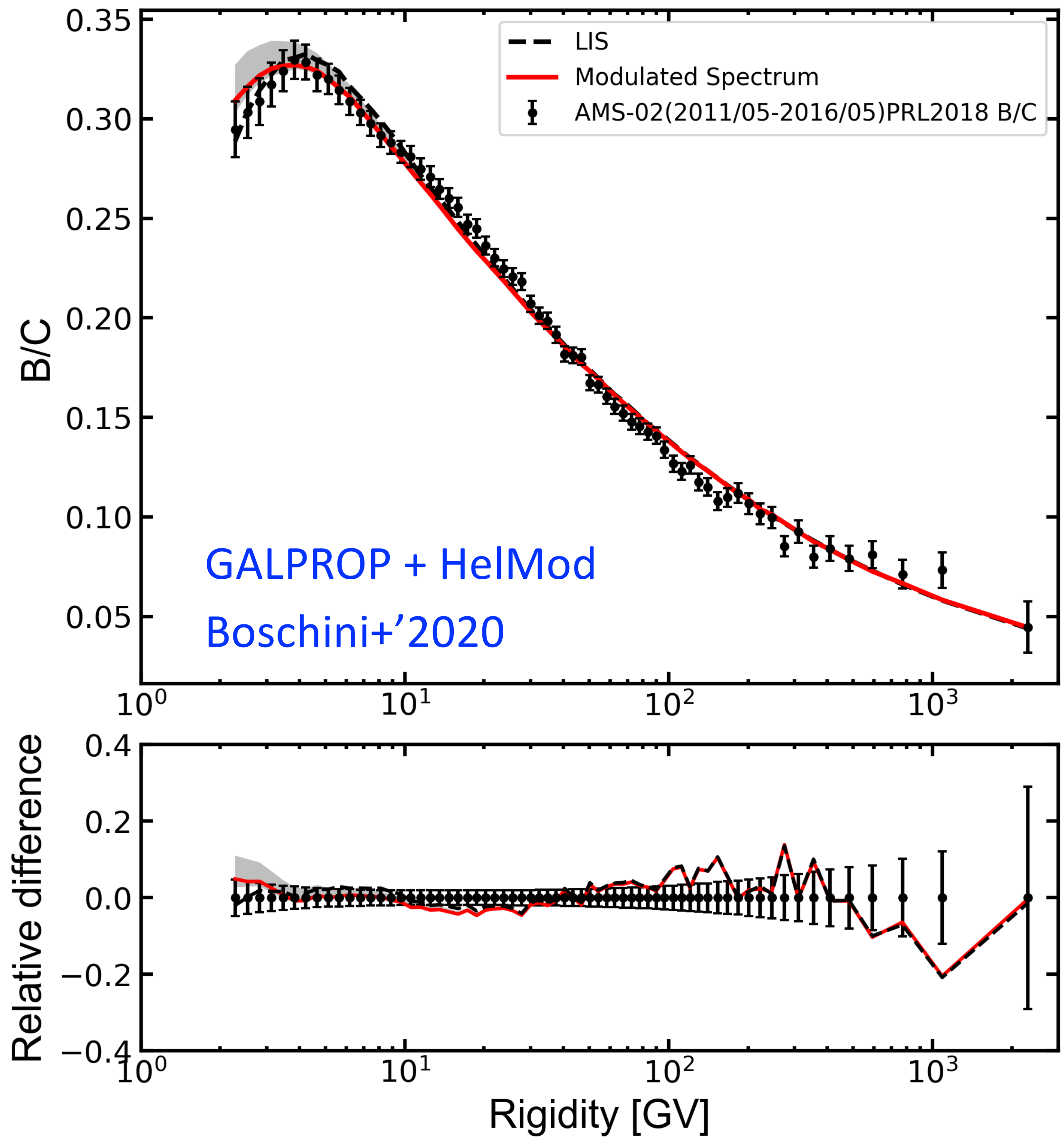

Positron excess: Old friends – pulsars

- ✧ Jon Arons 1981 "Particle acceleration by pulsars"
- ✧ Harding & Ramaty 1987 "The pulsar contribution to Galactic cosmic ray positrons"
- ✧ Ahmed Boulares 1989 "The nature of the cosmic-ray electron spectrum, and supernova remnant contributions"

"Therefore, the only role observed pulsars might play as direct cosmic ray sources is in providing positrons and electrons…"

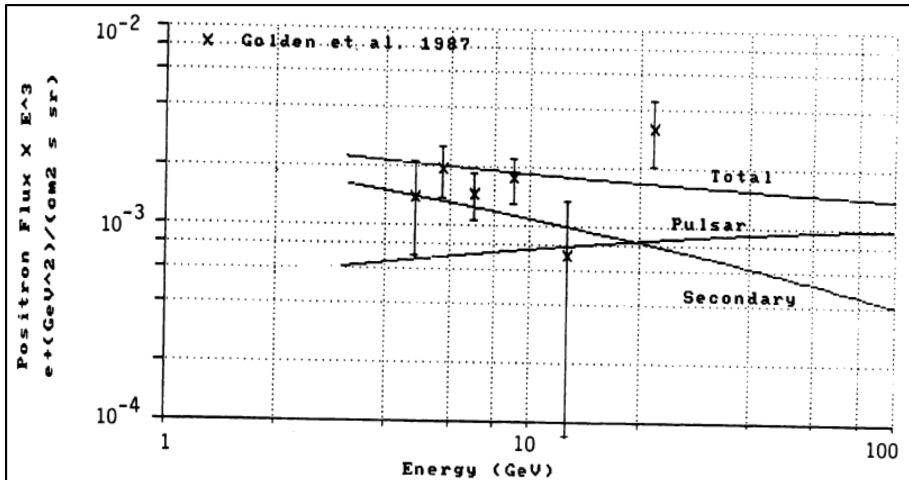

3 components:

- ✧ Secondary $e^{+/-}$
- ✧ Primary e^{-} from SNR
- ✧ Primary $e^{+/-}$ from pulsars

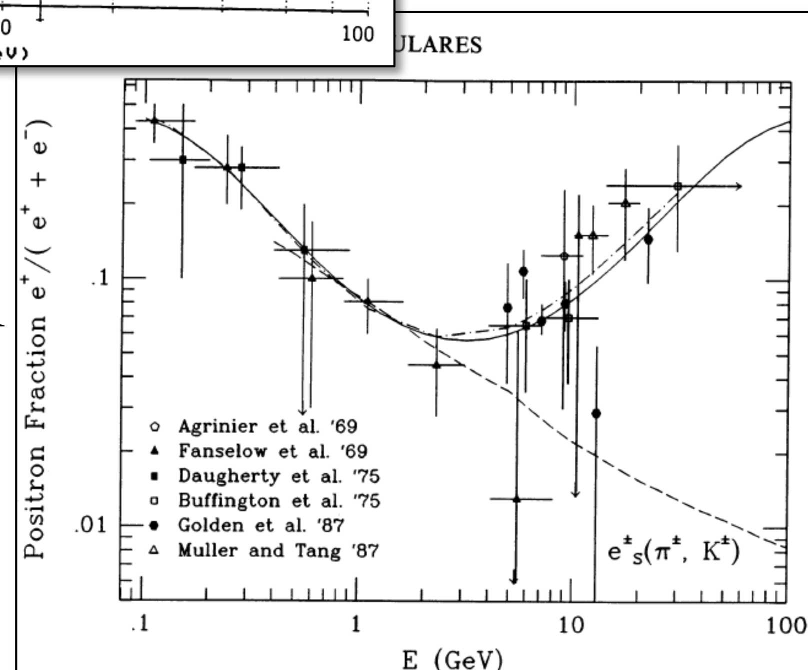

Pulsars as sources of CR positrons (& electrons)

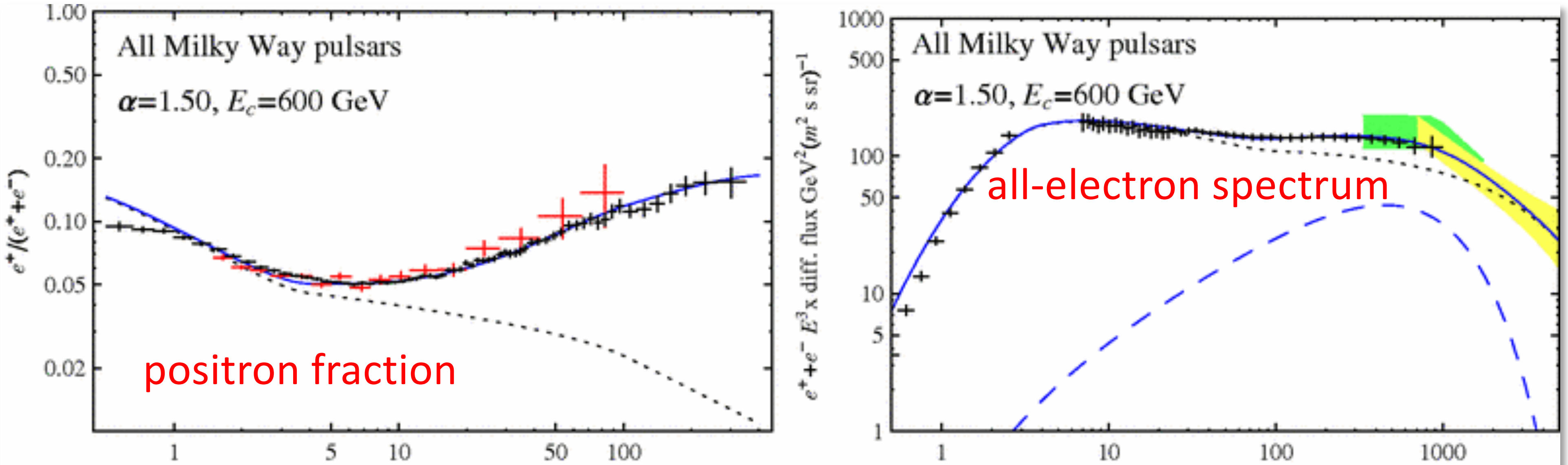

Example: Cholis & Hooper '13

Pulsar spectrum is parametrized as: $$\frac{dN}{dE} \sim E^{-\alpha} e^{\left(-\frac{E}{E_c}\right)}$$

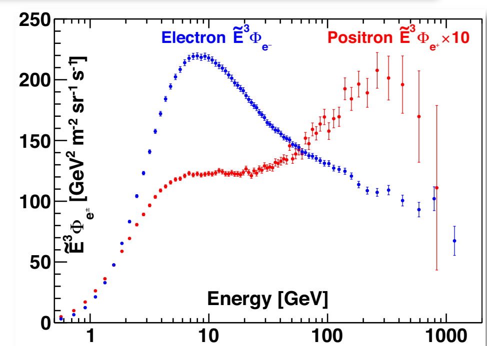

✧ α, E_c – free parameters

✧ Free injection spectrum of electrons from SNRs

Good:

✓ Affects only electrons and positrons, does not affect other CR species

✓ Given enough free parameters, it is possible to fit the positron fraction

Bad:

– Pulsar-only-model cannot reproduce all-*e* spectrum and the cutoff in e^+ spectrum at ~300 GeV

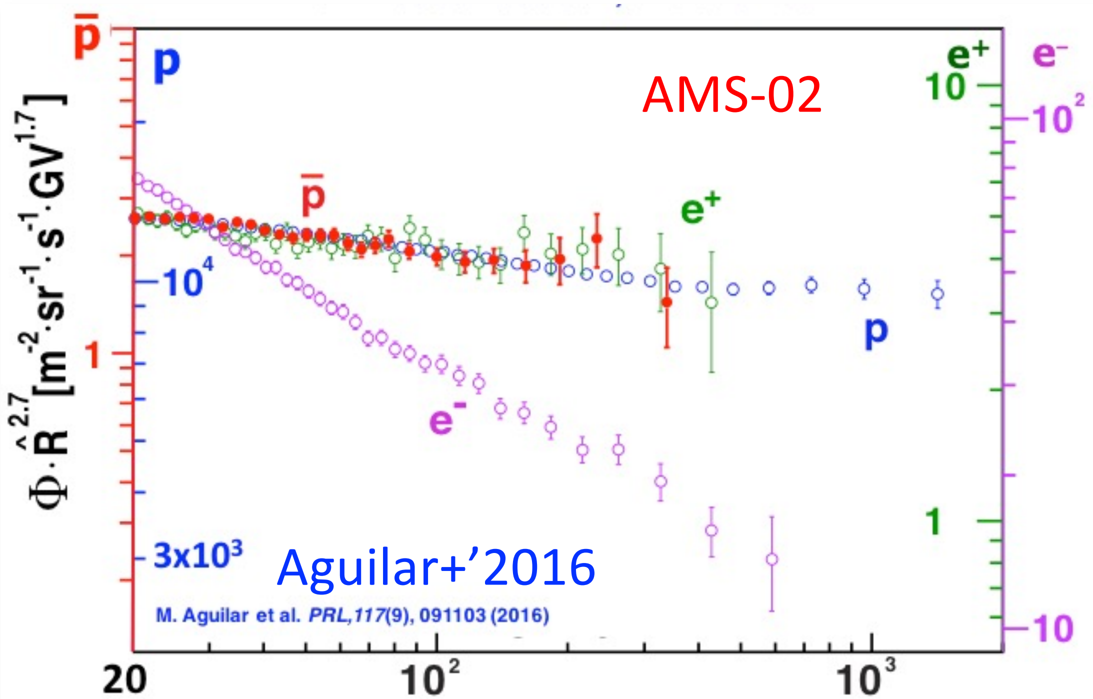

What do pulsars know about CR protons?

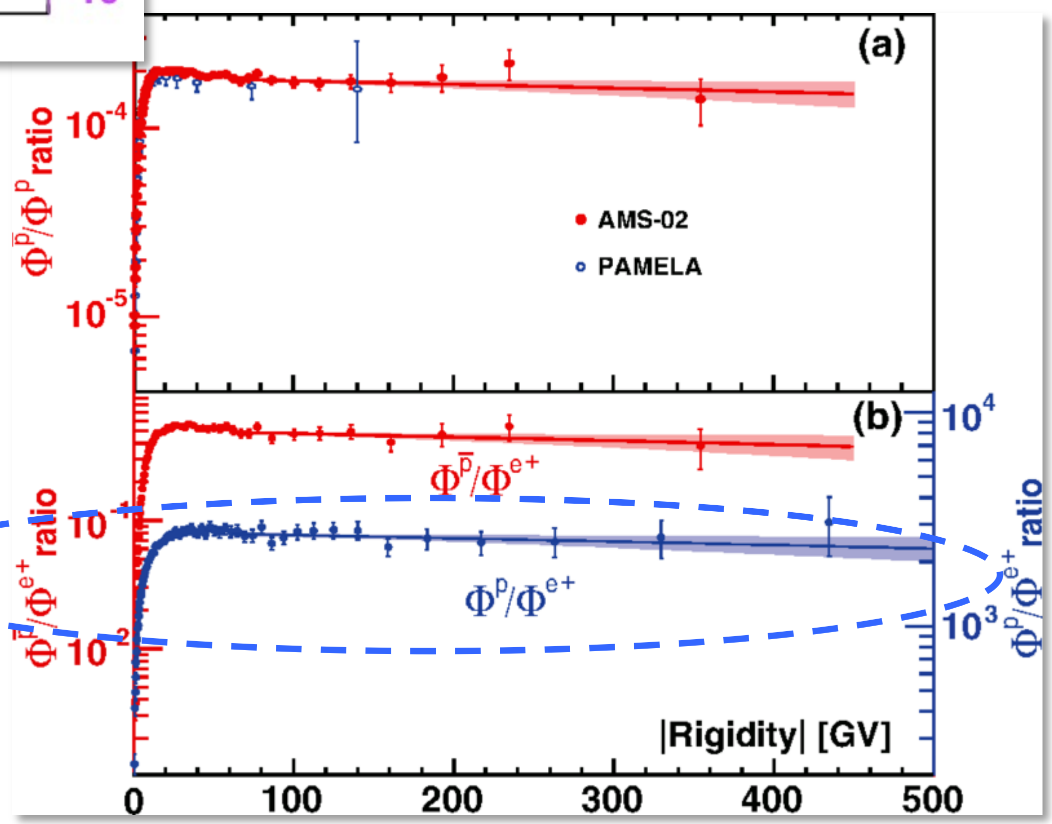

- ✧ If excess positrons are produced in pulsars or DM decays why the p/e⁺ ratio is flat?
- ✧ The flat p/e⁺ ratio perhaps indicates a common origin of the spectra of p and e⁺!

Pulsar bow shock model by A. Bykov et al. (2017)

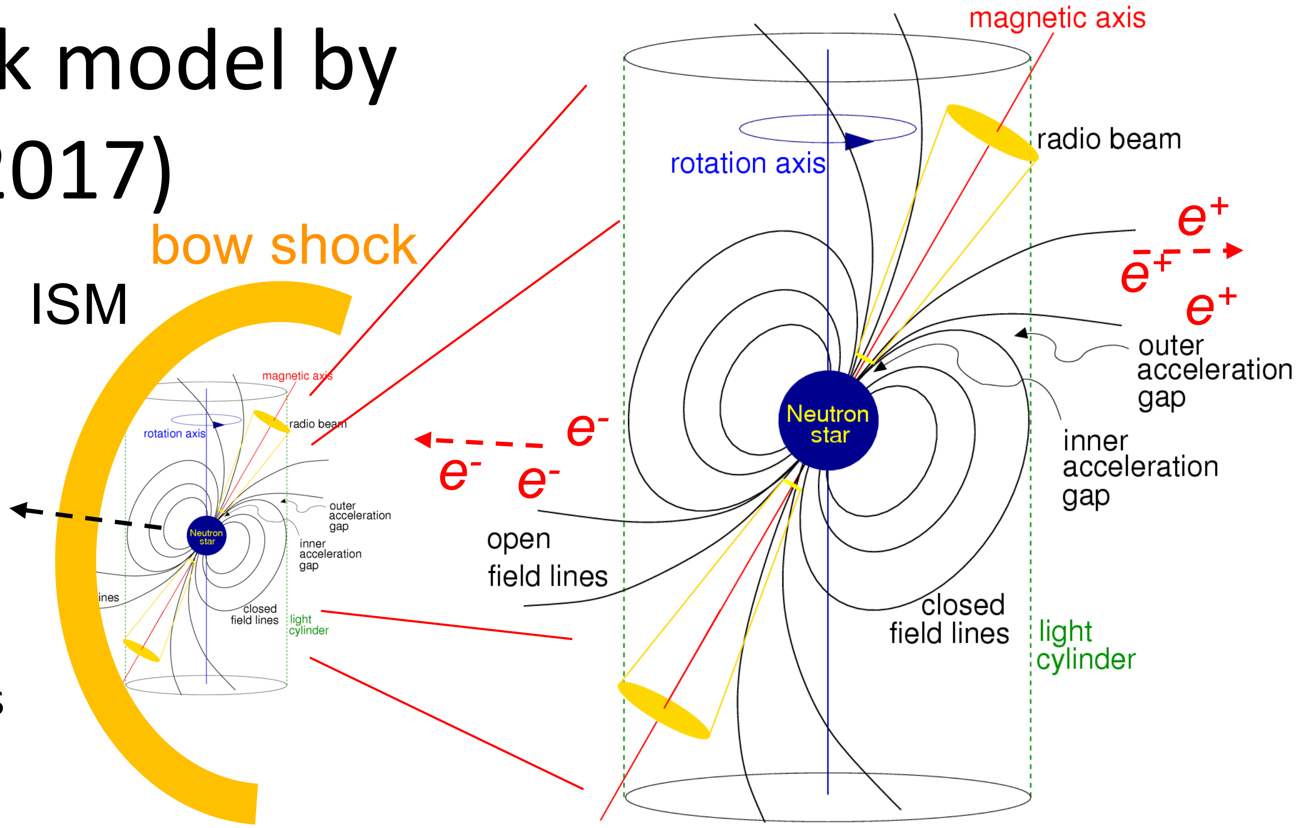

- Pulsars with high spin-down power produce relativistic winds
- Some of the PWNe are moving relative to the ambient ISM with supersonic speeds producing bow shocks
- Ultrarelativistic particles accelerated at the termination surface of the pulsar wind may undergo reacceleration in the converging flow system → produces universal spectrum, same as for protons
- Similar spectra for electrons and positrons

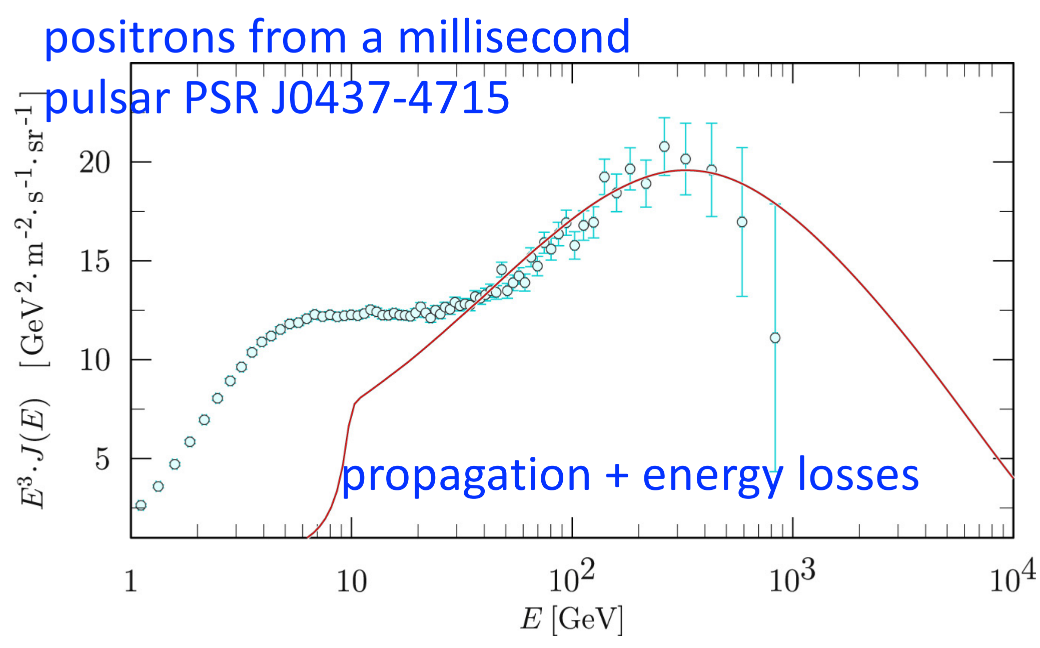

See also Bykov+’2019, Petrov’+2020,

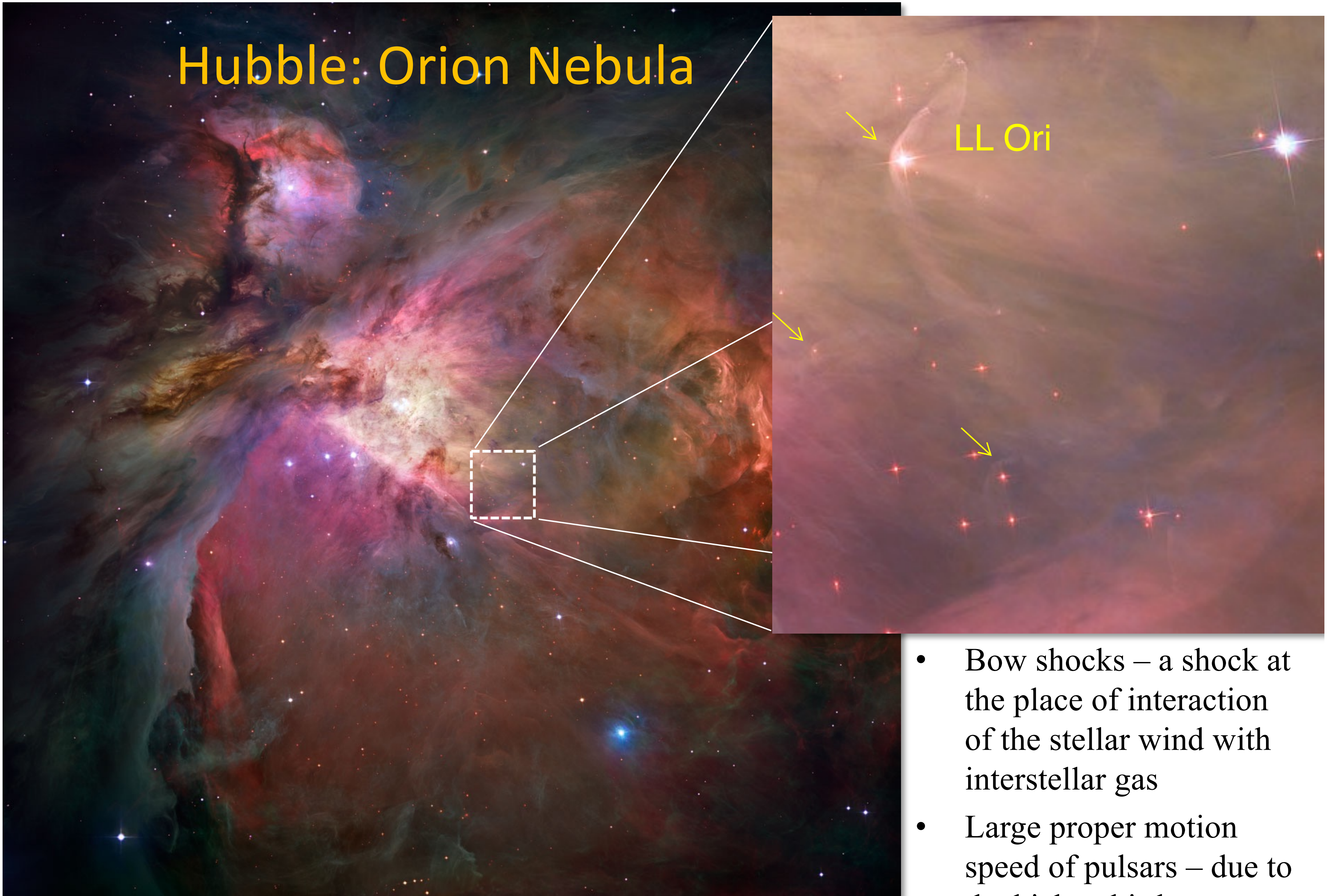

- Bow shocks – a shock at the place of interaction of the stellar wind with interstellar gas
- Large proper motion speed of pulsars – due to the kick at birth

The 5.7 millisecond pulsar PSR J0437-4715

- ◇ Distance: 156.79±0.25pc
- ◇ Closest and brightest millisecond pulsar (MSP), in a binary system with a white dwarf companion and an orbital period of 5.7 days
- ◇ Velocity ~100 km/s
- ◇ Observed in optical, far-ultraviolet (FUV), and X-ray bands
- ◇ It exhibits the greatest long-term rotational stability of any pulsar
- ◇ It is the first pulsar for which the full three-dimensional orientation of the binary orbit was determined, enabling a new test of General Relativity

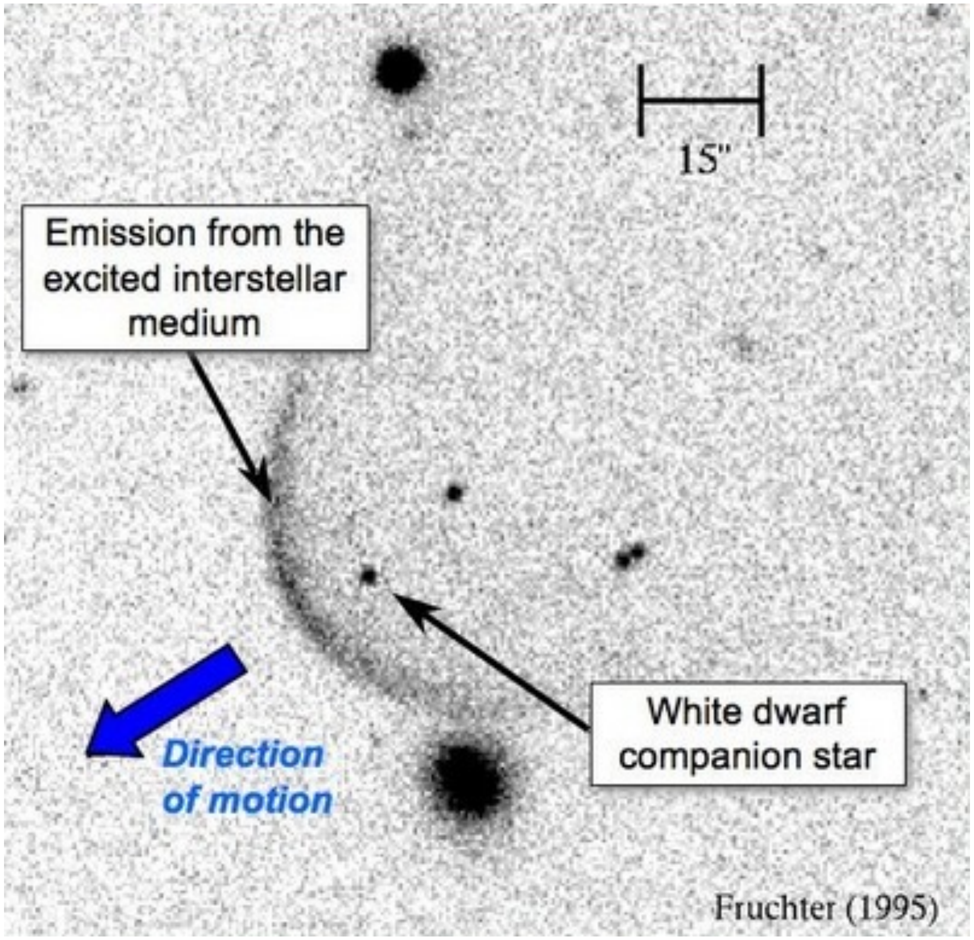

Optical image of the binary system containing PSR J0437-4715

ISSN 1062-8738, Bulletin of the Russian Academy of Sciences: Physics, 2009, Vol. 73, No. 5, pp. 564–567. © Allerton Press, Inc., 2009.
Original Russian Text © A.D. Panov, J.H. Adams Jr., H. S. Ahn, G.L. Bashinzhagyan, J.W. Watts, J.P. Wefel, J. Wu, O. Ganel, T.G. Guzik, V.I. Zatsepin, I. Isbert, K.C. Kim, M. Christl, E.N. Kouznetsov, M.I. Panasyuk, E.S. Seo, N.V. Sokolskaya, J. Chang, W.K.H. Schmidt, A.R. Fazely, 2009, published in Izvestiya Rossiiskoi Akademii Nauk. Seriya Fizicheskaya, 2009, Vol. 73, No. 5, pp. 602–605.

2009

Energy Spectra of Abundant Nuclei of Primary Cosmic Rays from the Data of ATIC-2 Experiment: Final Results

A. D. Panov[a], J. H. Adams Jr.[b], H. S. Ahn[c], G. L. Bashinzhagyan[a], J. W. Watts[b], J. P. Wefel[d], J. Wu[c], O. Ganel[c], T. G. Guzik[d], V. I. Zatsepin[a], I. Isbert[d], K. C. Kim[c], M. Christl[b], E. N. Kouznetsov[d], M. I. Panasyuk[a], E. S. Seo[c], N. V. Sokolskaya[a], J. Chang[f, g], W. K. H. Schmidt[g], and A. R. Fazely[e]

[a] *Skobel'tsyn Institute of Nuclear Physics, Moscow State University, Moscow, Russia*
e-mail: panov@dec1.sinp.msu.ru

[b] *Marshall Space Flight Center, United States*

[c] *University of Maryland, United States*

[d] *Southeastern Louisiana University, United States*

[e] *Southern University, Baton Rouge, Louisiana, United States*

[f] *Purple Mountain Observatory, China*

[g] *Max Planck Institute, Germany*

The final results of processing the data from the balloon-born experiment ATIC-2 (Antarctica, 2002–2003) for the energy spectra of protons and He, C, O, Ne, Mg, Si, and Fe nuclei, the spectrum of all particles, and the mean logarithm of atomic weight of primary cosmic rays as a function of energy are presented.

The preliminary conclusions on the significant difference in the spectra of protons and helium nuclei (the proton spectrum is steeper) and the non-power character of the spectra of protons and heavier nuclei (flattening of carbon spectrum at energies above 10 TeV) are confirmed.

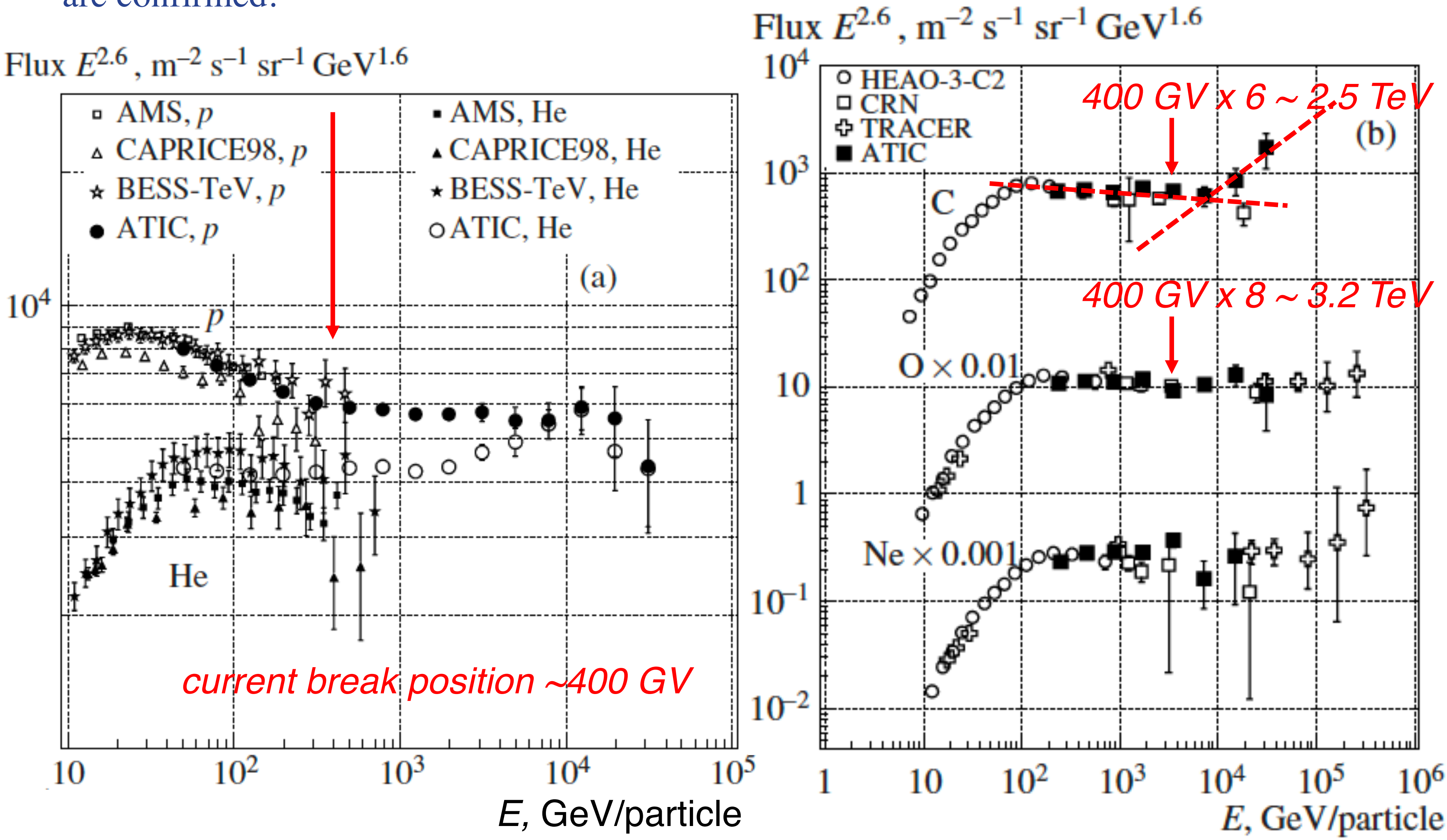

Earlier experiments pre-2000

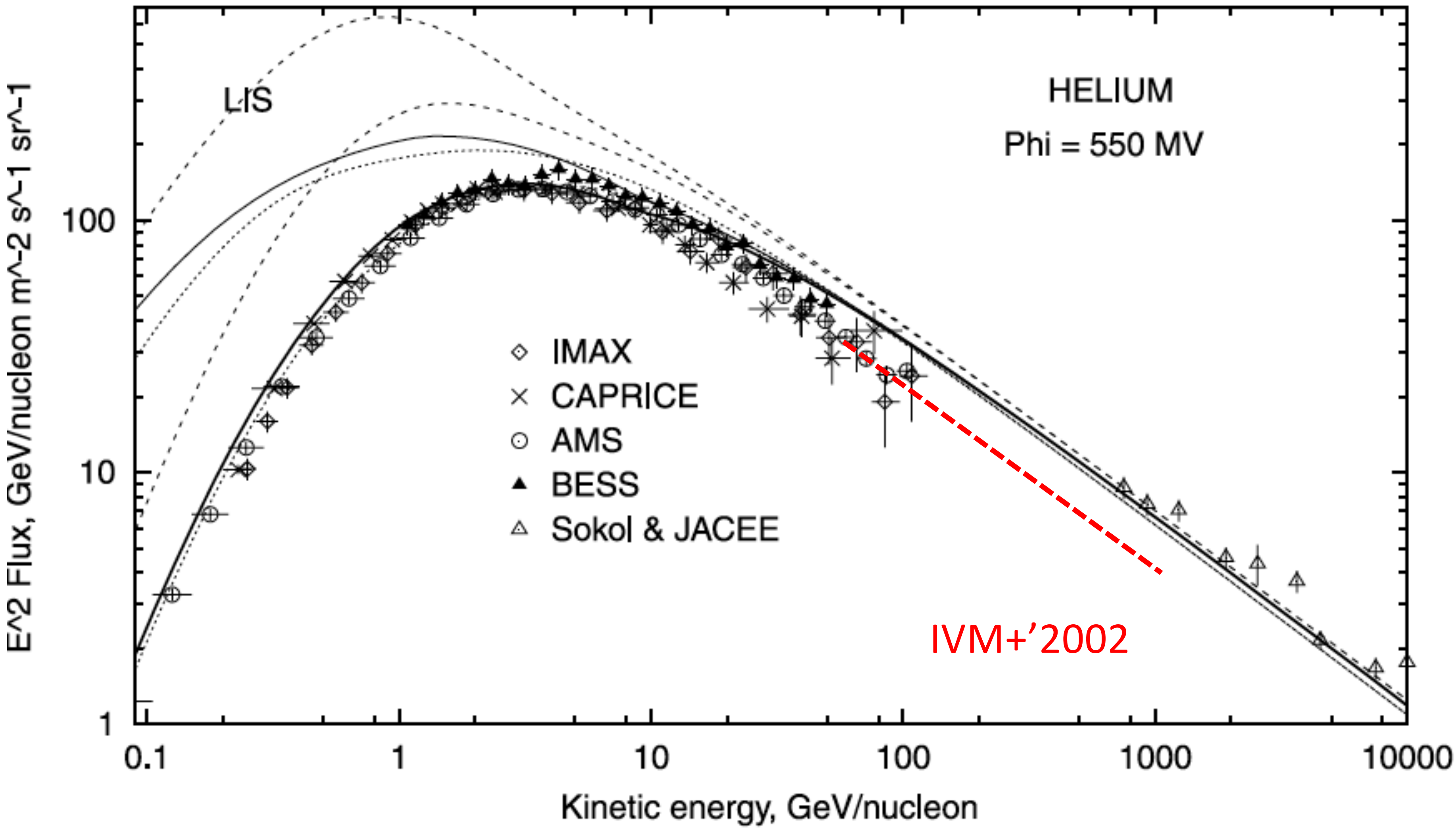

Strictly speaking, the inconsistency of *p* and *He* spectra with a single power-law could be already seen in earlier data, but was considered as a likely result of the energy calibration issues

Break in the spectra of CR nucleons

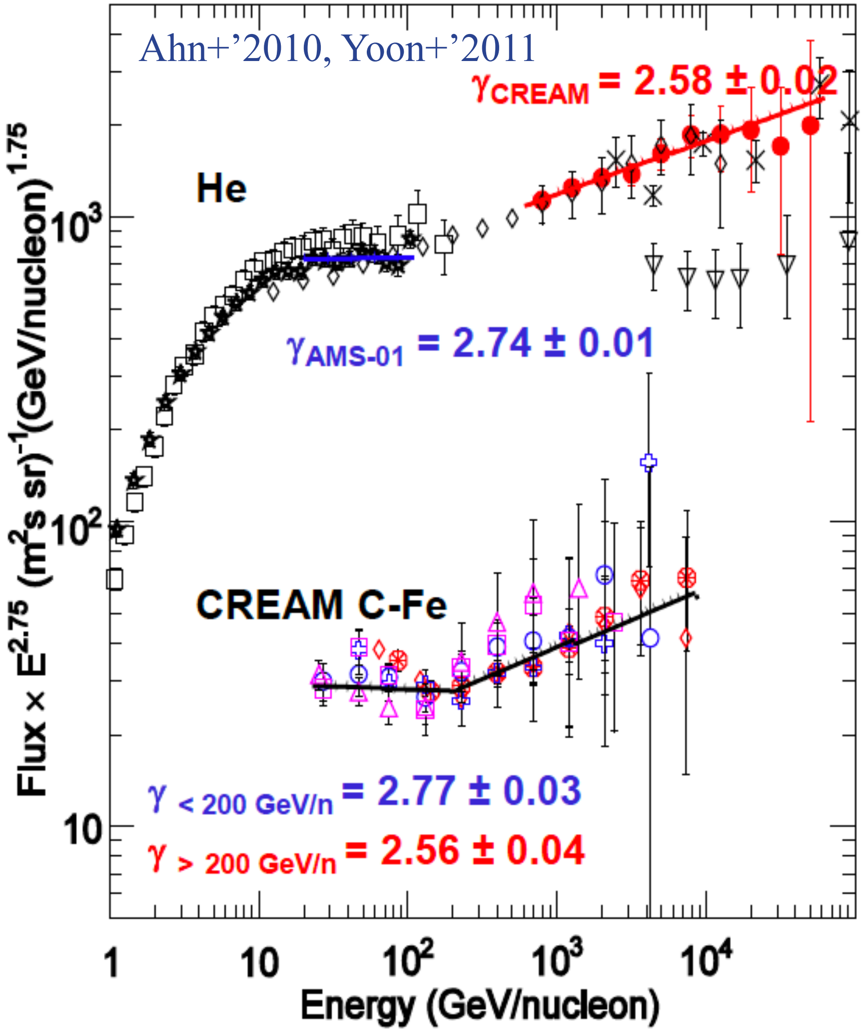

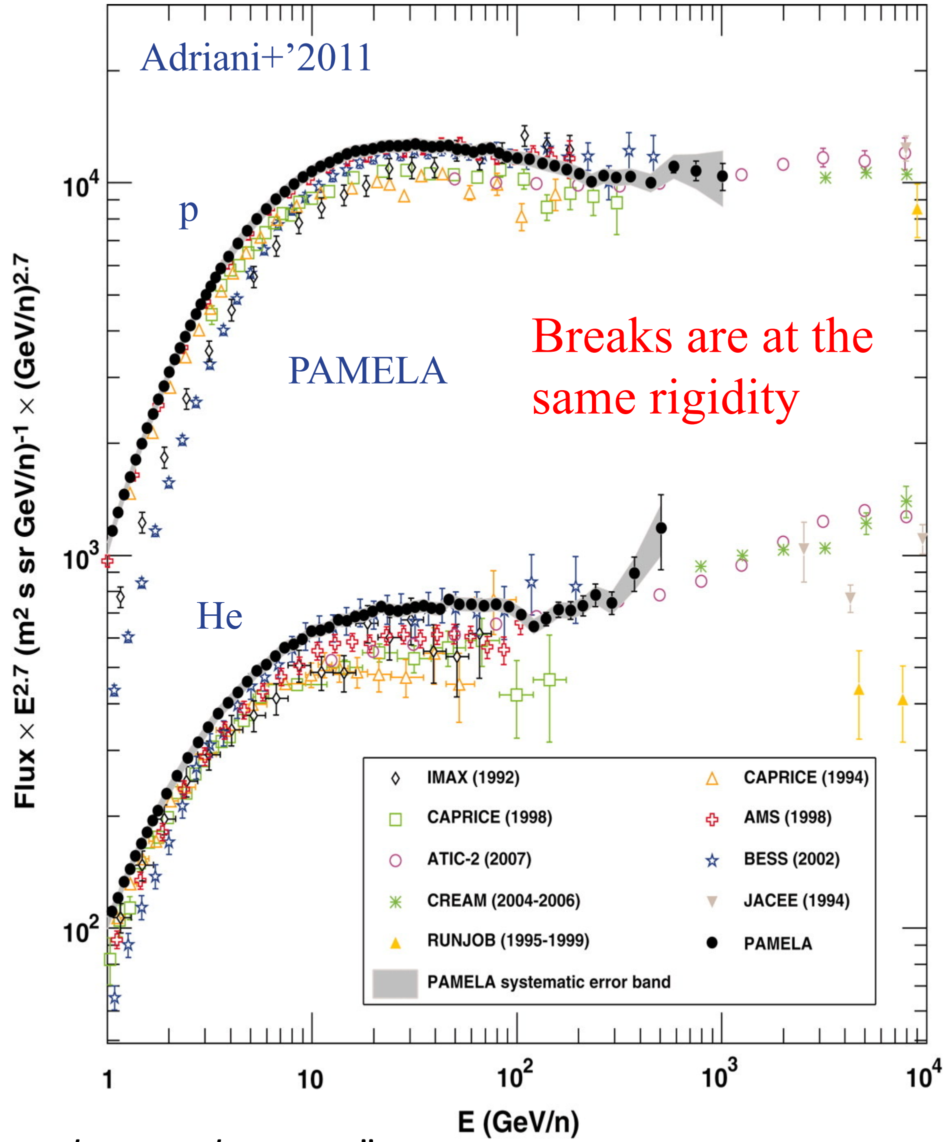

- ✧ CREAM "*Discrepant hardening observed in cosmic-ray elemental spectra*" (Ahn+'2010) and ATIC-2 (Panov+'2009)
- ✧ Initially looked like an energy calibration issue…
- ✧ …until it was confirmed by PAMELA and with more statistics by AMS-02

Interpretation of the break at ~300-400 GV

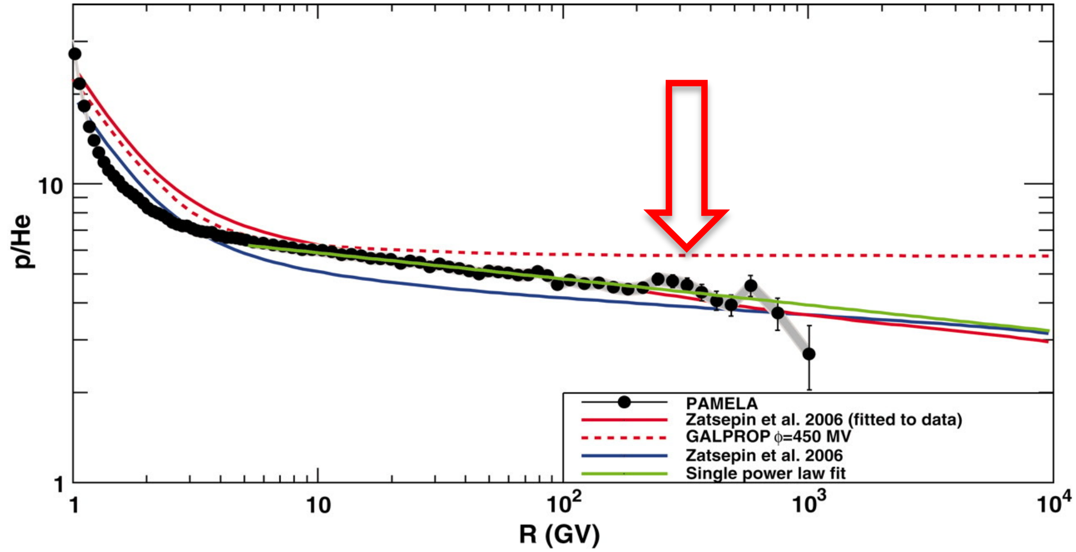

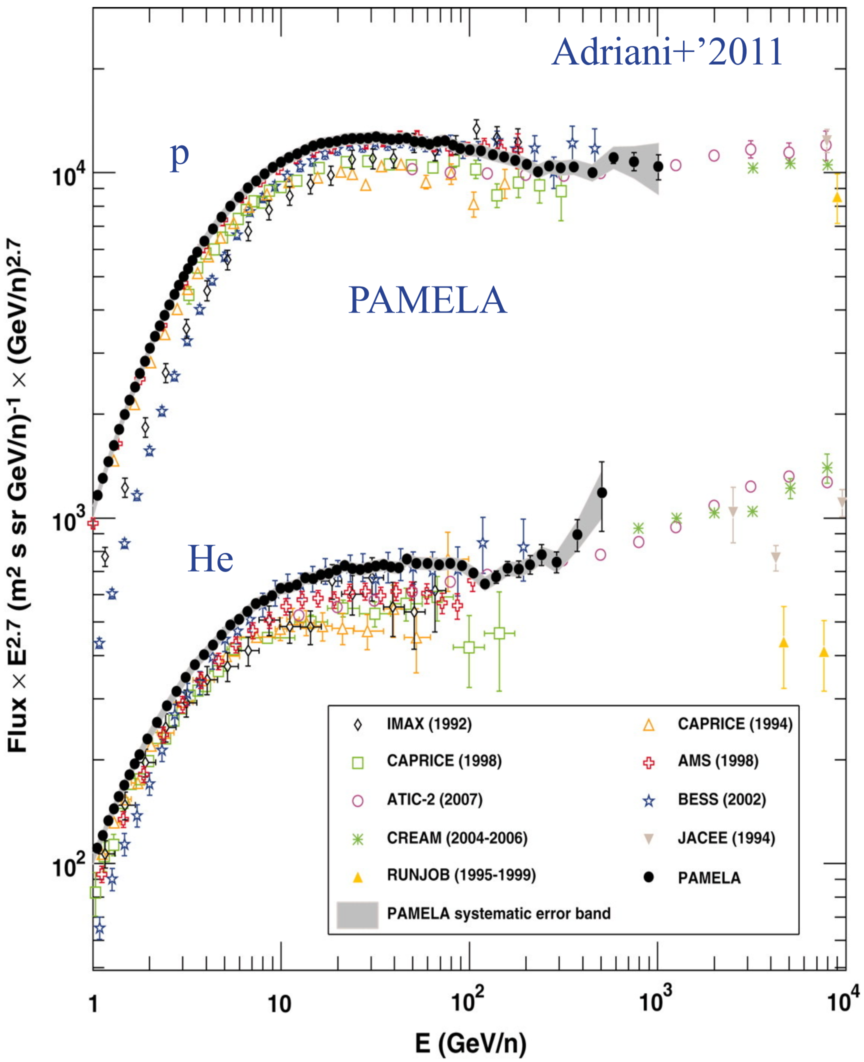

Based on PAMELA data Vladimirov+'2012 considered 6 scenarios of the break:

- ✧ Injection scenario: associated with injection
  - – prediction for secondaries – change in the spectral index below/above the break $\Delta\gamma_{\rm sec} \sim \Delta\gamma_{\rm prim}$
- ✧ Propagation scenario: result of the diffusion (preferred)
  - – The ratio p/He shows no break
  - – Prediction for secondaries – change in the spectral index below/above the break $\Delta\gamma_{\rm sec} \sim 2\Delta\gamma_{\rm prim}$
  - – Index of the diffusion coeff.: $\delta \sim \gamma_{\rm sec} - \gamma_{\rm prim}$

AMS-02: Breaks in the spectra of CR species

- ◇ Spectral shapes of primary species are similar
- ◇ Spectral shapes of secondary species are similar, but different from primaries
- ◇ Spectra of secondaries are steeper than primaries in the whole energy range
- ◇ The break is at about the same rigidity

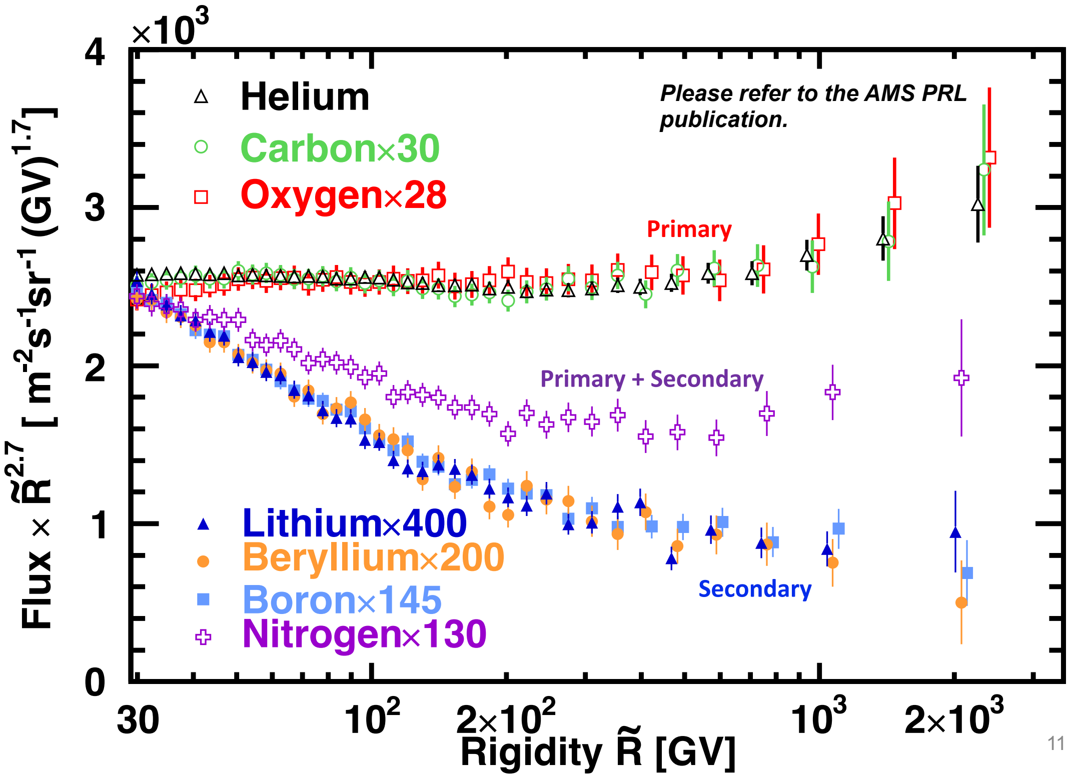

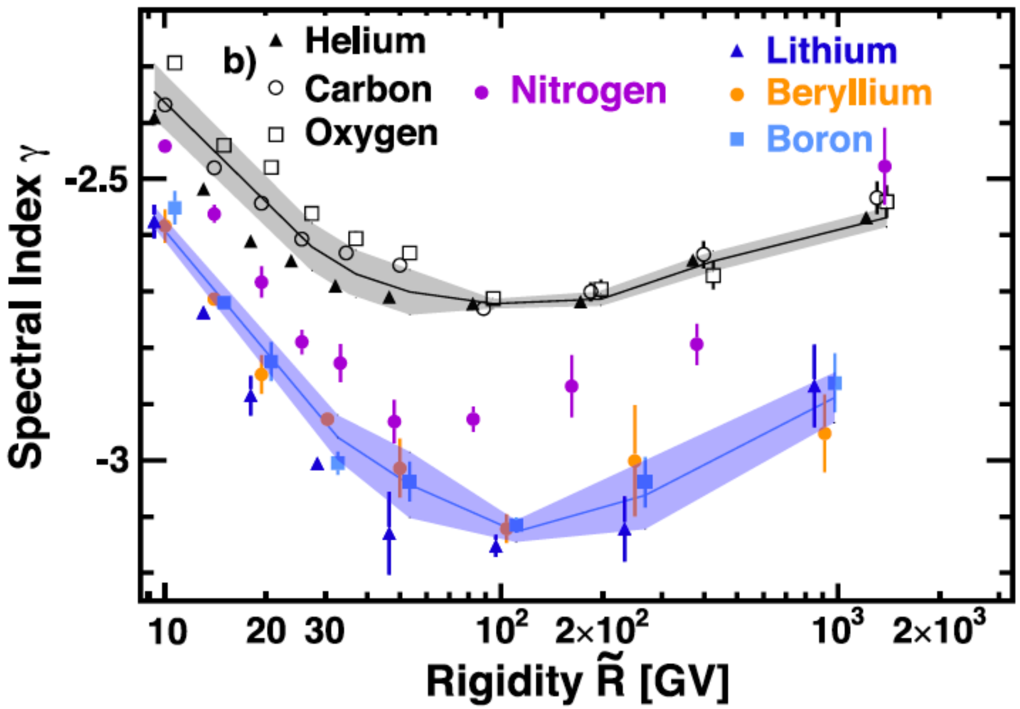

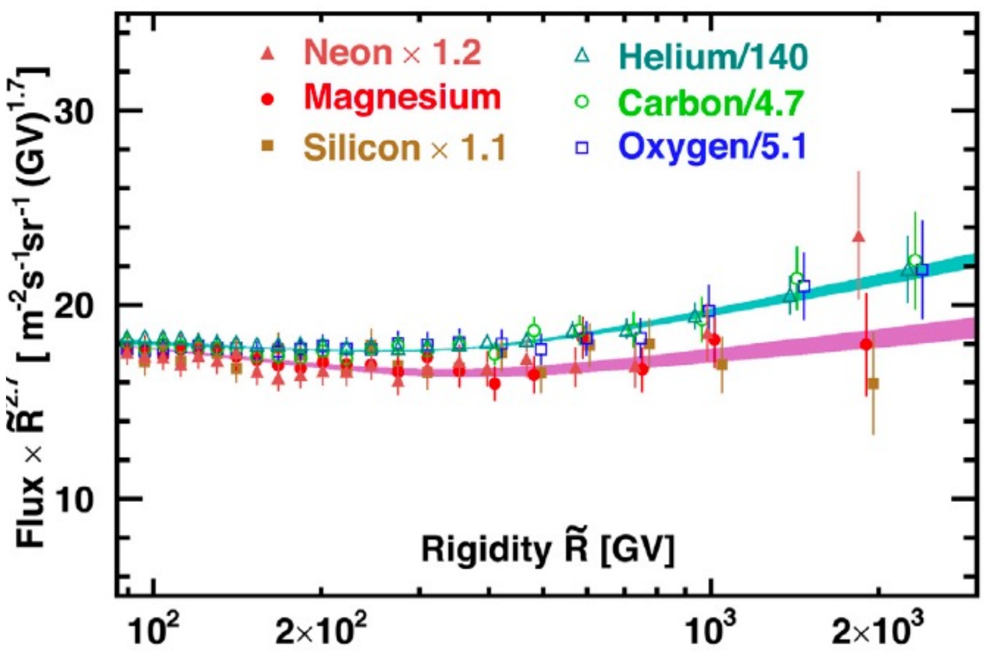

Effect of interstellar propagation

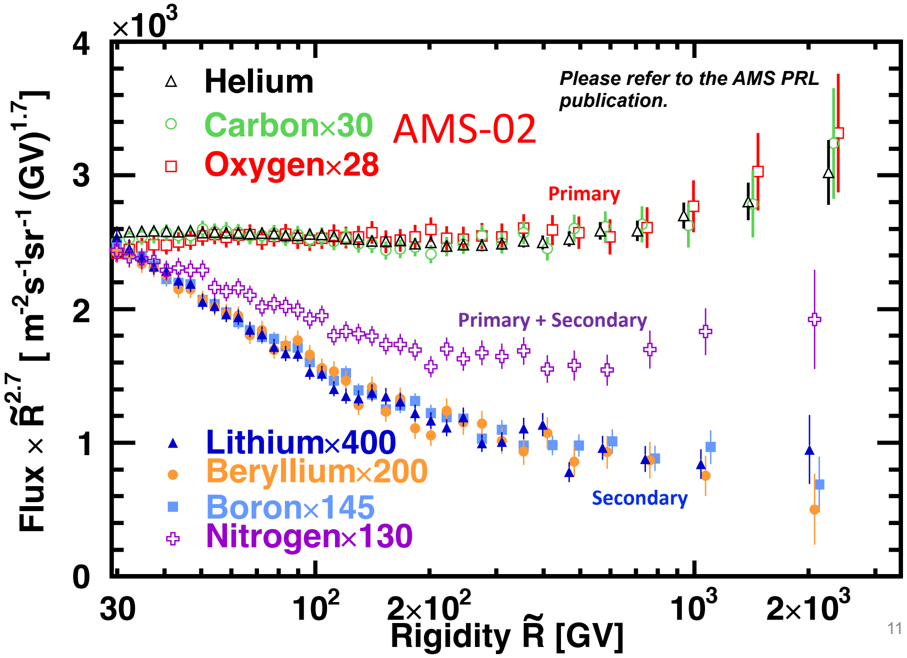

Such behavior was predicted (Vladimirov+'12, Blasi+'12):

$$\Delta\gamma_{\rm sec} \sim 2\Delta\gamma_{\rm prim}$$

if the break is due to the break in the spectrum of interstellar turbulence

Index of the diffusion coefficient:

$$\delta = |\gamma_{\rm sec} - \gamma_{\rm prim}|$$

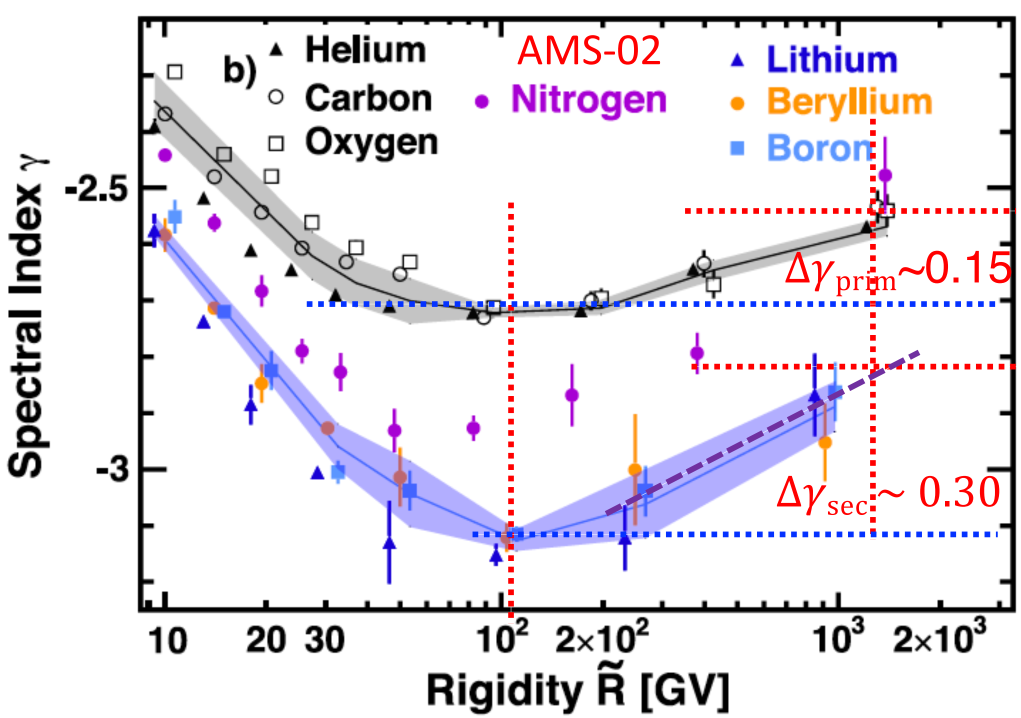

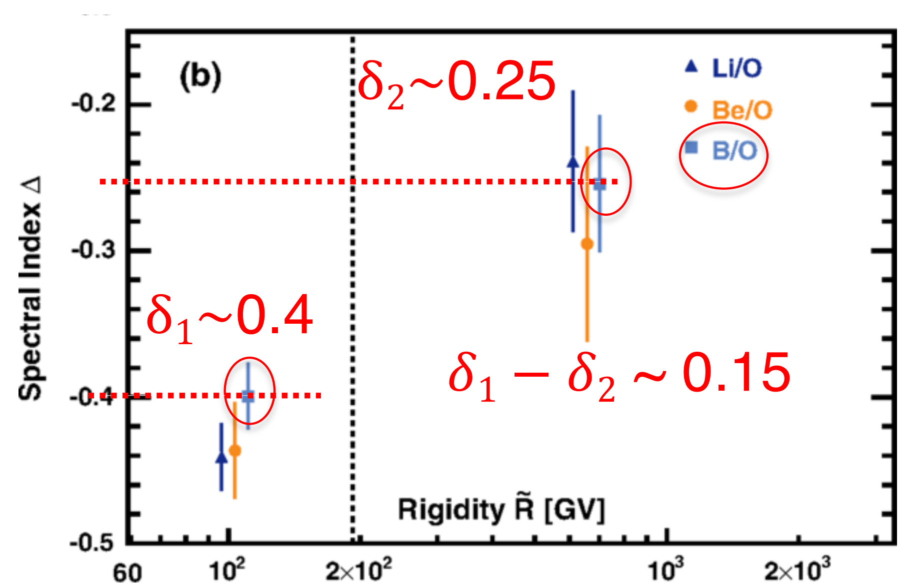

B/C in different scenarios

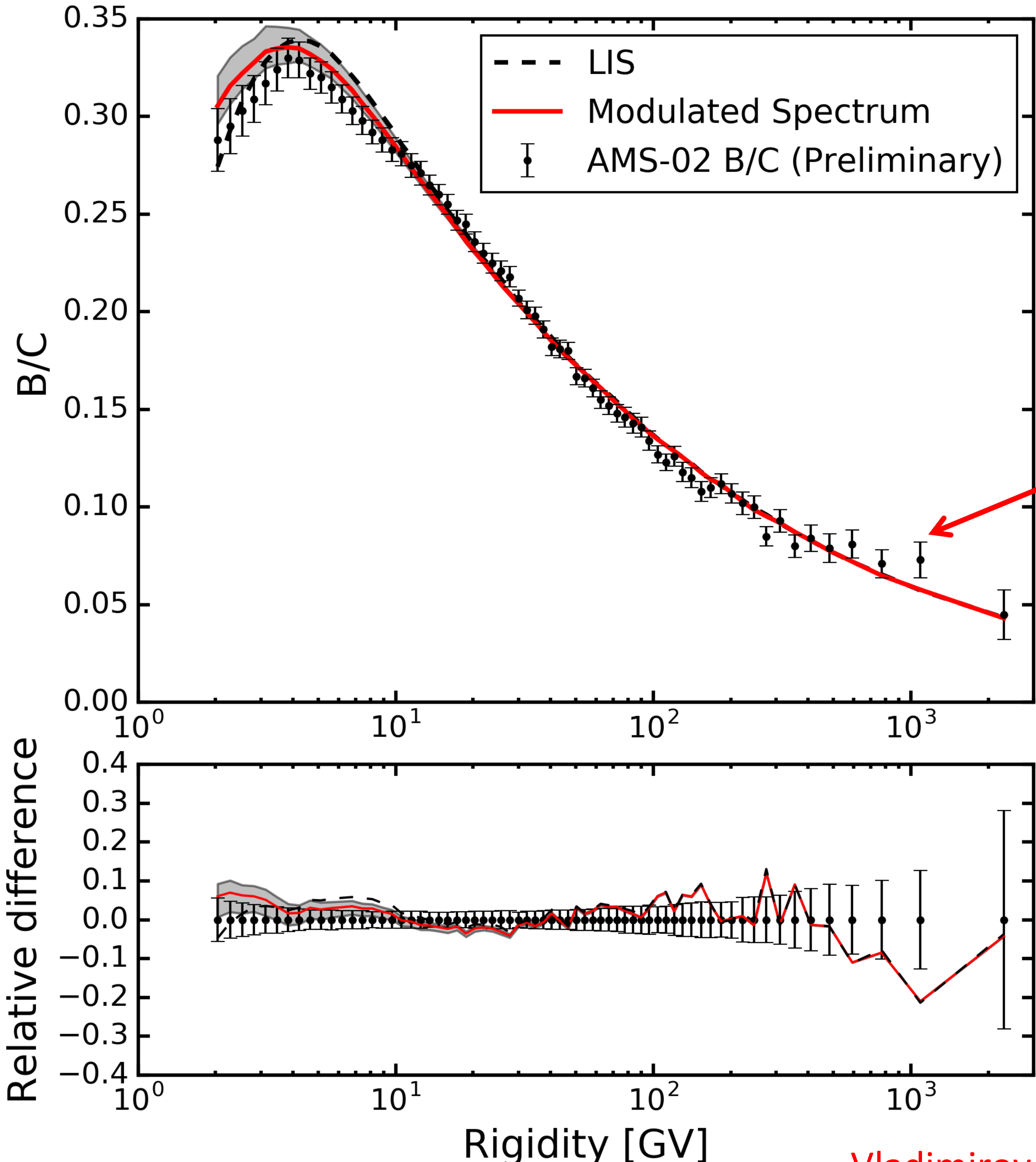

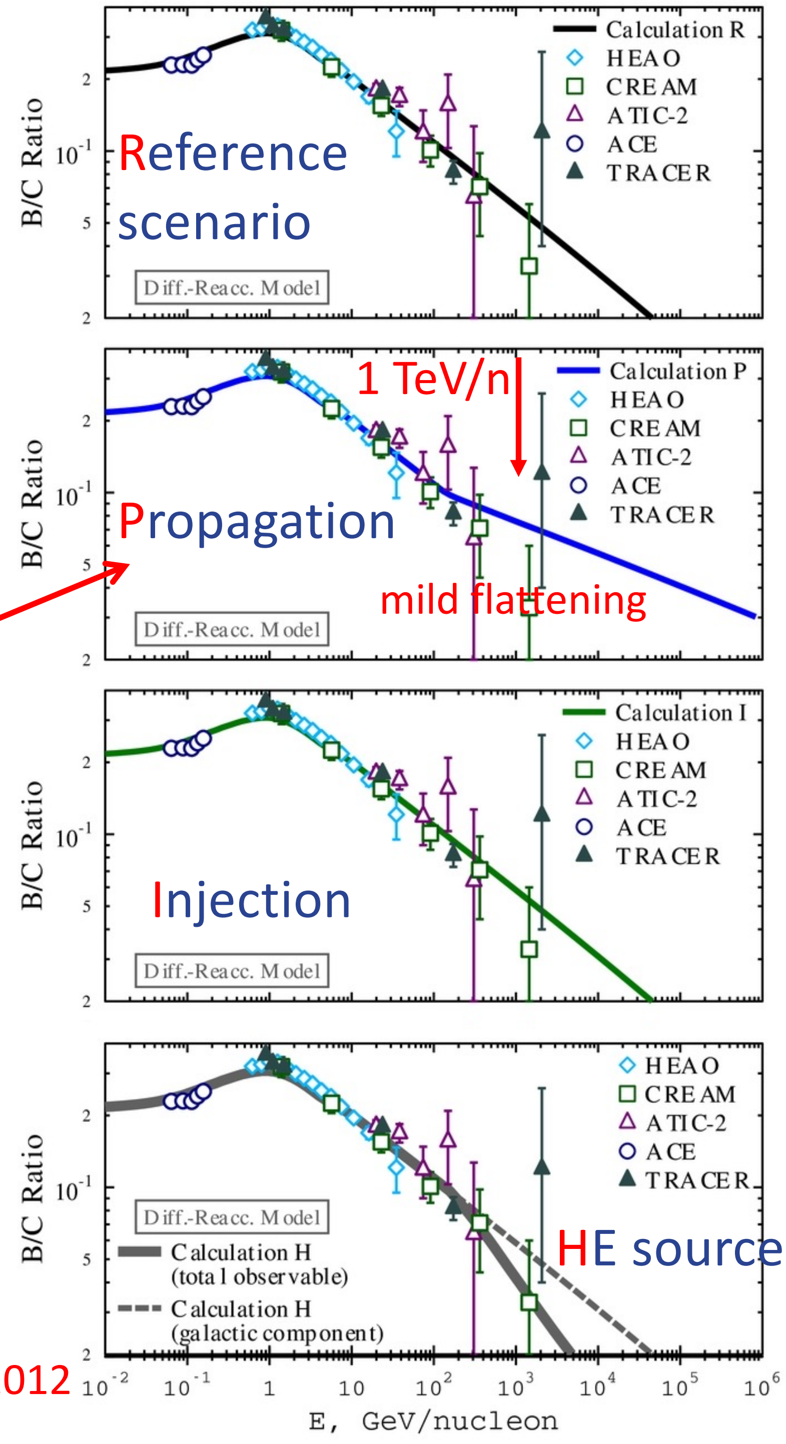

Vladimirov+'2012

Interstellar turbulence and the diffusion coeff.

- 300 GV break: A transition from the self-generated turbulence to the cascading of externally generated turbulence (for instance due to supernova bubbles) from large spatial scales to smaller scales

- The agreement with AMS-02 data is pretty good, but does not explain the difference between the spectra of *p* and heavier species (He-O)

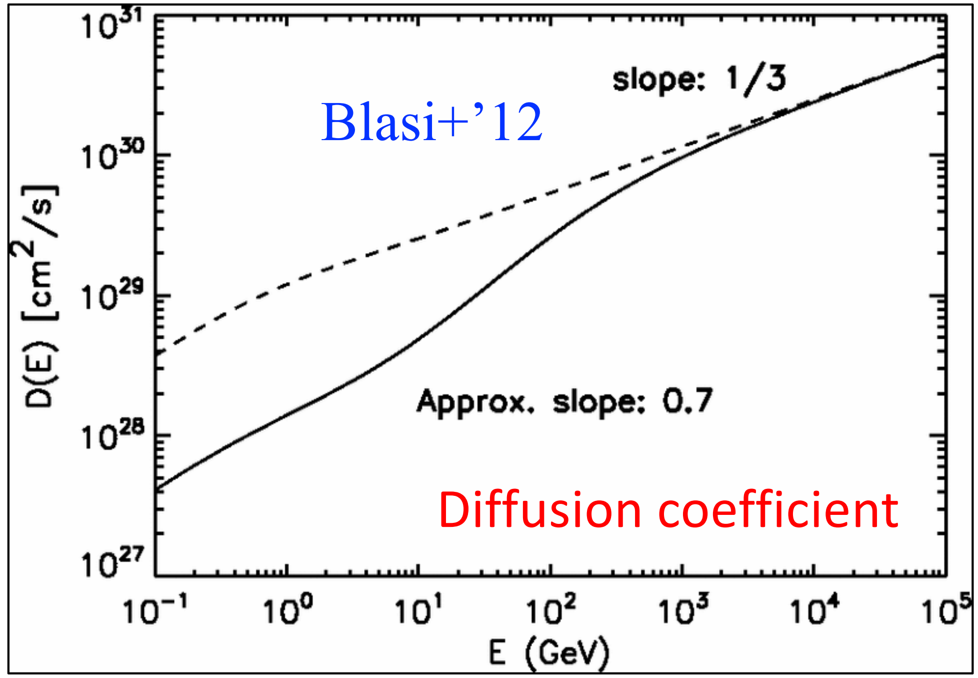

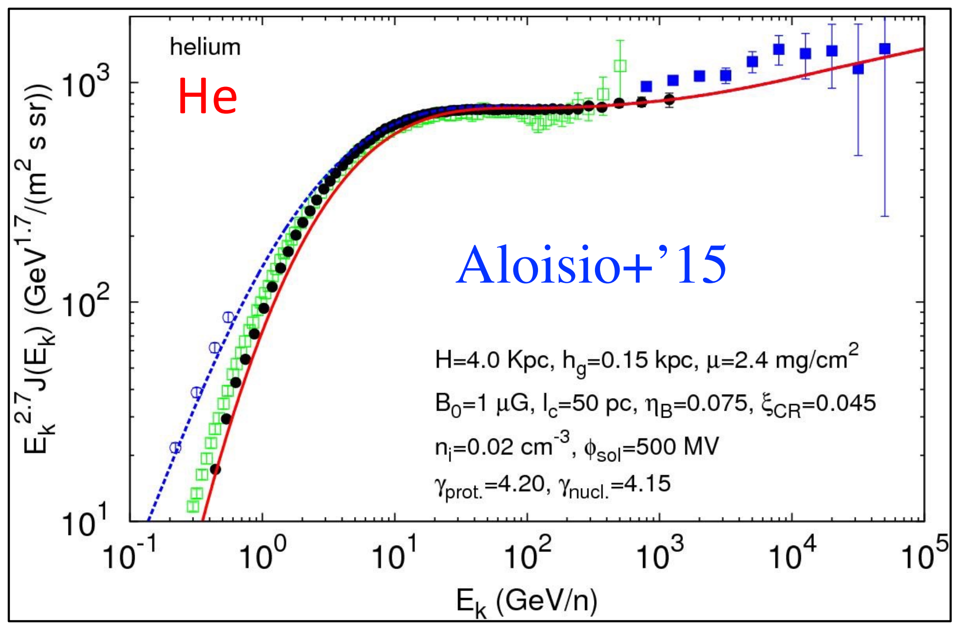

AMS-02 data

- Spectra of CR species from AMS-02:
  - Primary
  - Intermediate
  - Secondary (steeper spectra)
- Local Interstellar Spectra (LIS) – dashed lines
- Primary Li at HE?

Boschini+'2020

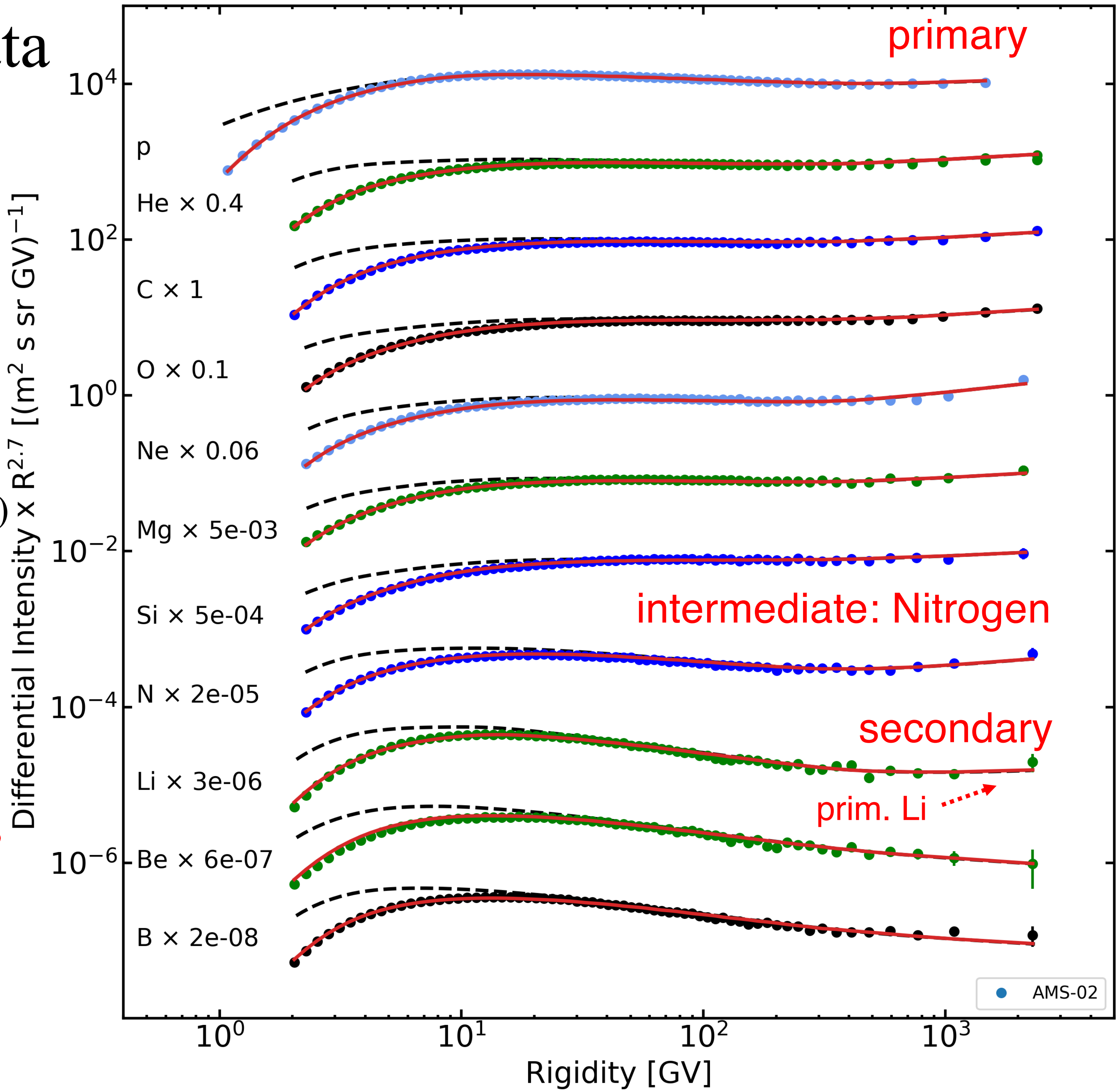

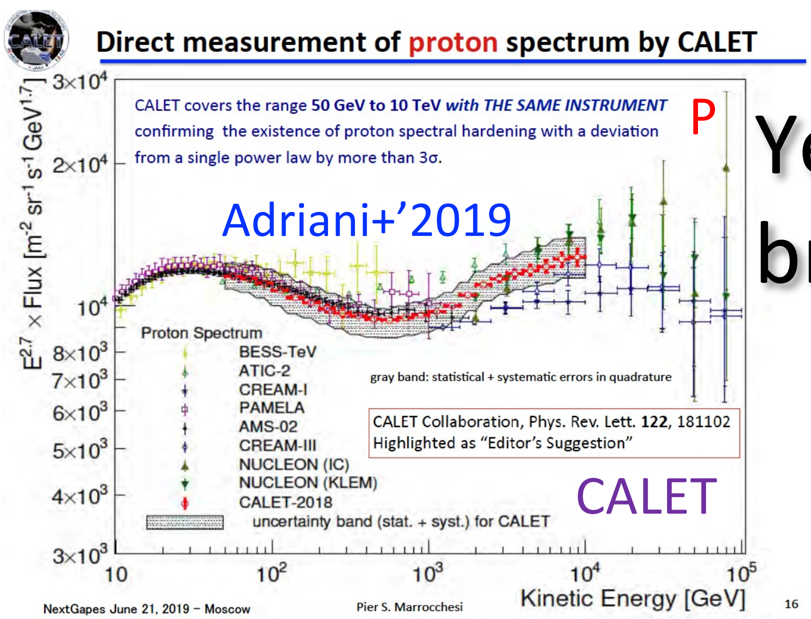

Yet another break at 10TV?

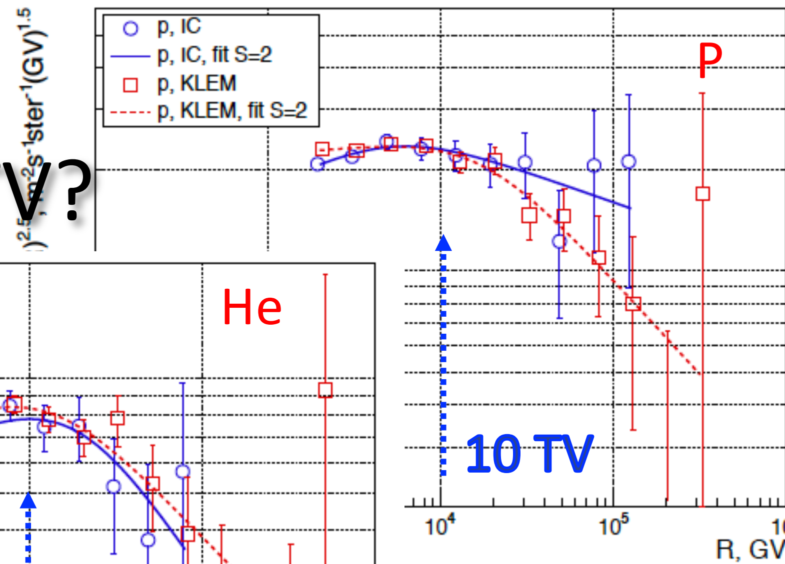

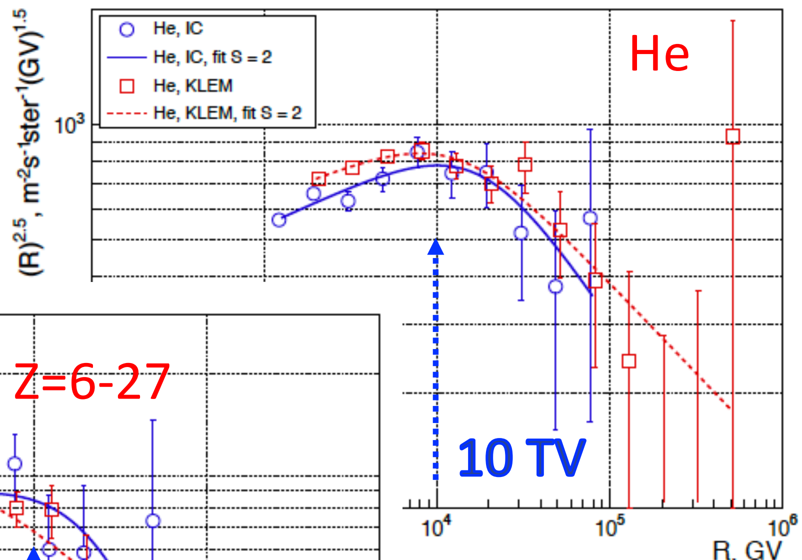

NUCLEON
Atkin+'2018

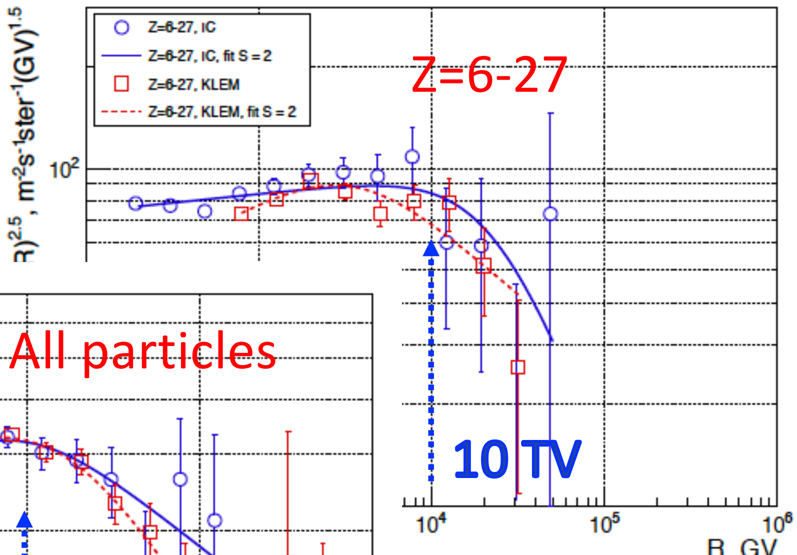

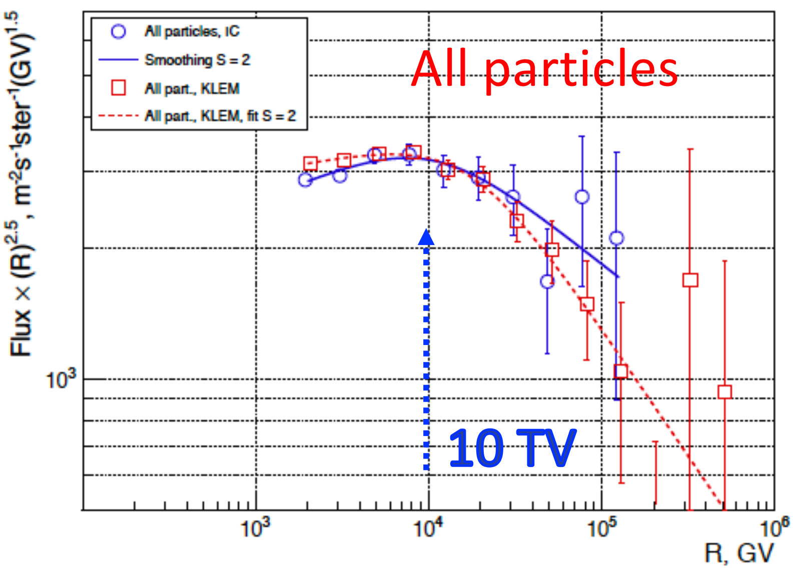

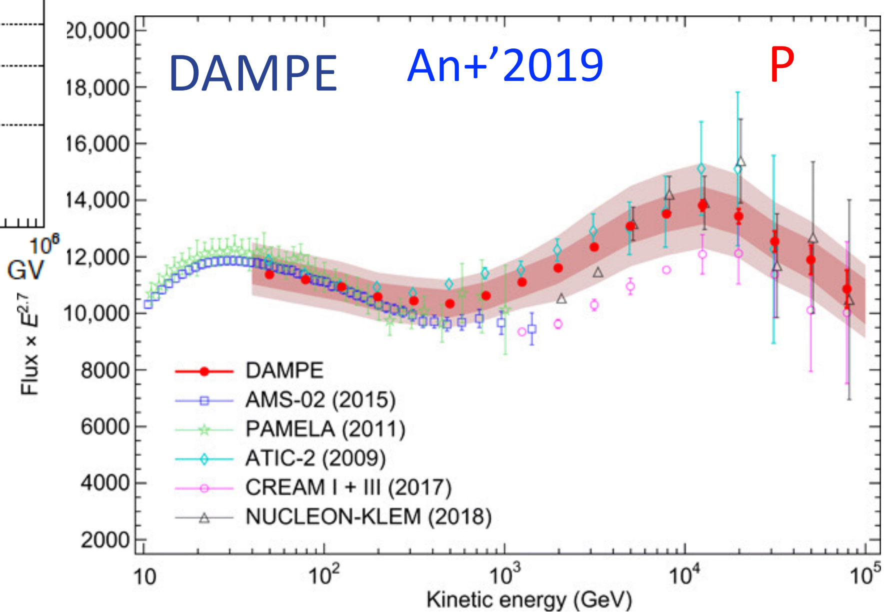

A collection of data indicates two breaks in H and He spectra @ the same rigidity

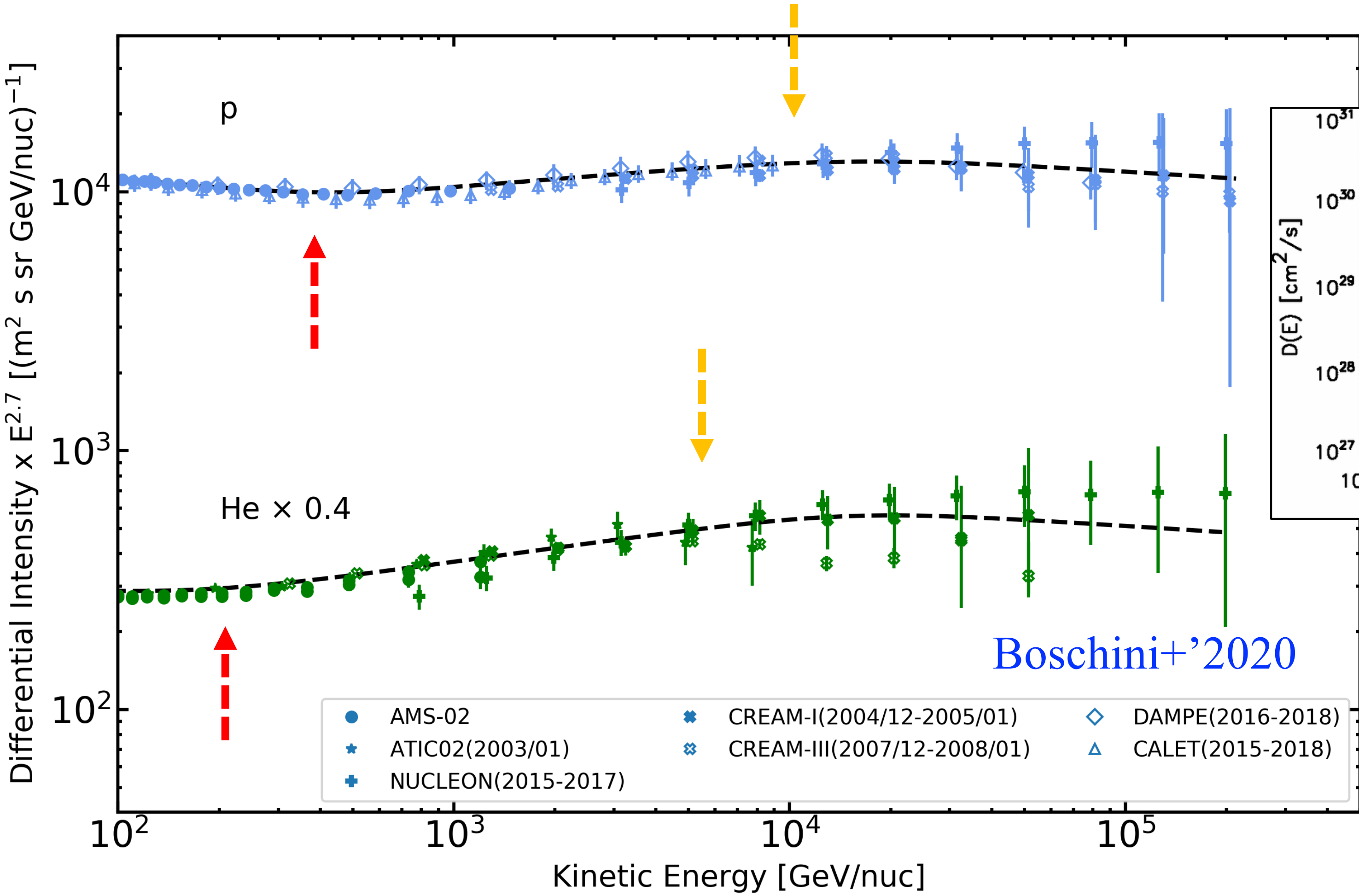

Diffusion coefficient?

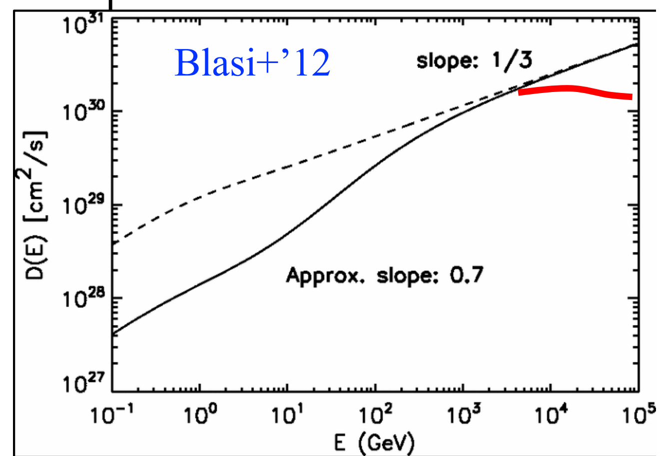

- ✧ Apparently, there are 2 breaks that very close to each other (at the same rigidity for p and He)
- ✧ Sharpness of the break is in conflict with large scale properties of the interstellar medium

Anisotropy

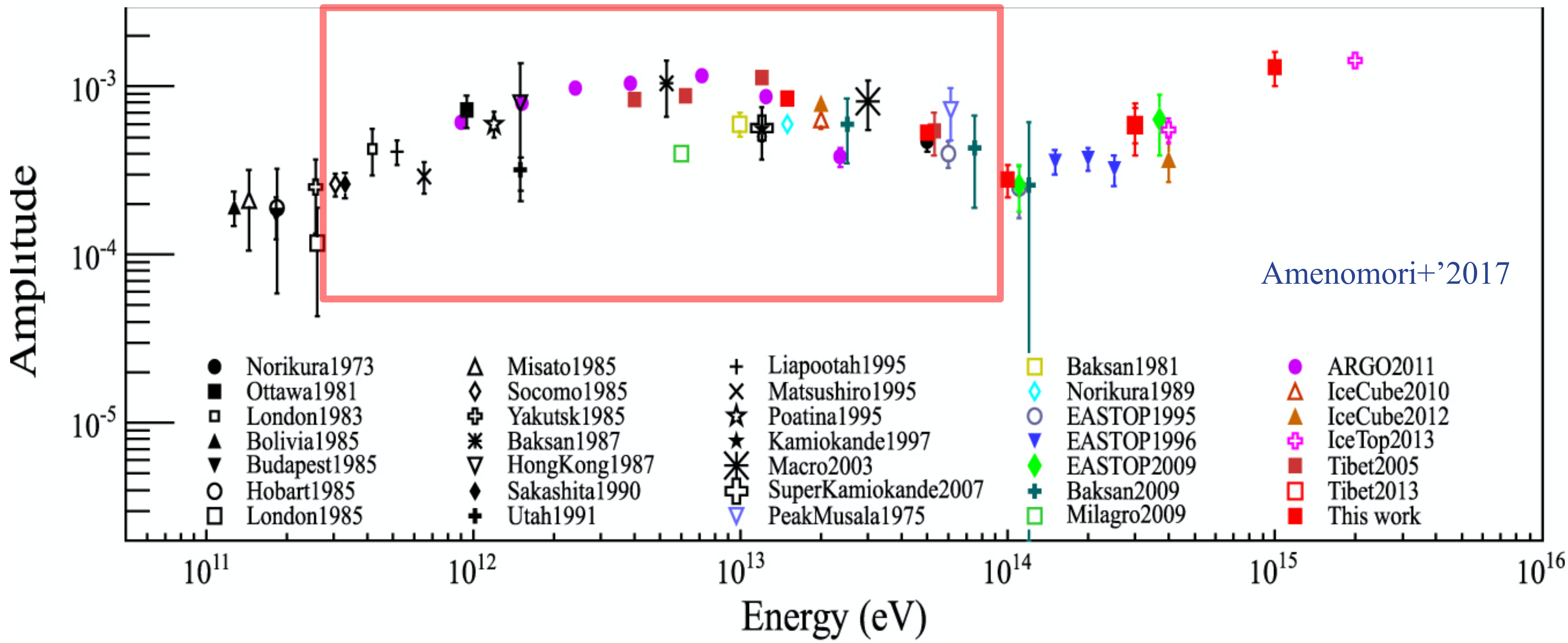

✧ CR anisotropy has an enhancement in exactly the range of the bump

✧ Indicates the local origin of the bump

Local SNR?

The TeV bump has to be made of the preexisting CRs with all their primaries and secondaries that have spent millions of years in the Galaxy! – weak local shock that reaccelerates CR particles

Local SNR scenario is proposed by:

Fang et al. 2020

Fornieri et al. 2021

Yuan et al. 2020

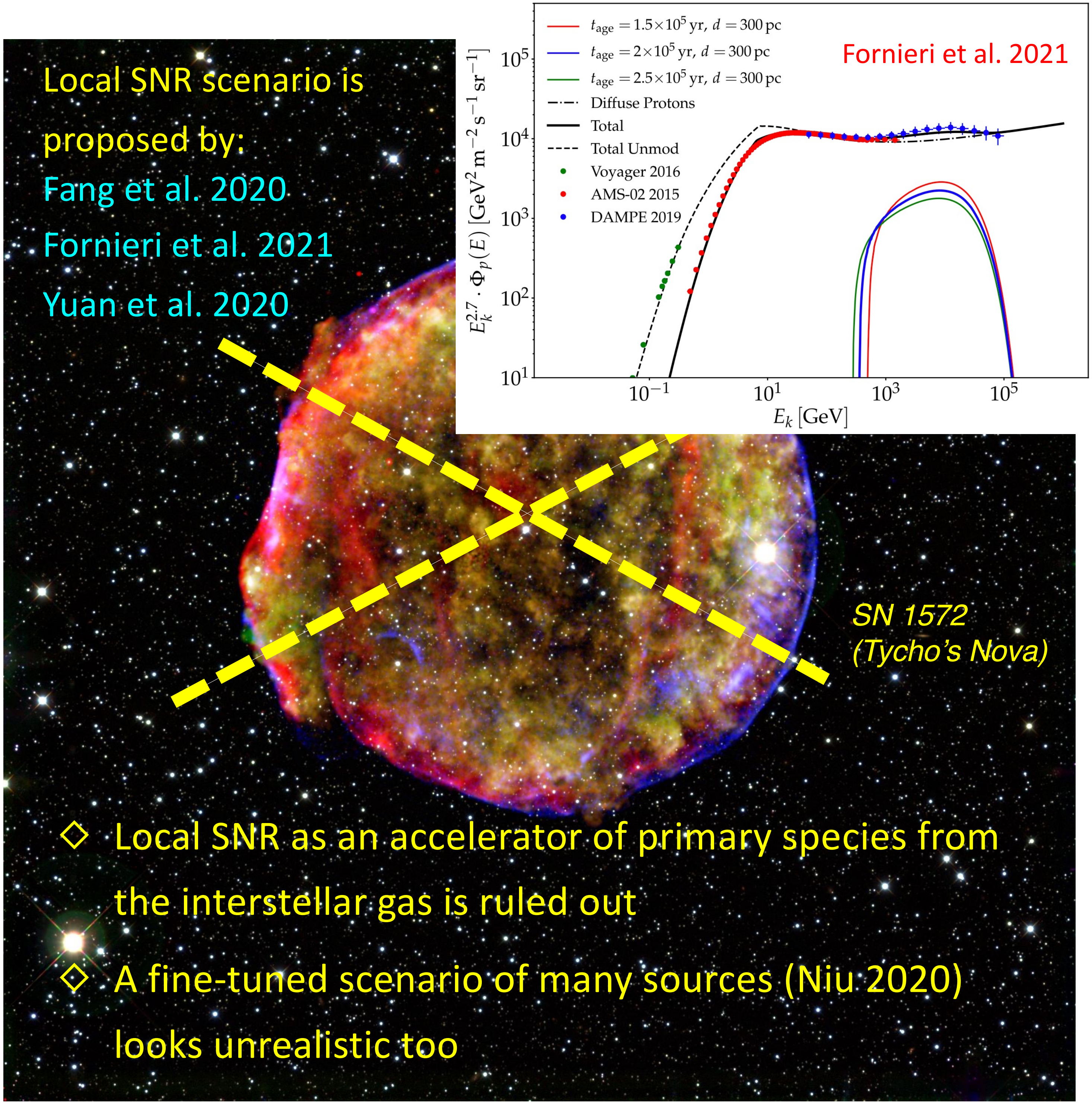

◇ Local SNR as an accelerator of primary species from the interstellar gas is ruled out

◇ A fine-tuned scenario of many sources (Niu 2020) looks unrealistic too

Local SNR scenario

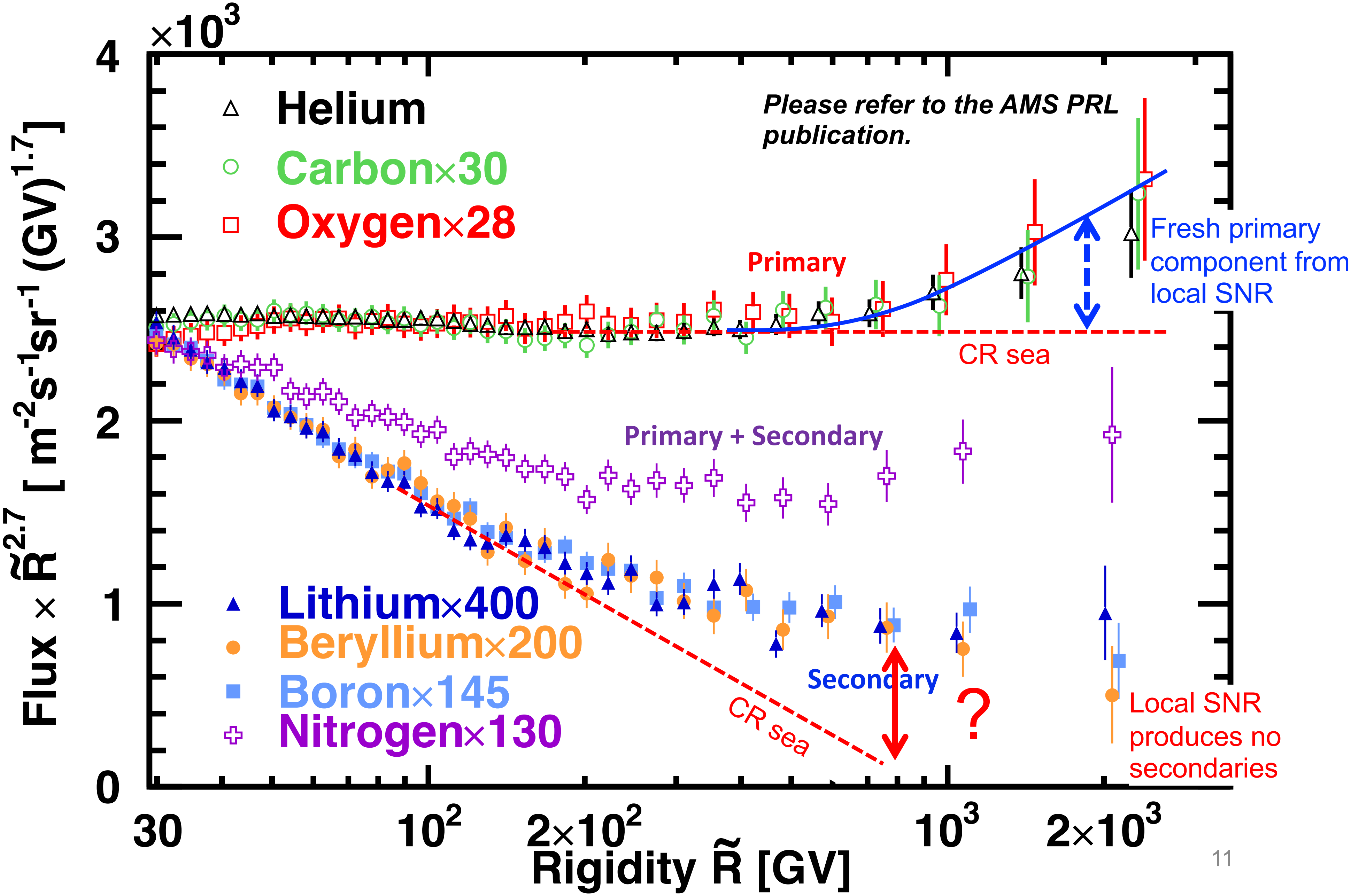

Galactic Loops

- ✧ WMAP *K*-band polarization intensity map
- ✧ Unsharp mask version of the Haslam et al. (1982) map
- ✧ The origin of the Loops is unknown
- ✧ If these are old SNRs, accelerated particles may still be present in the shell
- ✧ Signatures of the past (recent?) activity in the Solar neighborhood
- ✧ How strong does this past activity affect the current fluxes of CR species?

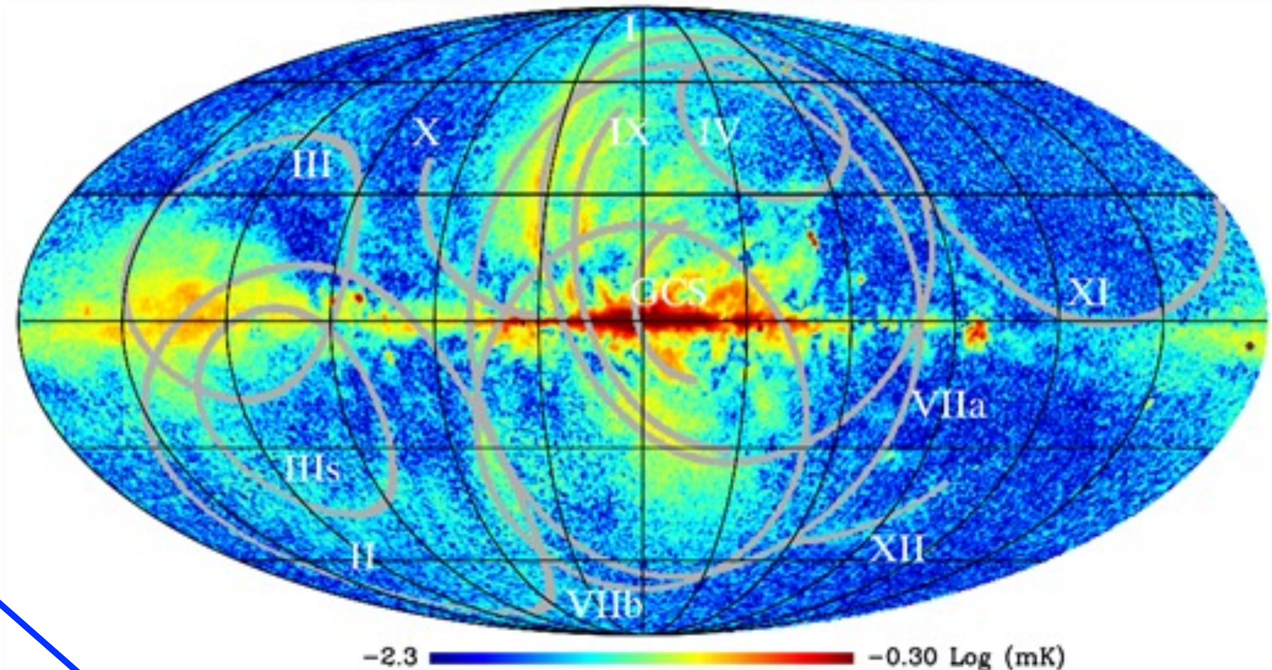

WMAP *K*-band polarization intensity map

Vidal+'2015

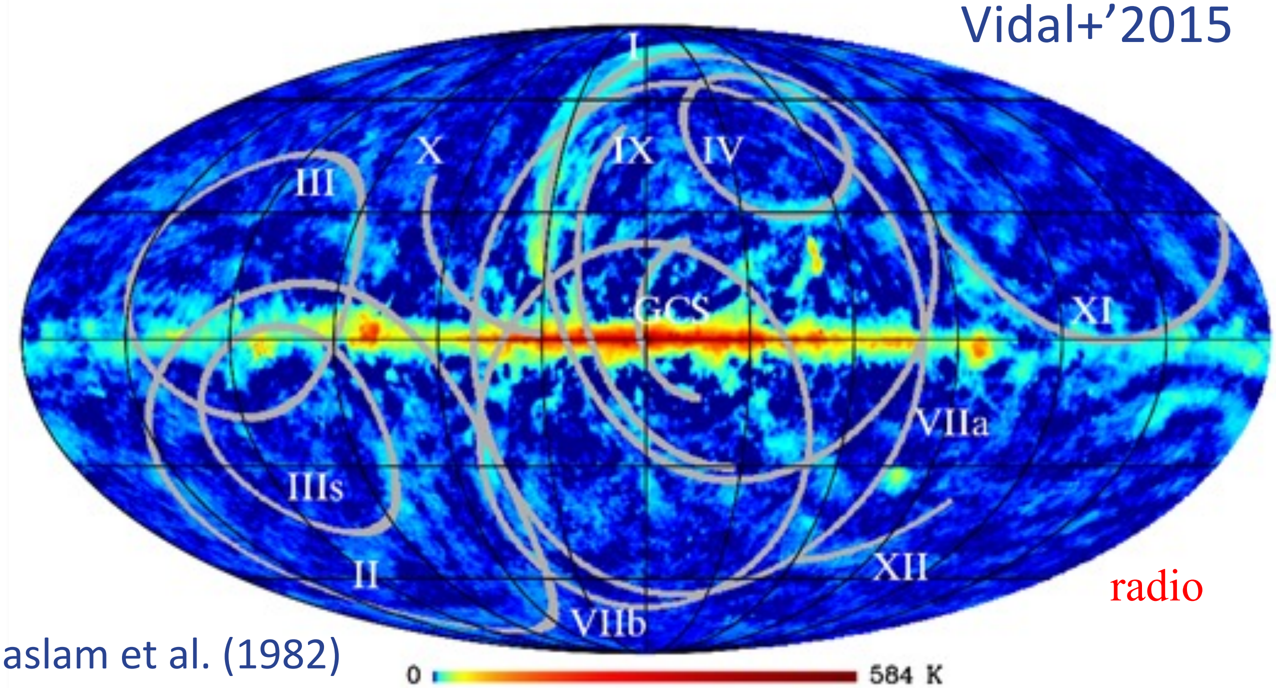

radio

Haslam et al. (1982)

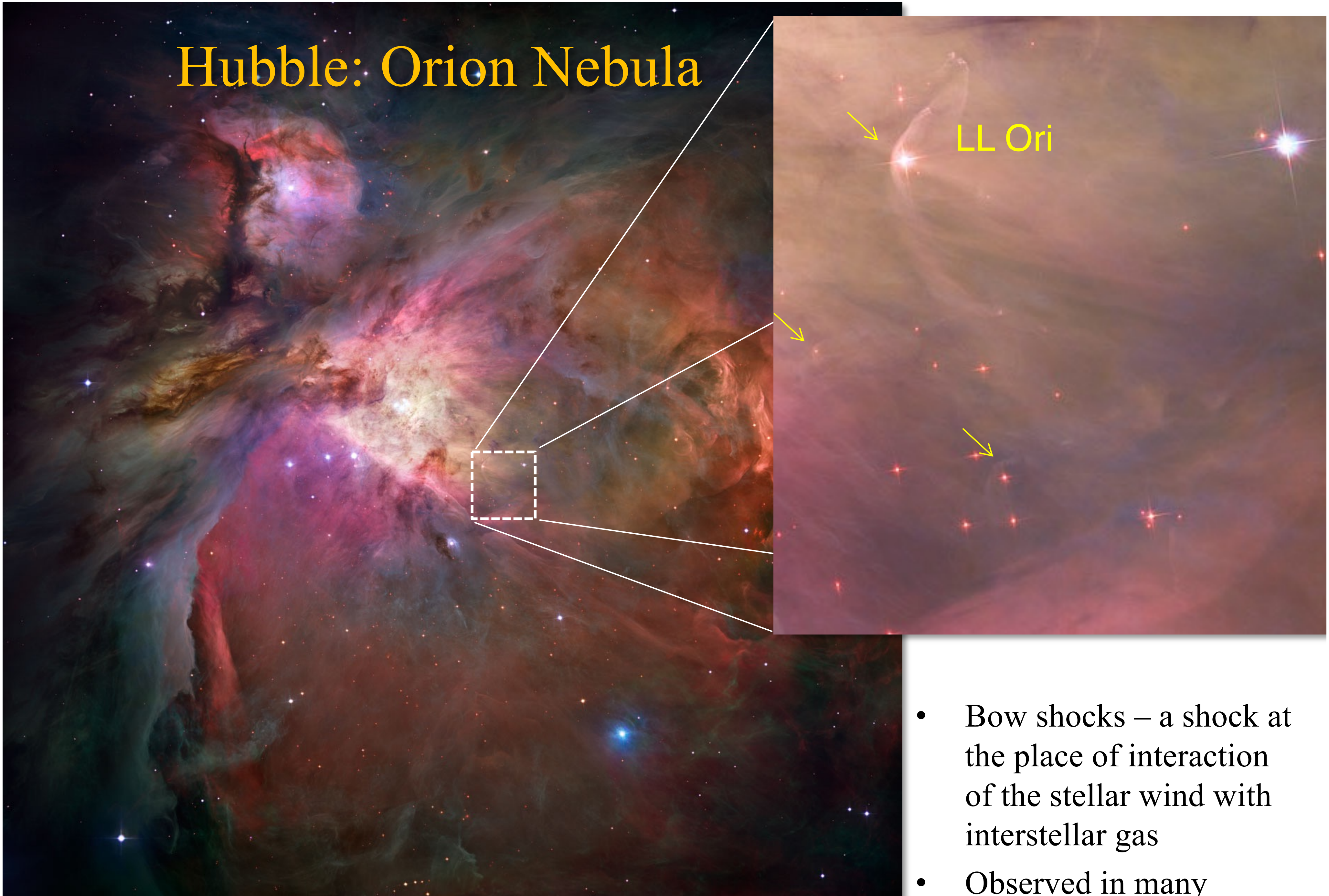

- Bow shocks – a shock at the place of interaction of the stellar wind with interstellar gas
- Observed in many systems

Bow shock of a passing star

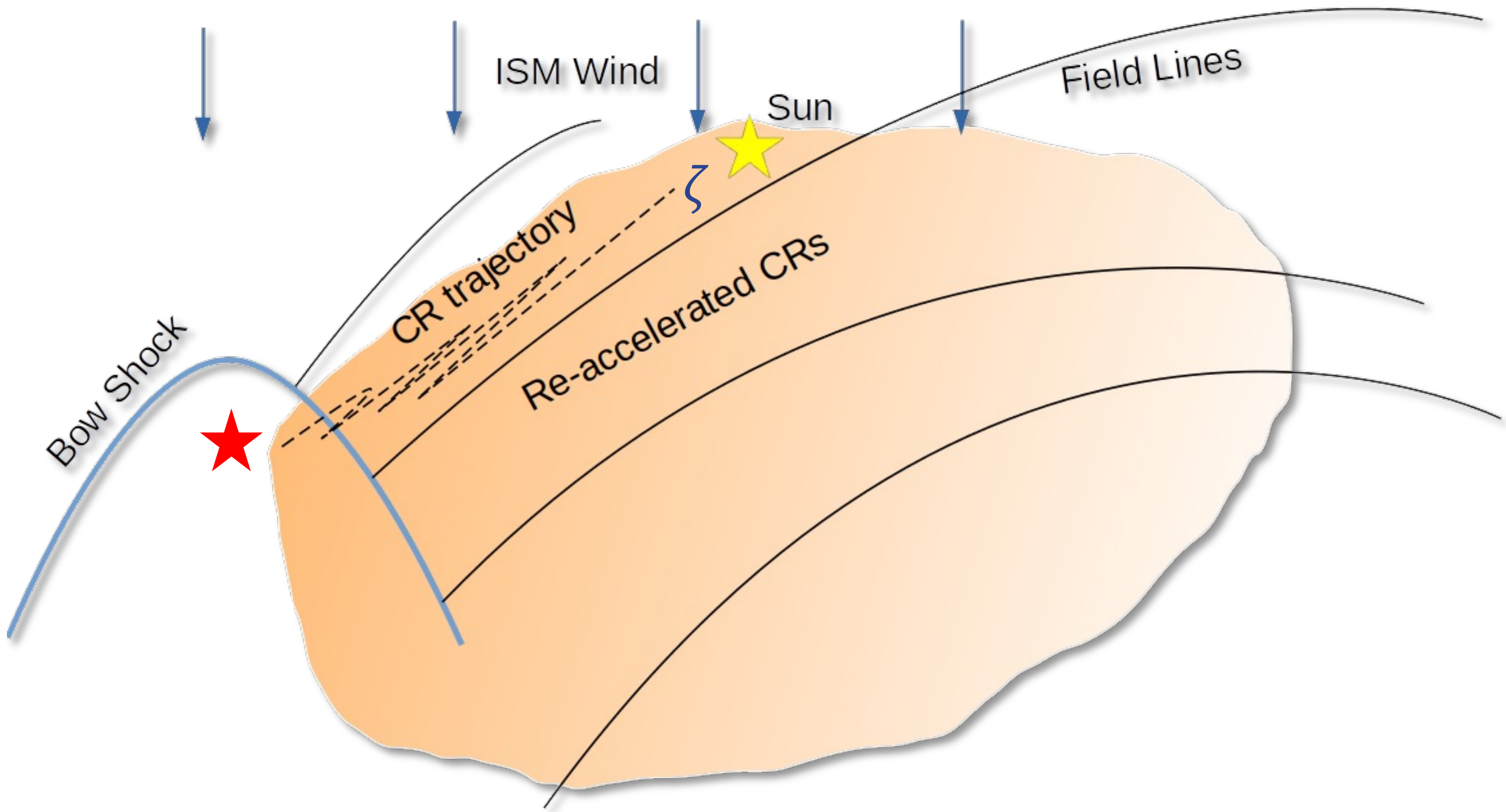

- CRs propagate along the magnetic flux tube while self-generating turbulence;
- Distance-size relationship ζ_{obs}(pc) ~ $10^2\sqrt{l_\perp\,(\mathrm{pc})}$, $l_\perp$ – size of the bow shock;
- Assuming $l_\perp = 10^{-3}$-10^{-2} pc, the path length along the B-field lines: ζ_{obs} = 3-10 pc.

Malkov & IVM'2021, 2022

Epsilon Eridani and passing stars

- ε Eri: K2 dwarf (5000K), 0.82 $M_\odot$, 0.74 $R_\odot$
- Distance – 3.2 pc
- Speed – 20 km/s (a bit small, but has a strong stellar wind)
- Well aligned with the direction of the local magnetic field – within 6.7°
- Huge astrosphere – 8000 au, 47’ as seen from Earth (larger than the Moon!)
- Mass loss rate – 30 $\dot{M}_\odot$

- ε Indi: triplet K4.5V (0.77 $M_\odot$) + T1.5 (0.072 $M_\odot$) + T6 (0.067 $M_\odot$)
- Distance – 3.6 pc
- Speed – 40.4 km/s (radial)

- Scholz’s Star: duplet M9.5 (0.095 $M_\odot$) + T5.5 (0.063 $M_\odot$)
- Distance – 6.8 pc
- Speed – 82.4 km/s (radial)

- Any local shock with a small Mach number

Bump formation

- ✧ Moderate reacceleration by ×1.5-2
- ✧ Low-energy particles do not reach the observer as they are convected downstream by the ISM flow
- ✧ High-energy particle loss from the flux tube

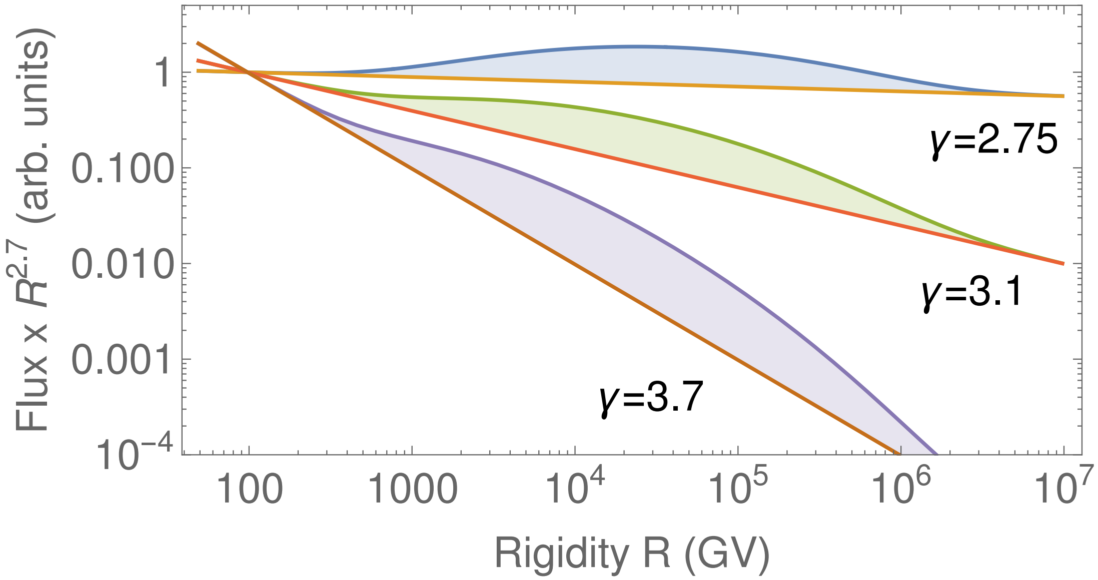

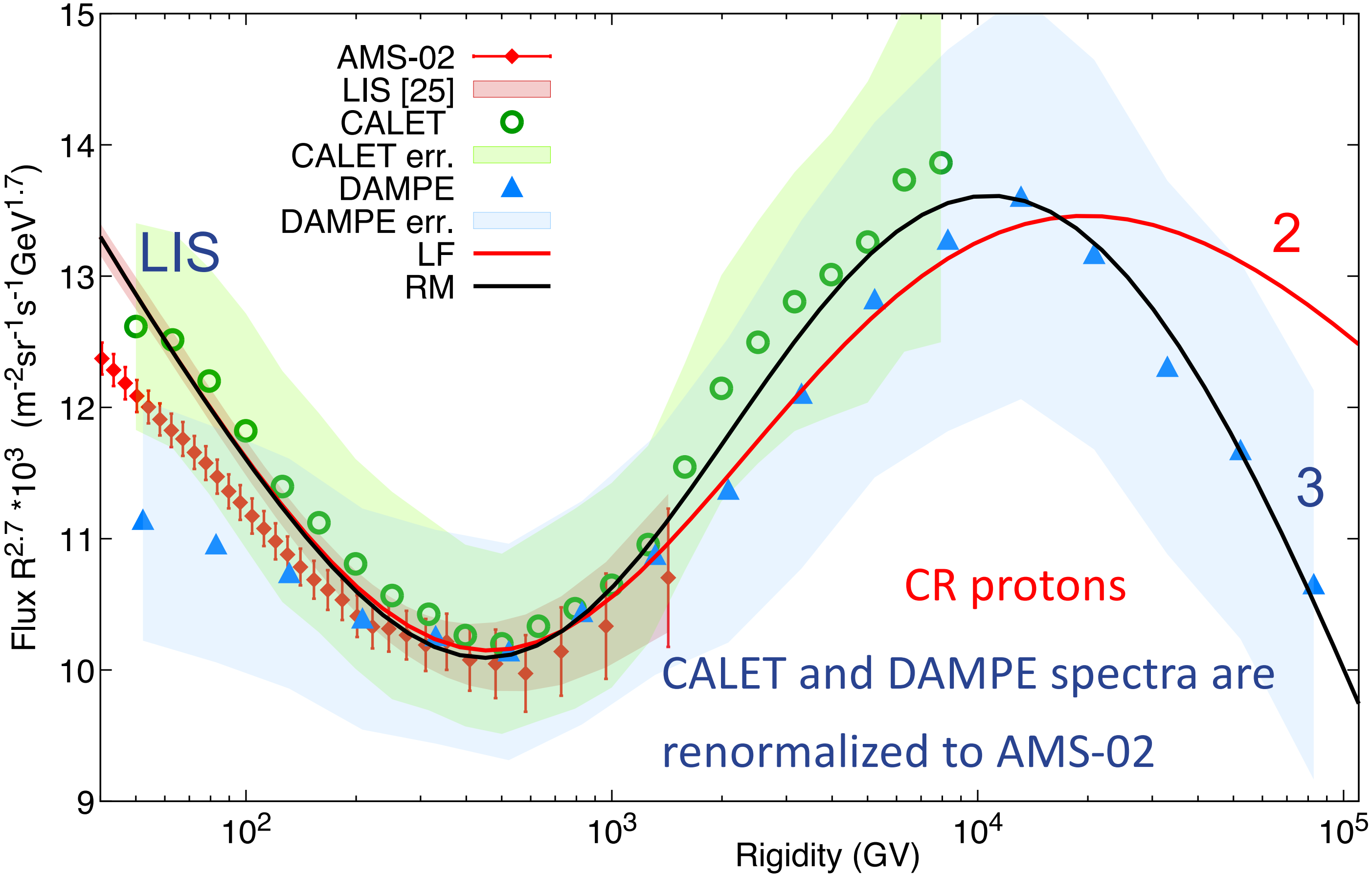

- ✧ Only 2 (3) free parameters – fixed from CR proton spectrum
- ✧ Use local interstellar spectrum (LIS) below the bump
- ✧ The steeper the spectrum of ambient particles – that larger the bump

Malkov & IVM’2021, 2022

Parameters

Table 1. Model parameters and fit results for the proton spectrum.

Parameter (St. err. %)	R_0(GV)	R_L(GV)	q	$K=(\gamma+2)/(q-\gamma)$	$\chi^2_{\min}$/dof	dof
Realistic Model (RM)	5878 (3.5%)	2.24×10^5 (28%)	4.2	3.59 (4.9%)	0.10	76-3
Loss-Free Model (LF)	4795 (3.2%)	∞	4.7	2.58 (2.9%)	0.19	76-2

$$f_s(R)=A_sR^{-\gamma_s}\left\{1+\frac{\gamma_s+2}{q-\gamma_s}\exp\left[-\sqrt{\frac{R_0}{R}}-\sqrt{\frac{R}{R_L}}\right]\right\}$$

Table 2. Input parameters for CR species derived from their LIS (Boschini et al. 2020b).

Parameters	protons	helium	boron	carbon
A_s (m^{-2} s^{-1} sr^{-1} GV^{-1})	2.32×10^4	3410	79	109
γ_s	2.85	2.76	3.1	2.76

- parameters fixed from CR proton spectrum

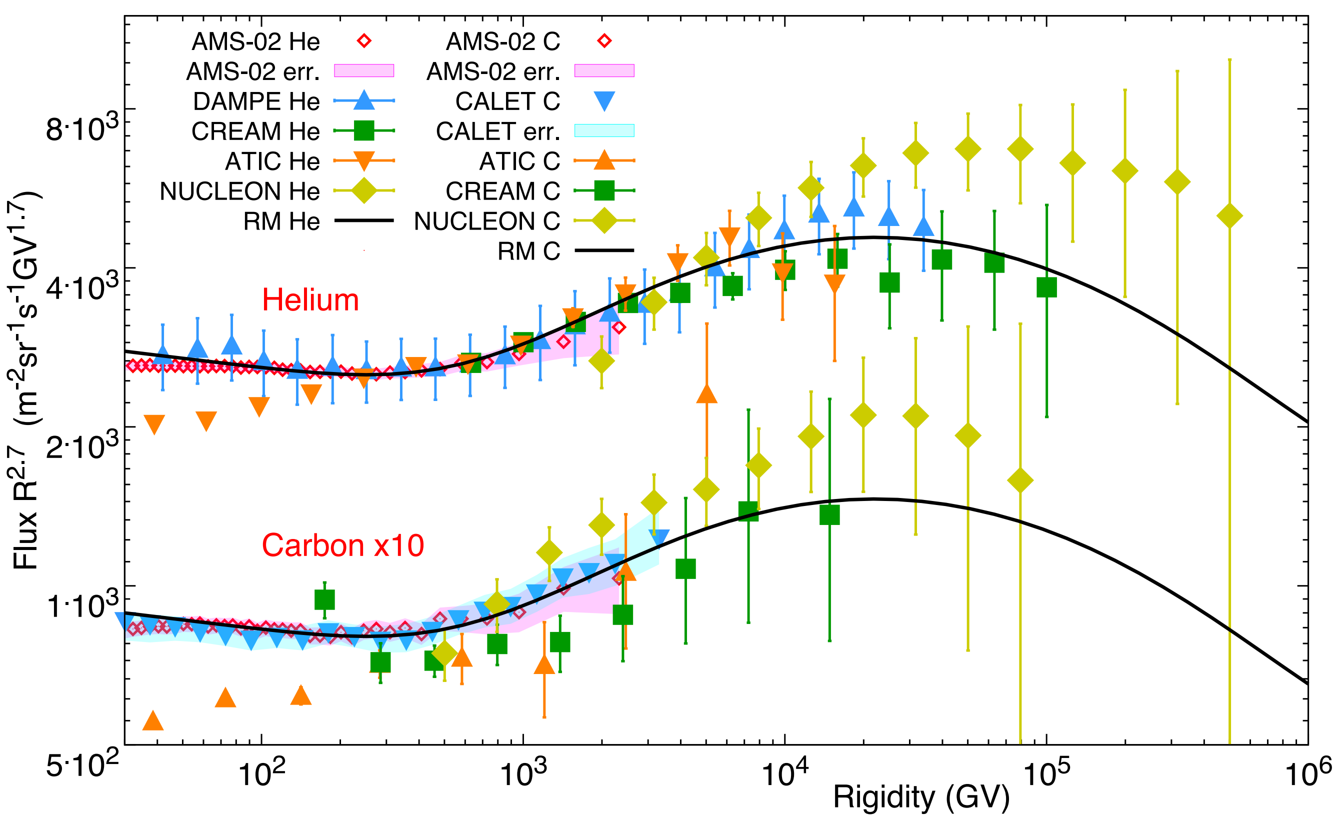

- A_s , γ_s – fixed normalization and spectral index of the LIS below the bump (individual for each species)
- LIS for H-Ni are given in Boschini+'2020
- Model reproduces spectra of ALL CR species with only 2 (3) parameters fixed from the proton spectrum

Malkov & IVM'2021, 2022

Example: B/C ratio

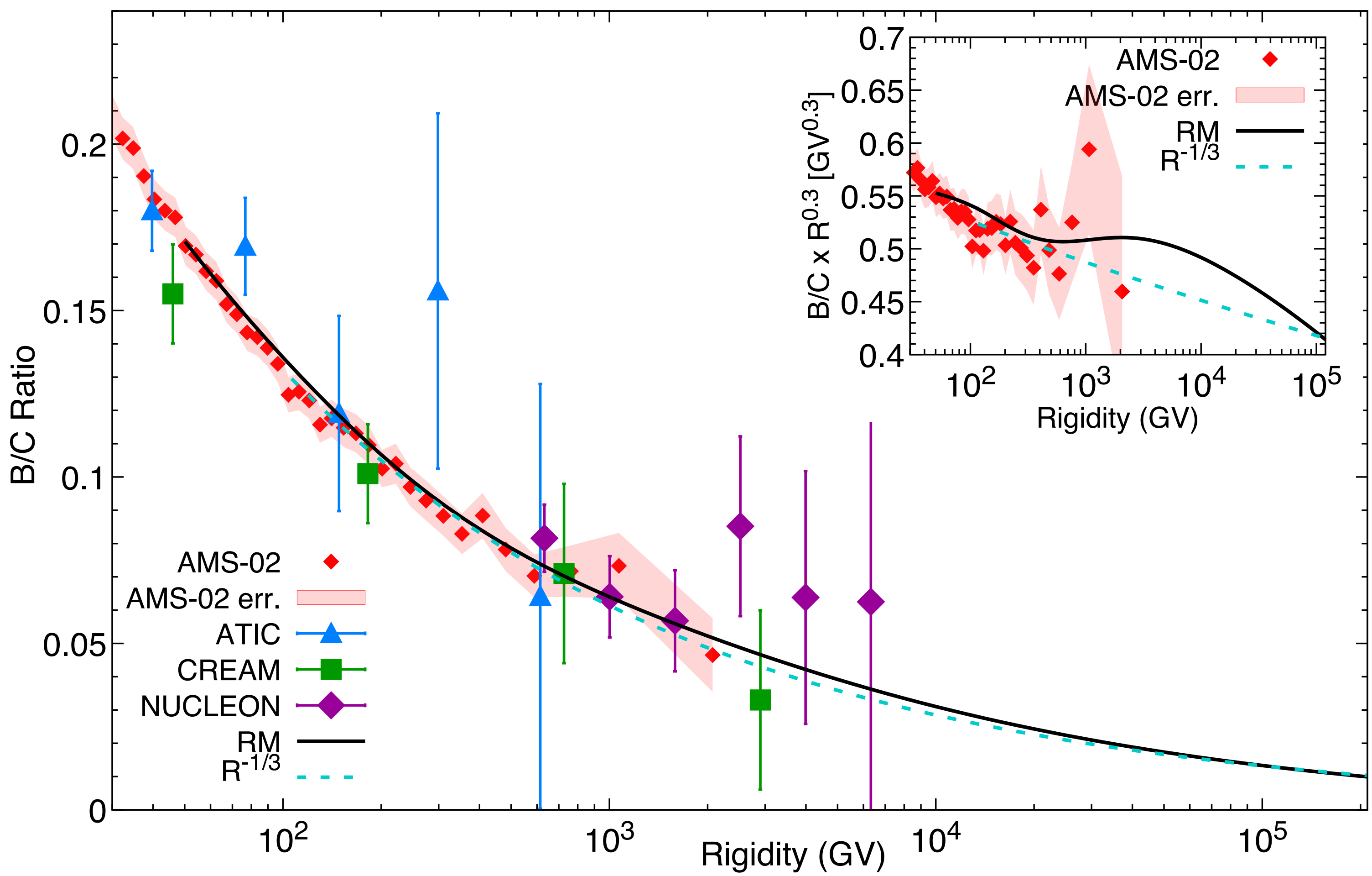

B/C is better measured than the spectrum of Boron

Malkov & IVM'2021, 2022

Low-energy cosmic rays: excesses

Precise spectra of CR species by AMS-02 reveal excesses when compared to ACE-CRIS and Voyager 1 measurements

Boschini+’2019, 2020, 2021, 2022

So far excesses were found in the spectra of

✧ Lithium (secondary)

✧ Fluorine (secondary)

✧ Aluminum (50-50 sec.-prim.)

✧ Iron (primary)

B/C tuned to the data

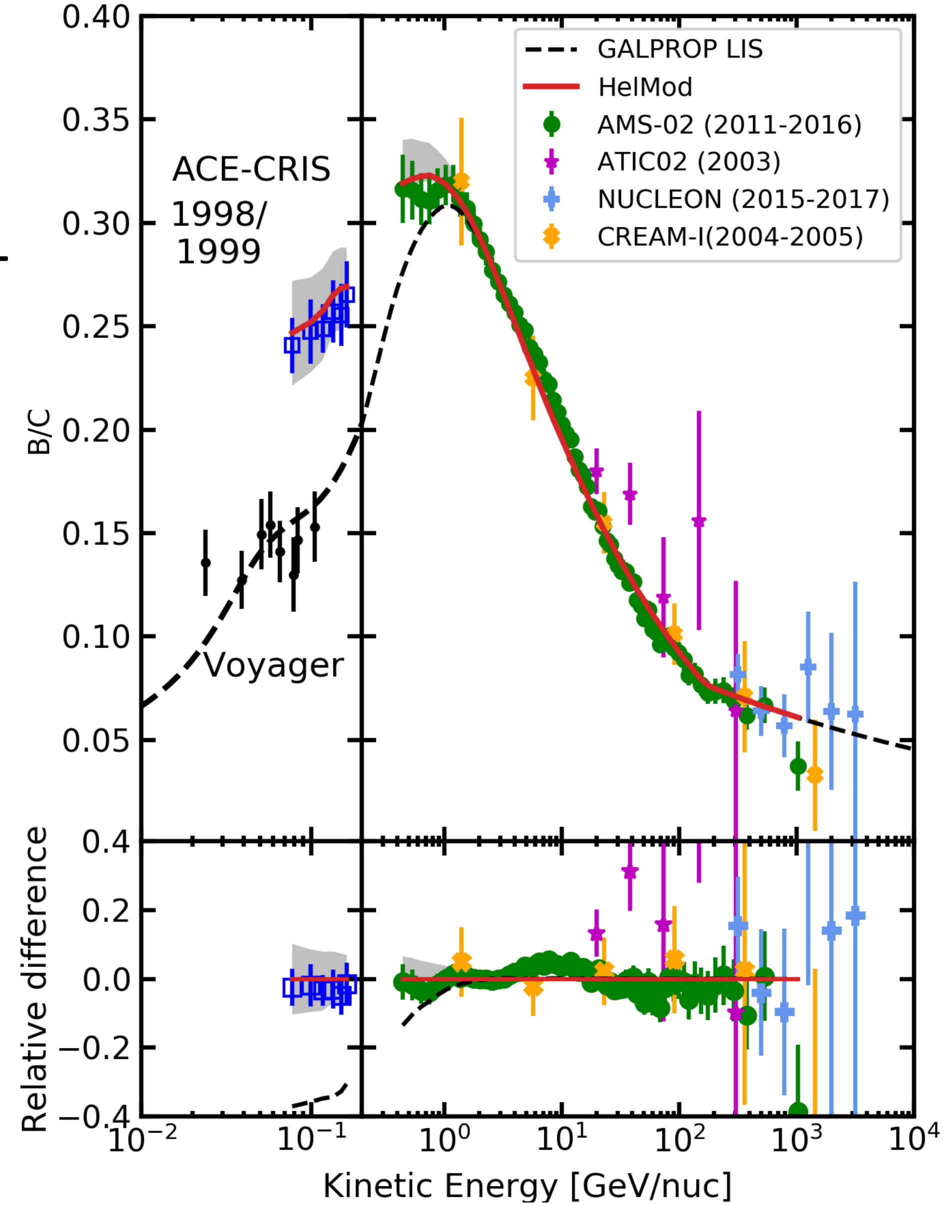

Primary Lithium

- Classical novae are the new type of sources of ^{7}Li
- Observation of blue-shifted absorption lines of partly ionized ^{7}Be (half-life 53.22 days) in the spectrum of a classical nova V339 Del ~40–50 days after the explosion (Tajitsu et al. 2015) is the first observational evidence that the mechanism proposed by Arnould & Norgaard (1975) and Starrfield et al. (1978) is working.
- Observations of other novae, V1369 Cen, V5668 Sgr, V2944 Oph, ASASSN-16kt [V407 Lupi], V838 Her, also reveal the presence of ^{7}Be lines in their spectra.
- The total mass of produced ^{7}Li per novae is estimated as $10^{-9}M_{\odot}$–$6\times10^{-9}M_{\odot}$.

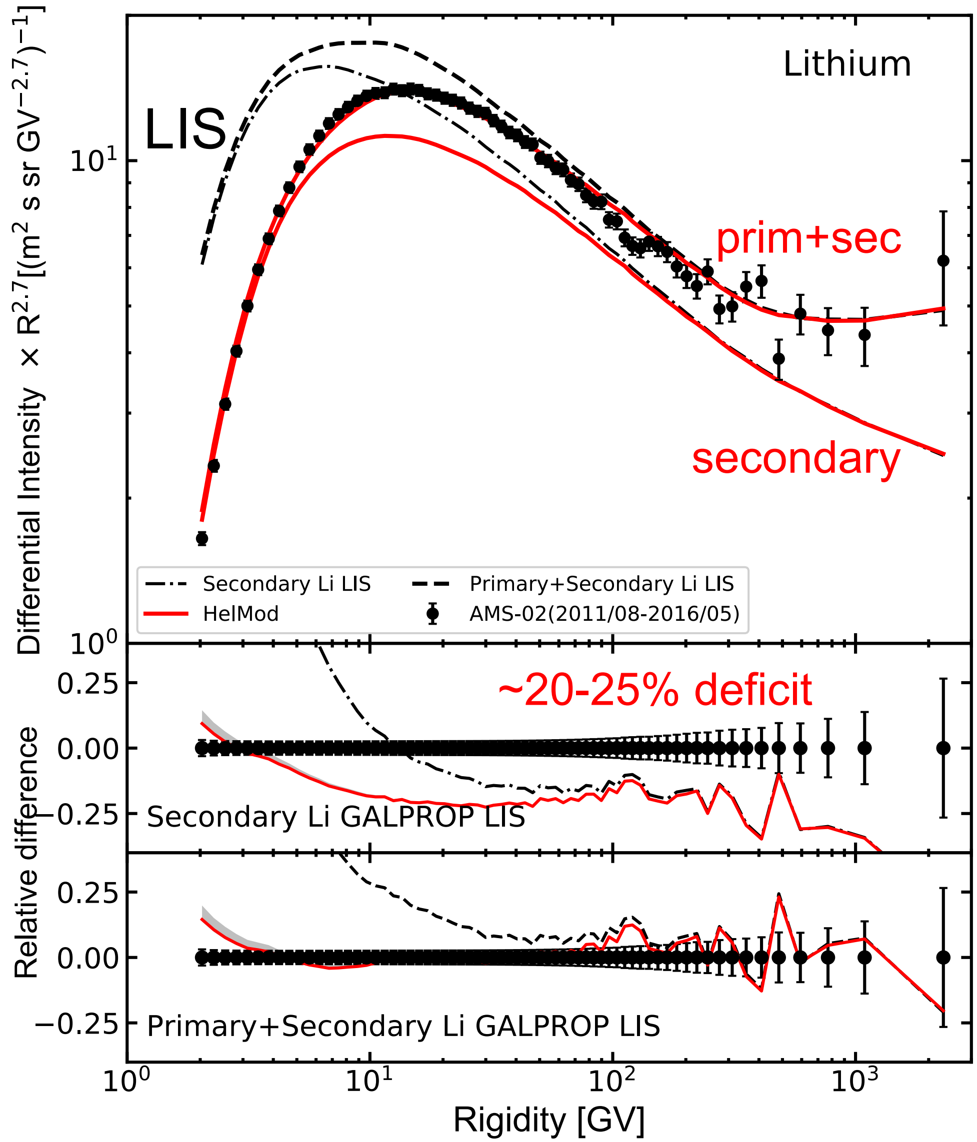

Fluorine excess

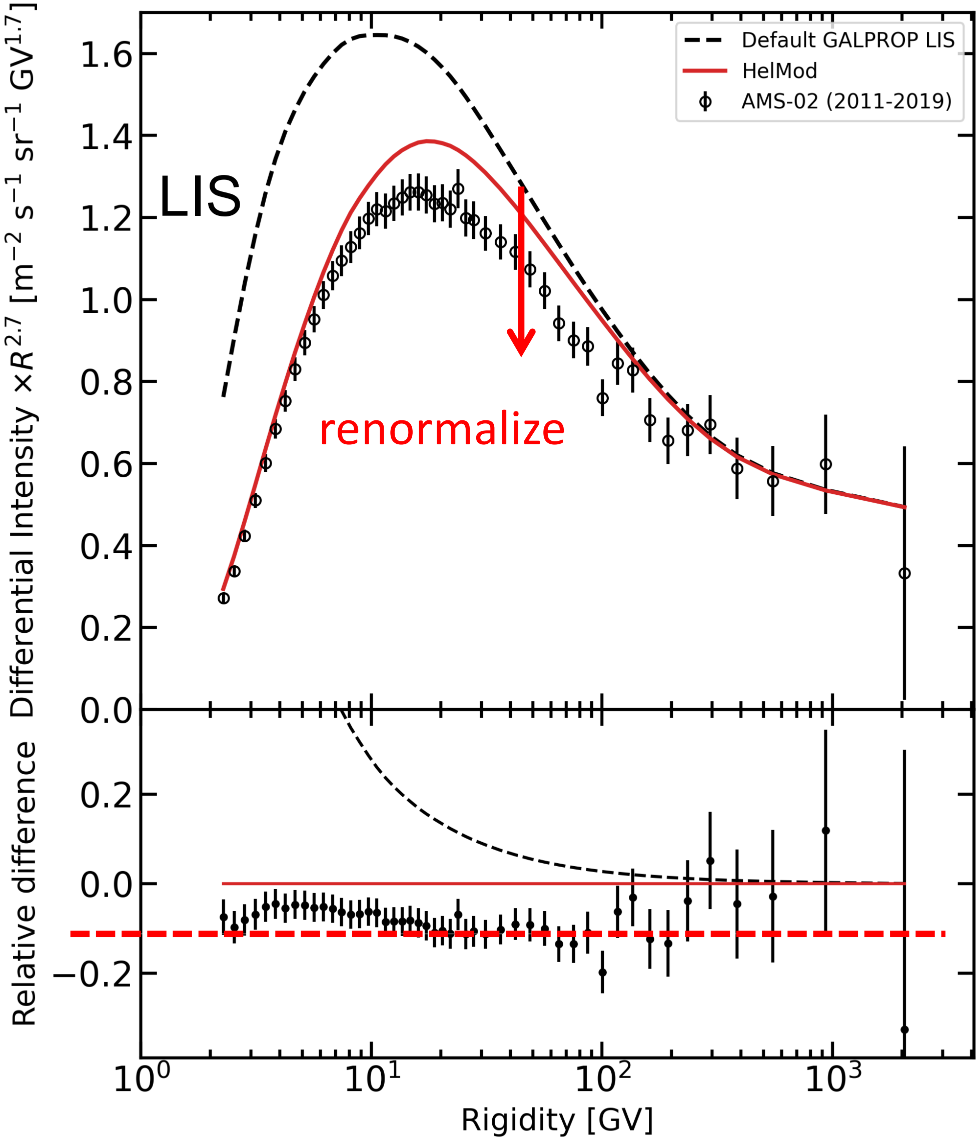

Deficit of secondary F, most likely a production cross section issue.

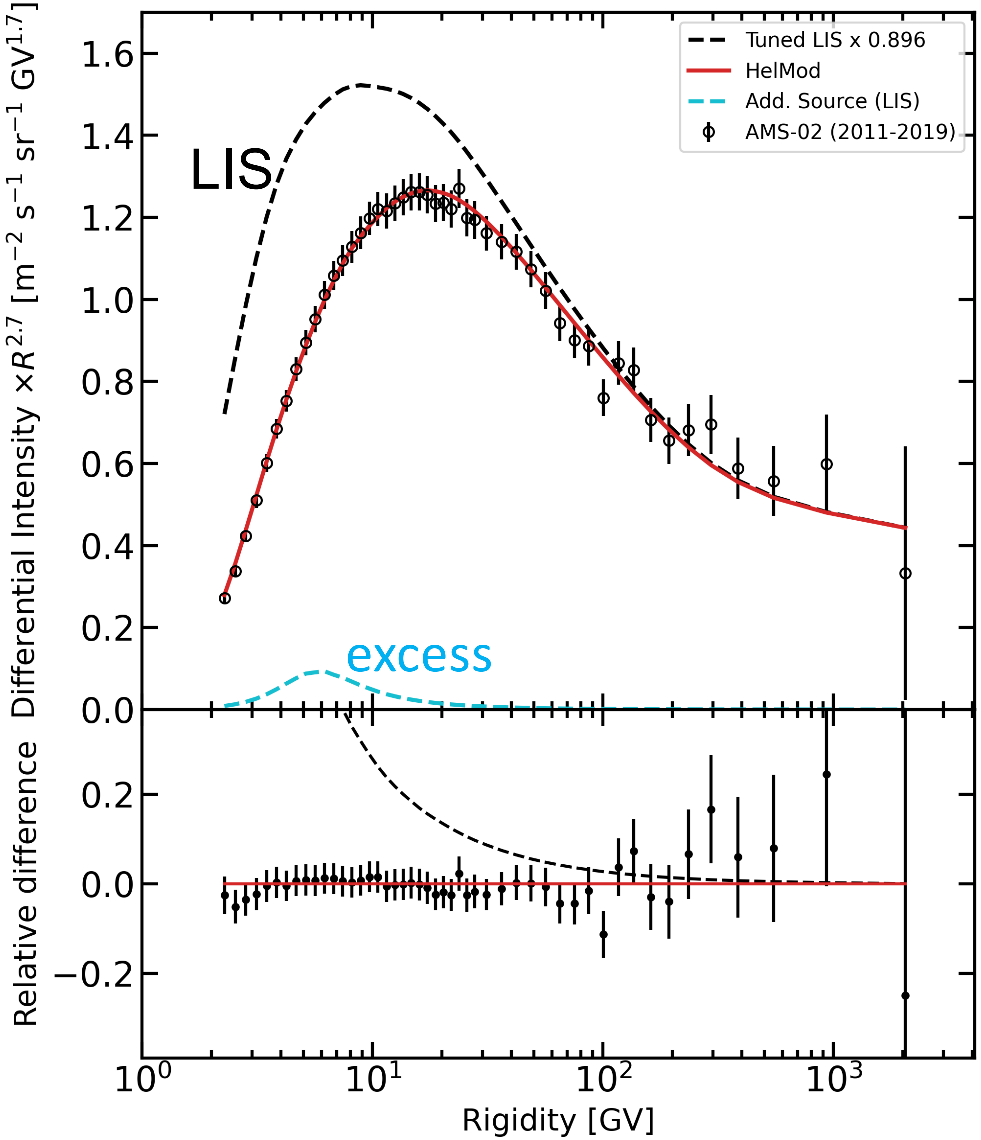

After renormalization, we see a low-energy excess.

Fluorine excess – II

- The ISM abundance of fluorine is anomalously low because it is easily destroyed in stars through either p- or α-captures
- The origin of cosmic fluorine is still not well constrained
- The main astrophysical sources of fluorine are thought to be supernovae Type II (SN II), Wolf–Rayet (WR) stars, and the asymptotic giant branch (AGB) of intermediate-mass stars

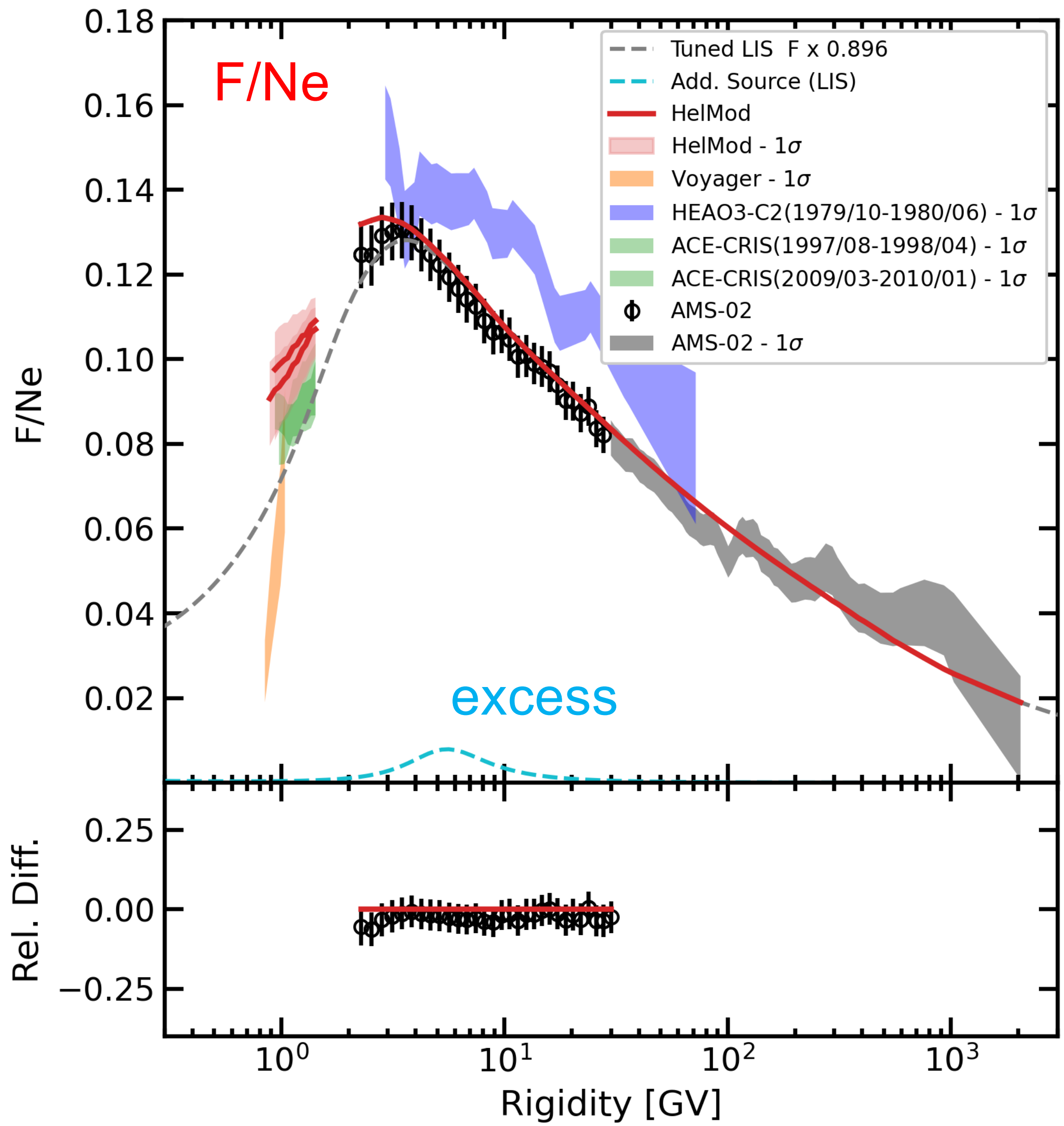

Iron excess

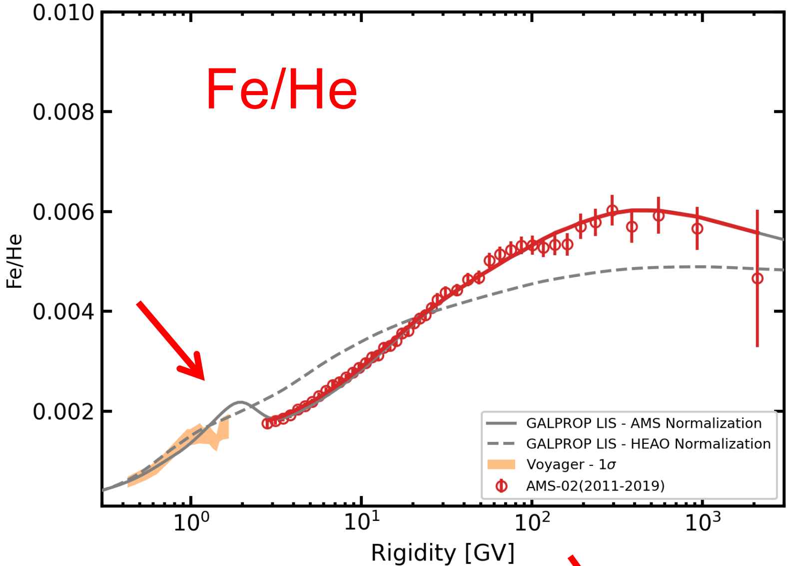

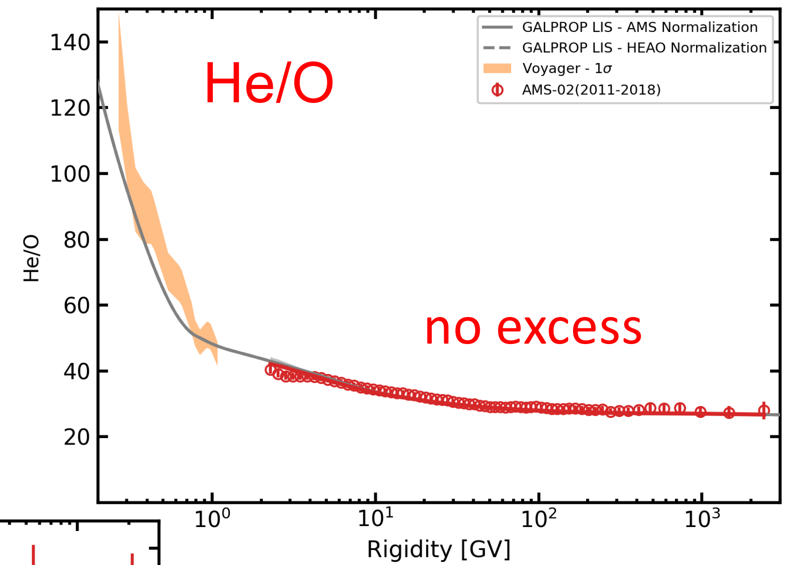

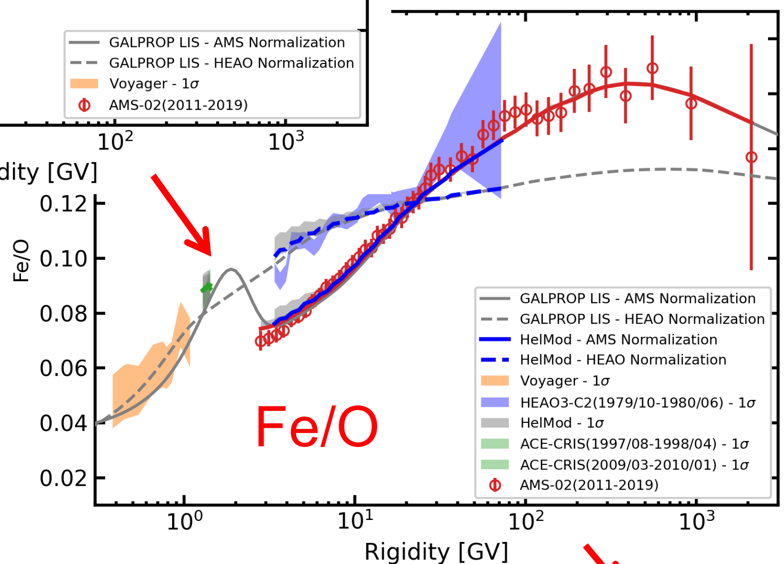

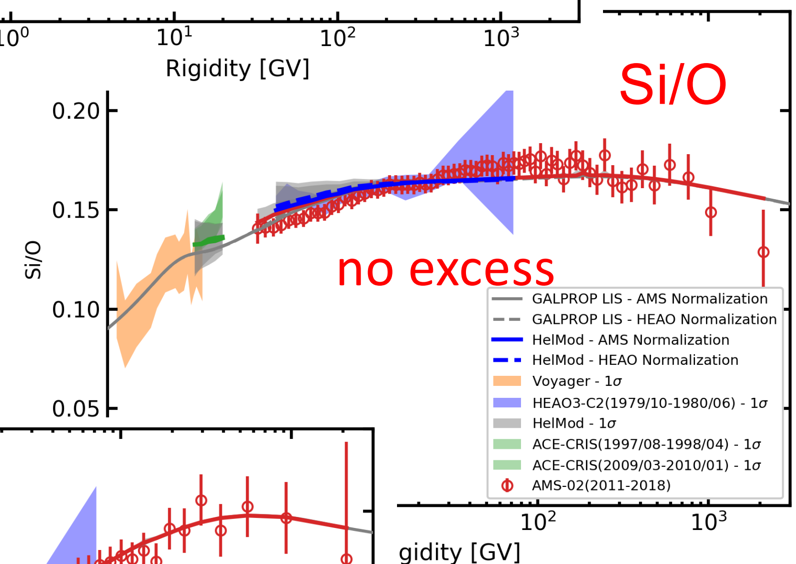

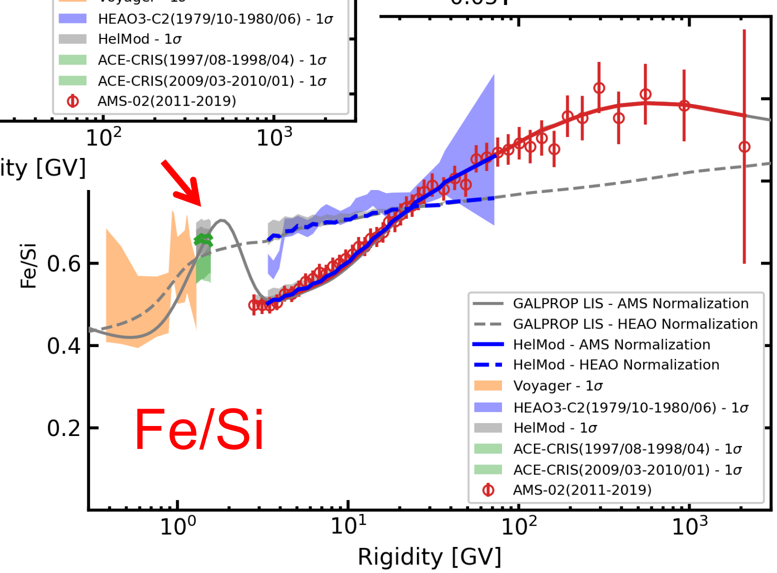

Most visible in Fe/He, Fe/O, Fe/Si ratios (arrows), while any such features are absent in He/O and Si/O ratios

Iron excess – II

- The excess in iron – follows from consistency between Voyager 1, ACE-CRIS, and AMS-02 data
- The likely source of the excess CR iron are the old SN remnants – falls in line with other evidences
- Excess of radioactive ^{60}Fe (half-life 2.6 Myr) in deep ocean sediments (Knie+’1999, 2004; Ludwig+’2016; Wallner+’2016)
- Lunar regolith samples (Cook+’2009; Fimiani+’2012, 2014)
- Antarctic snow (Koll+’2019).
- ACE-CRIS observations of ^{60}Fe (Binns+’2016)

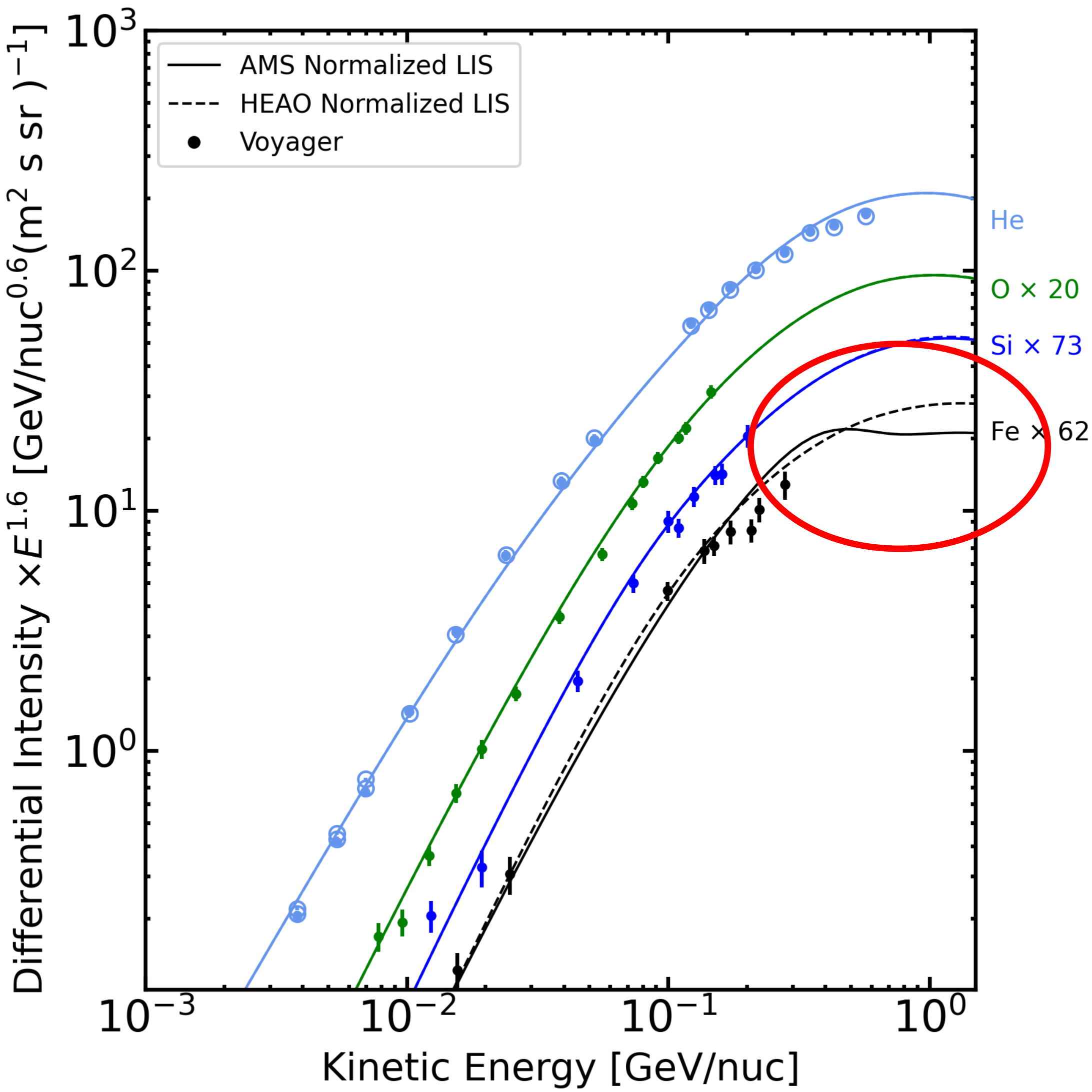

Aluminum excess

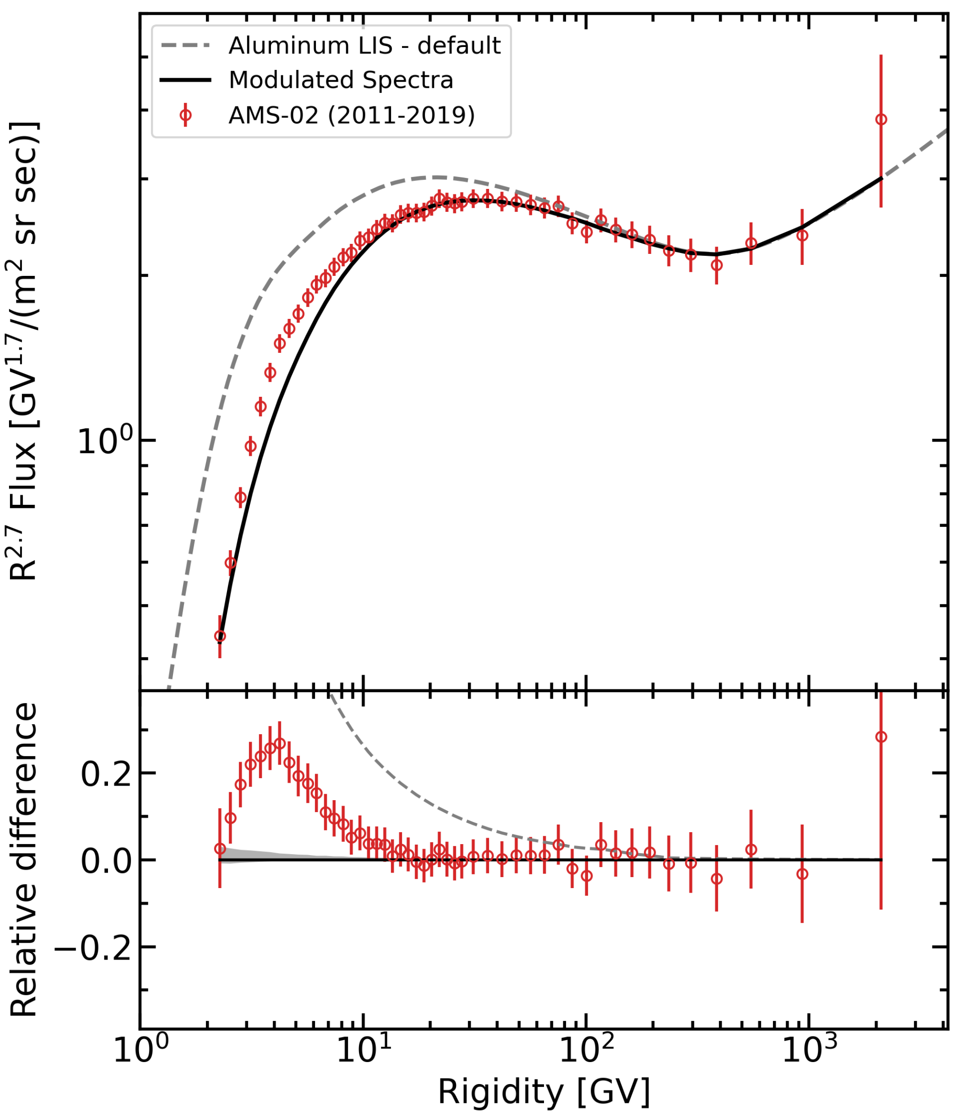

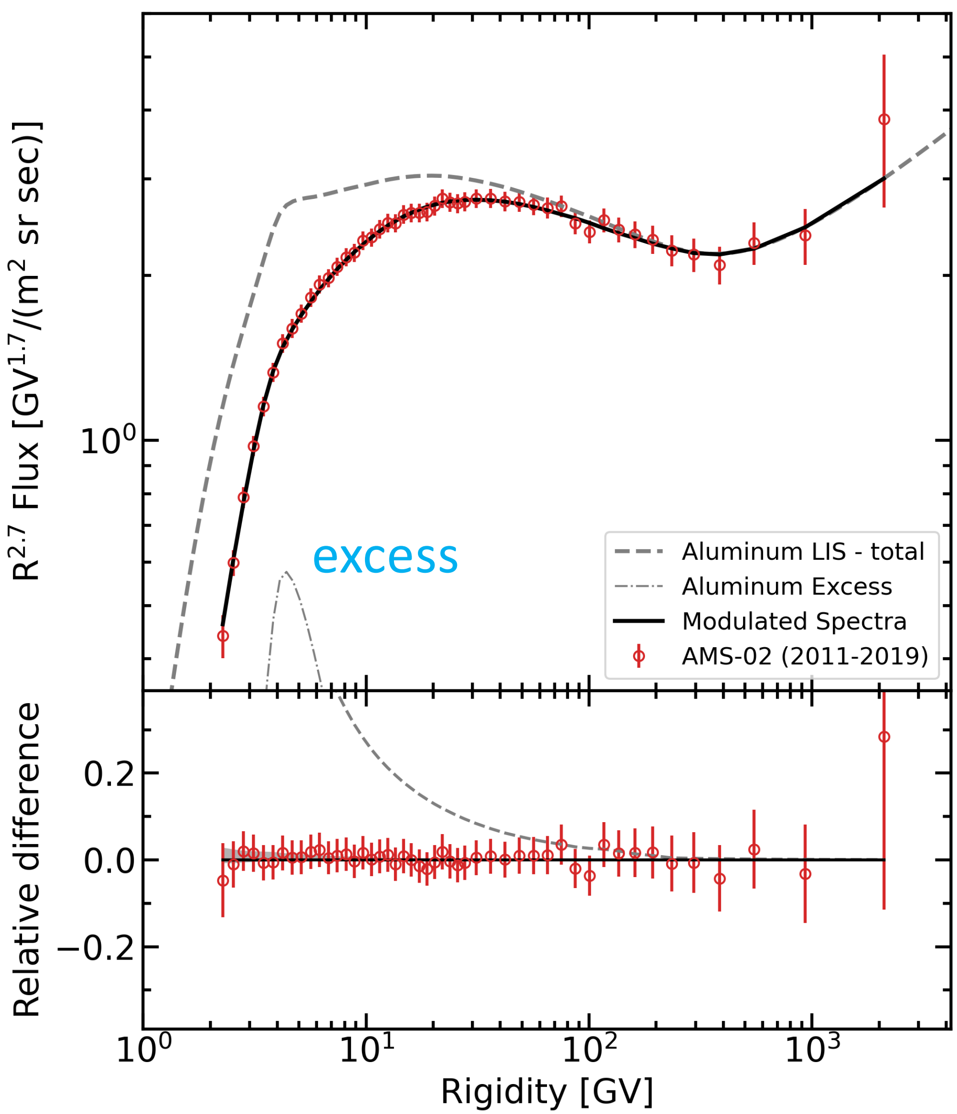

Aluminum excess – II

- Apparently, the sources of cosmic Al are numerous, and are simultaneously also the sources of other rare isotopes, such as ^{7}Li, ^{19}F, ^{60}Fe.
- Particularly interesting is a possible contribution of the massive WR stars proposed to explain the observed anomalous $^{22}Ne/^{20}Ne$ ratio and other observed ratios, $^{12}C/^{16}O$, and $^{58}Fe/^{56}Fe$, in CRs (Binns et al. 2008).
- Iron excess is likely the result of consequent SN explosions (in OB association)

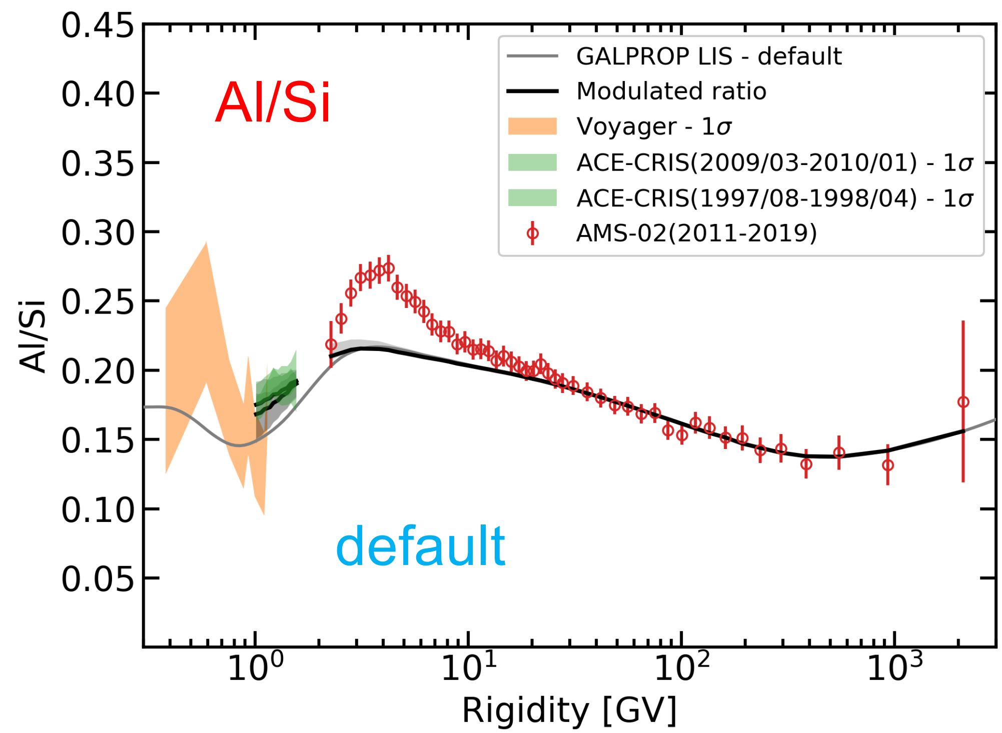

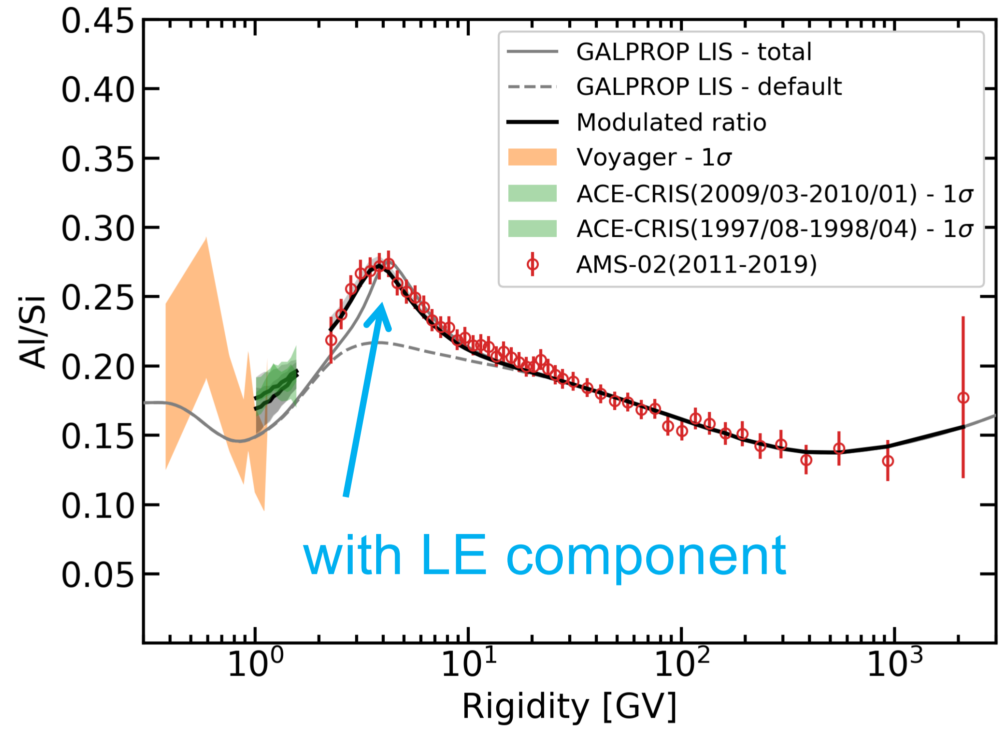

Local Bubble and OB associations

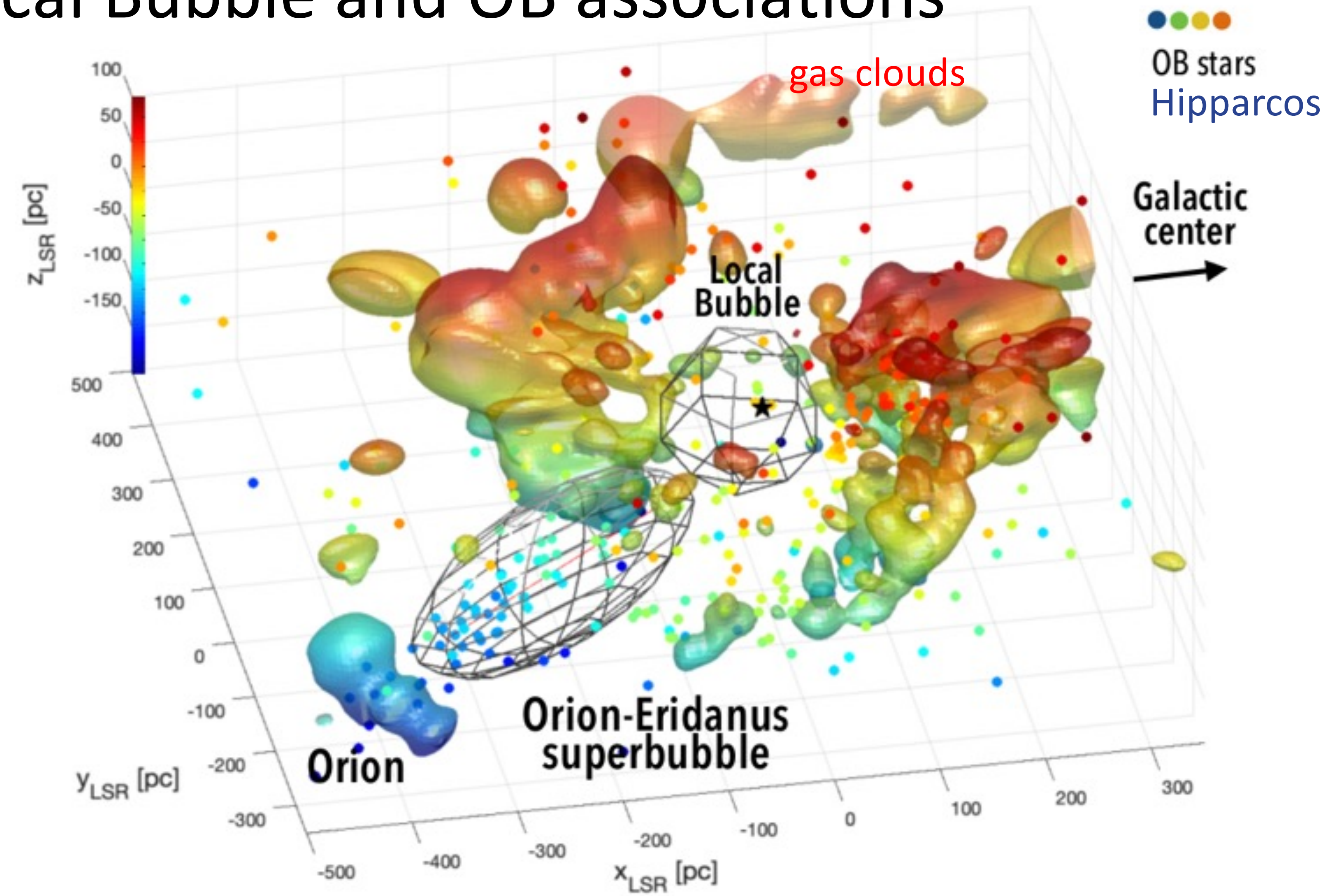

Perhaps we are at the very beginning of the journey to explore the place we live in and look through in our desire to understand the universe


June 11, 2008
12:05 pm (EDT)
14 years in orbit in 2022
Sky survey every 3 hours
41 000 sky surveys!

Fermi Highlights and Discoveries (GeV range)

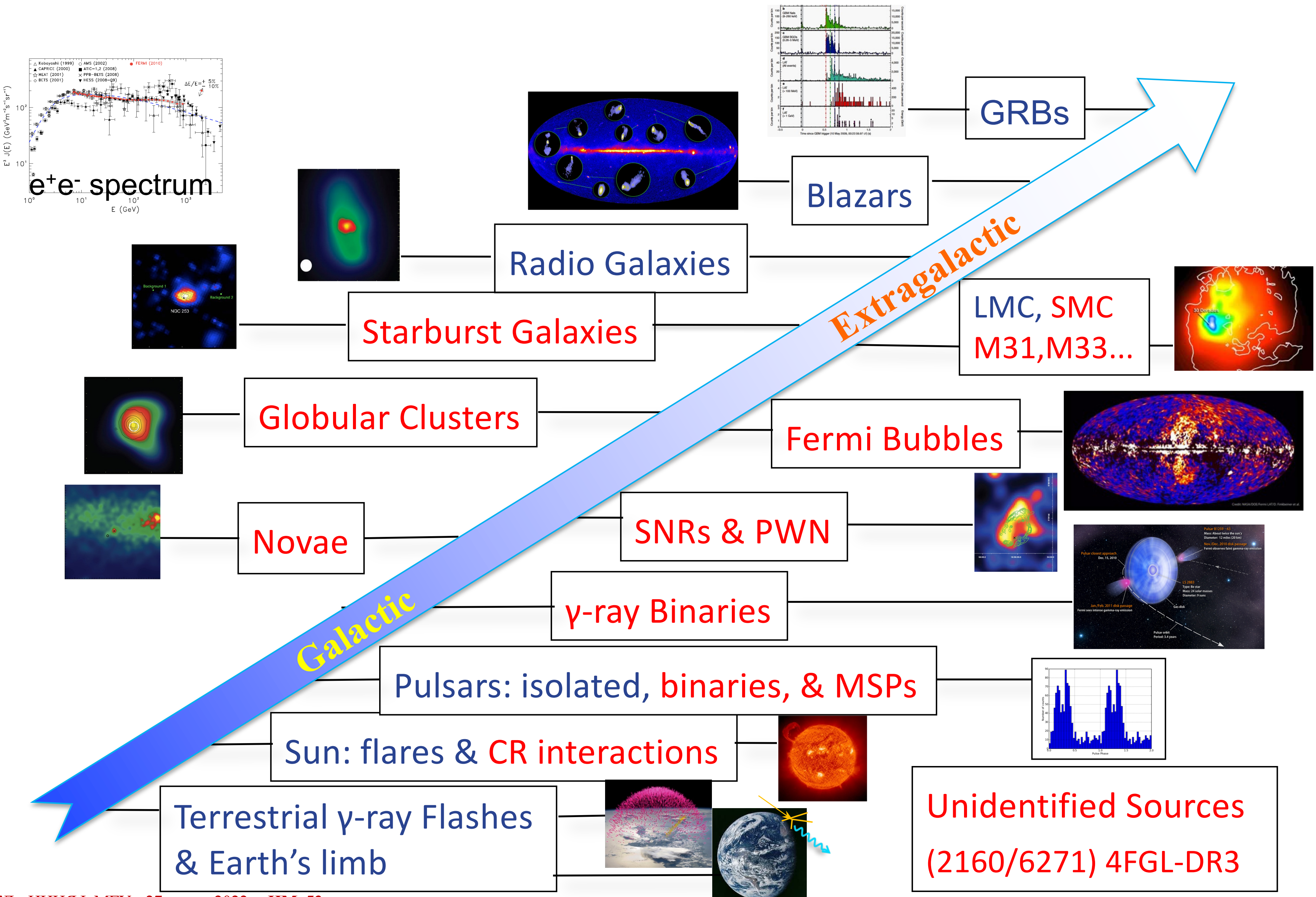

LAT Catalogs	Type	Energy range	No. of SRS
4FGL-DR3	General	50 MeV-1 TeV	6271 (2160 unid)
4LAC-DR2	AGN	50 MeV-1 TeV	3148
FLSF	Solar Flares	30 MeV-10 GeV	45
FAVA	Flaring Sources	0.1-300 GeV	4547
1FLE	Low Energy	30-100 MeV	198
2FHL	Hard Sources	>50 GeV	360
3FHL	High Energy	>10 GeV	1556
PC	Pulsars		234
FLGC	High Energy GRB		180
SNR	SN Remnants	1-100 GeV	30+14 margin+245 UL
FGES	Galactic Extended	10 GeV-2 TeV	46
FHES	High-Lat Extended		21
1FLT	Long-Term Transients	0.1-300 GeV	142
GBM Catalogs			
GRB	GRB spectra		2297
Mag	Magnetars		440
TGF	Terrestrial γ-ray Flashes		4144

Bl

4th Fermi-LAT Catalog

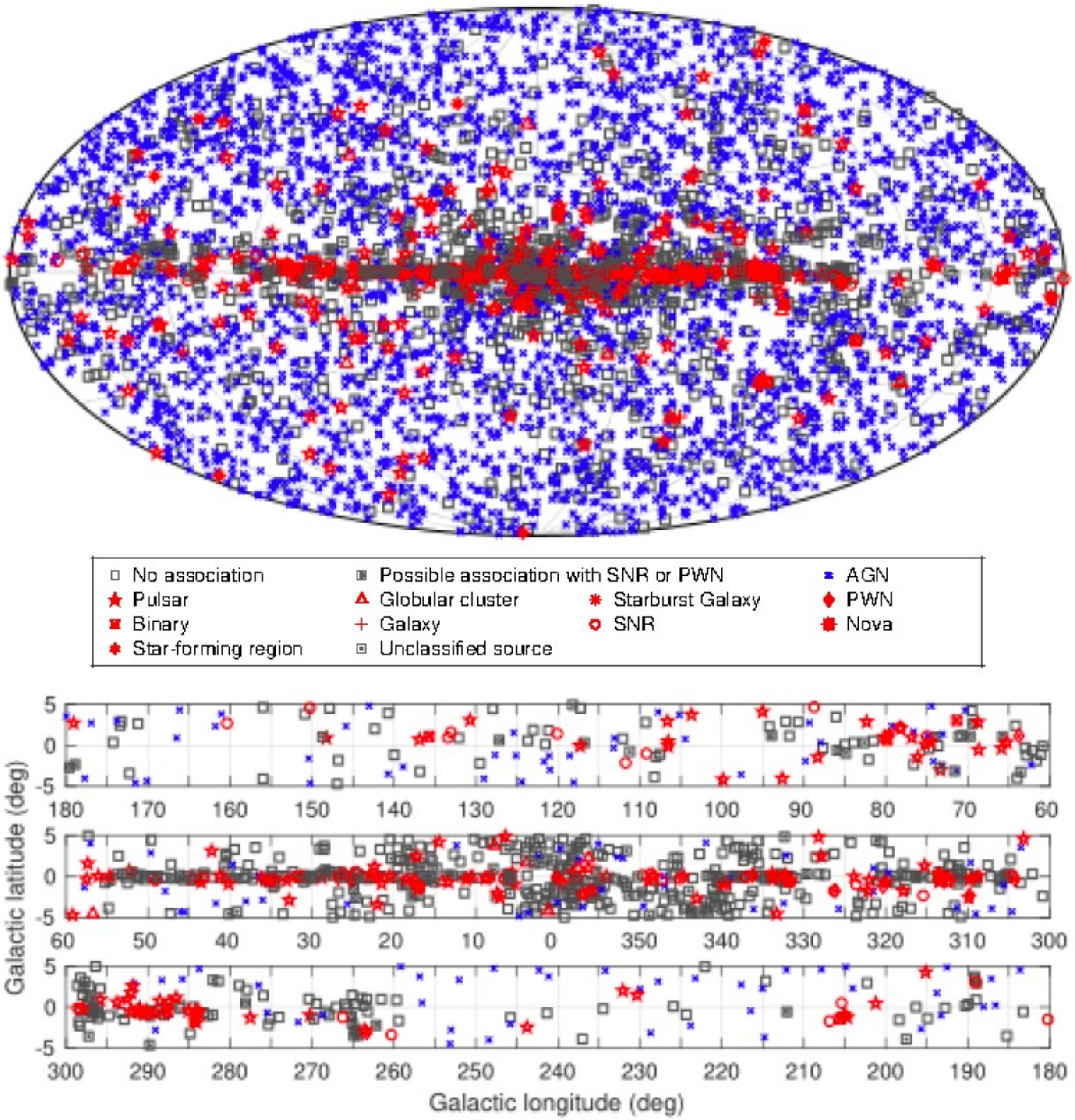

- 8 years of observations
- 50 MeV – 1 TeV
- 5065 sources above 4σ
- 75 extended sources
- 354 identified
- >3130 identified or associated sources are active galaxies (blazars)
- SMC, LMC, and M 31
- 7 Starburst galaxies
- 239 – pulsars
- Other Galactic sources:
  - 40 SNRs
  - 17 PWNe
  - 30 Globular clusters
  - 6 High-mass binaries
  - 3 Star-Forming Regions
  - 2 Low-mass Binaries
  - η Carinae (binary)
  - 1 Nova V5668 Sagittarii, other novae not included
- 1337 sources do not have any counterparts at other wavelength

Angular resolution: good, better, best!

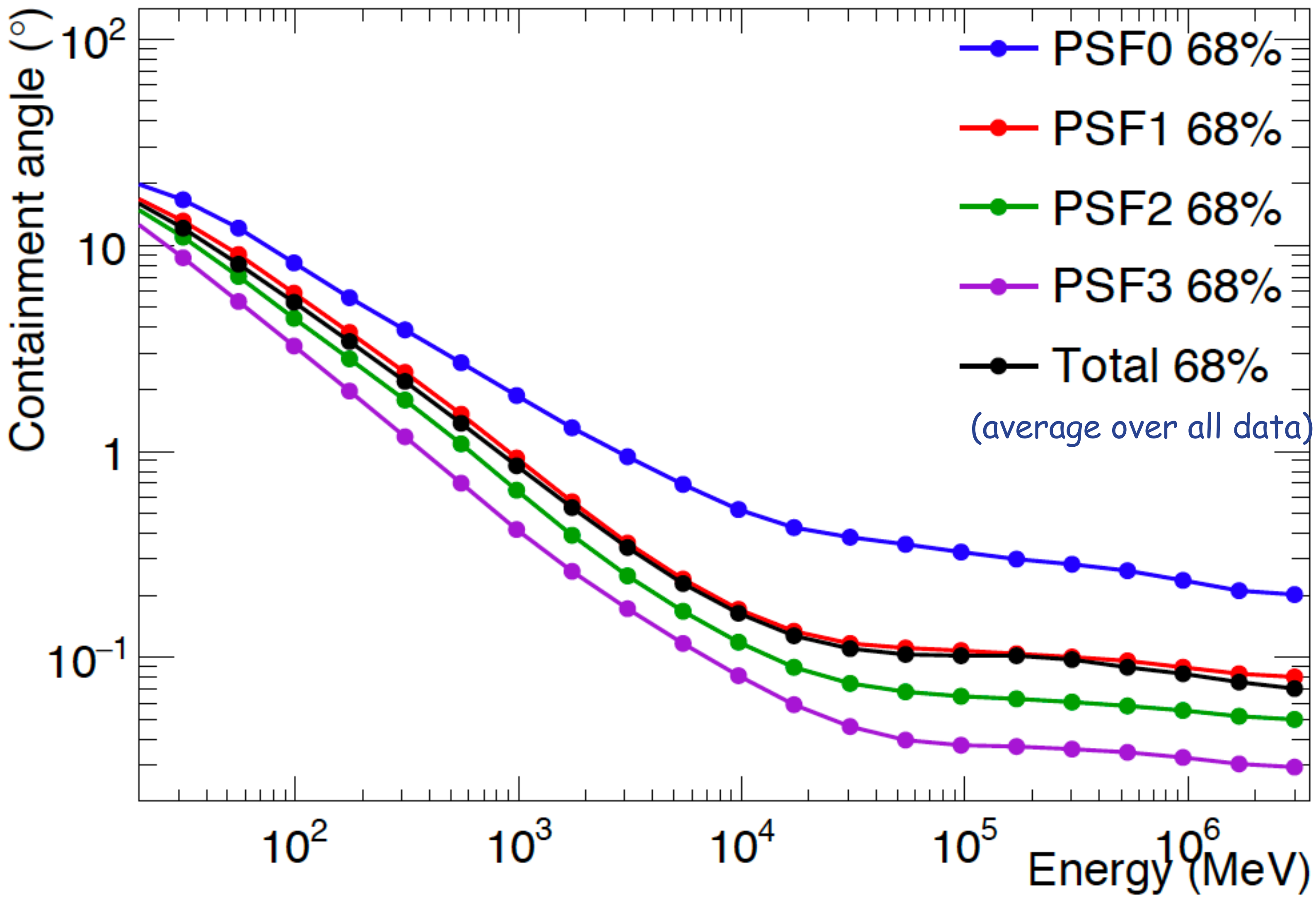

- ***Fermi*-LAT PSF as a function of energy, averaged over off-axis angle. The black line is the average over all data**

Example Templates – 36 (one energy band)

- These have been processed into predicted counts maps

GALPROP-based, independently scaled

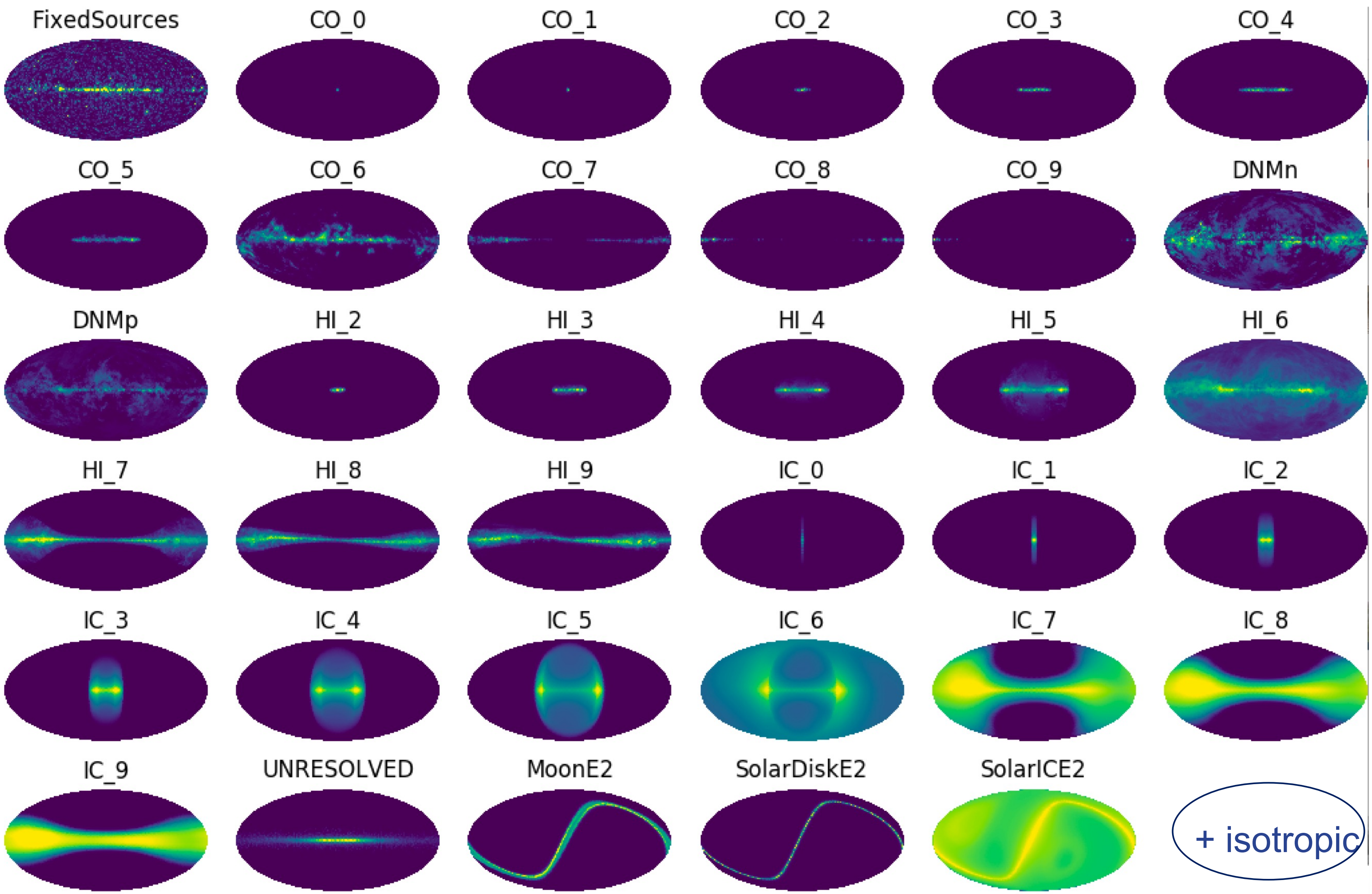

Fermi-LAT detection of normal galaxies

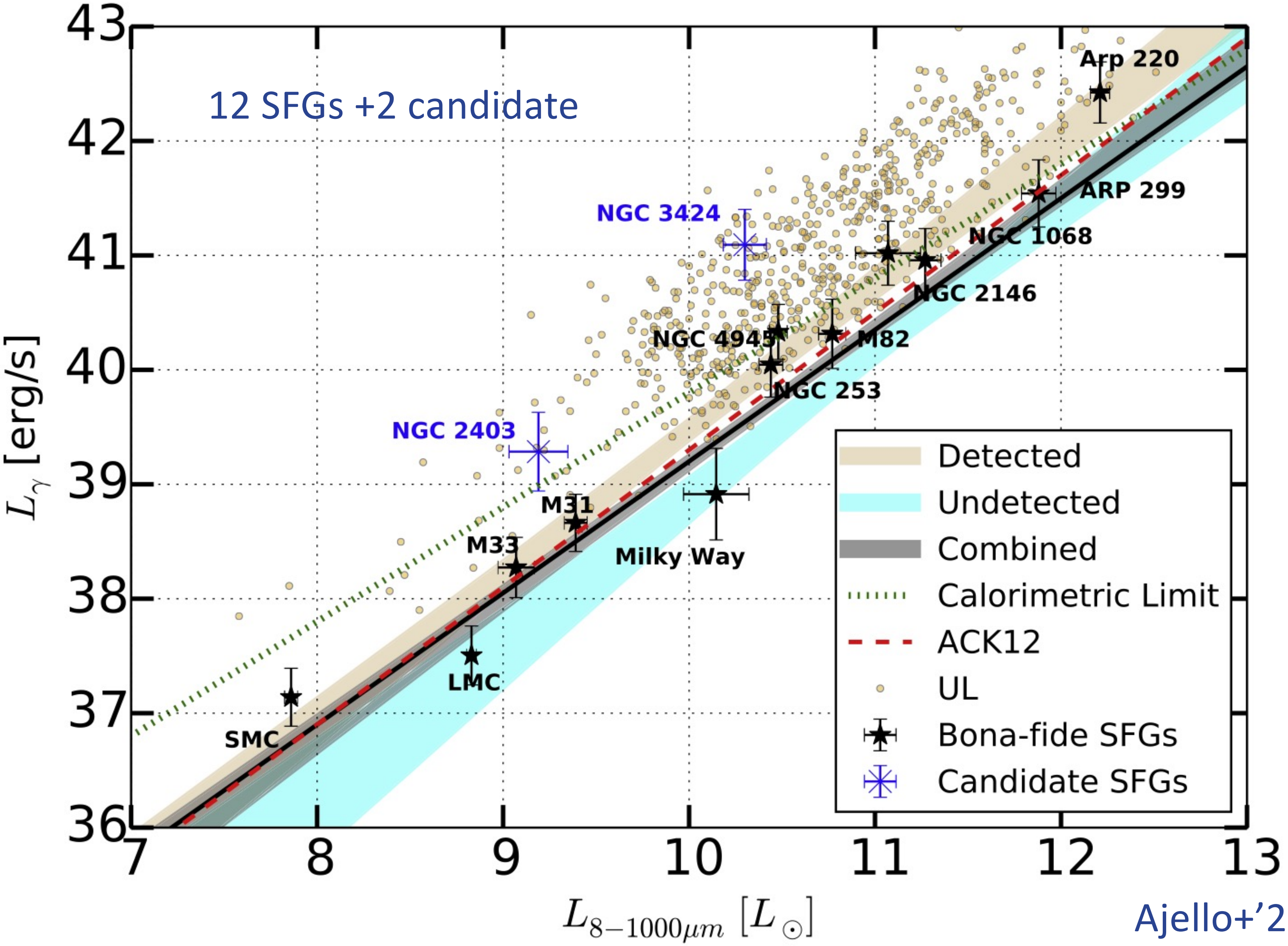

Ajello+'2020

HAWC observations of the extended emission from Geminga & PSR B0656

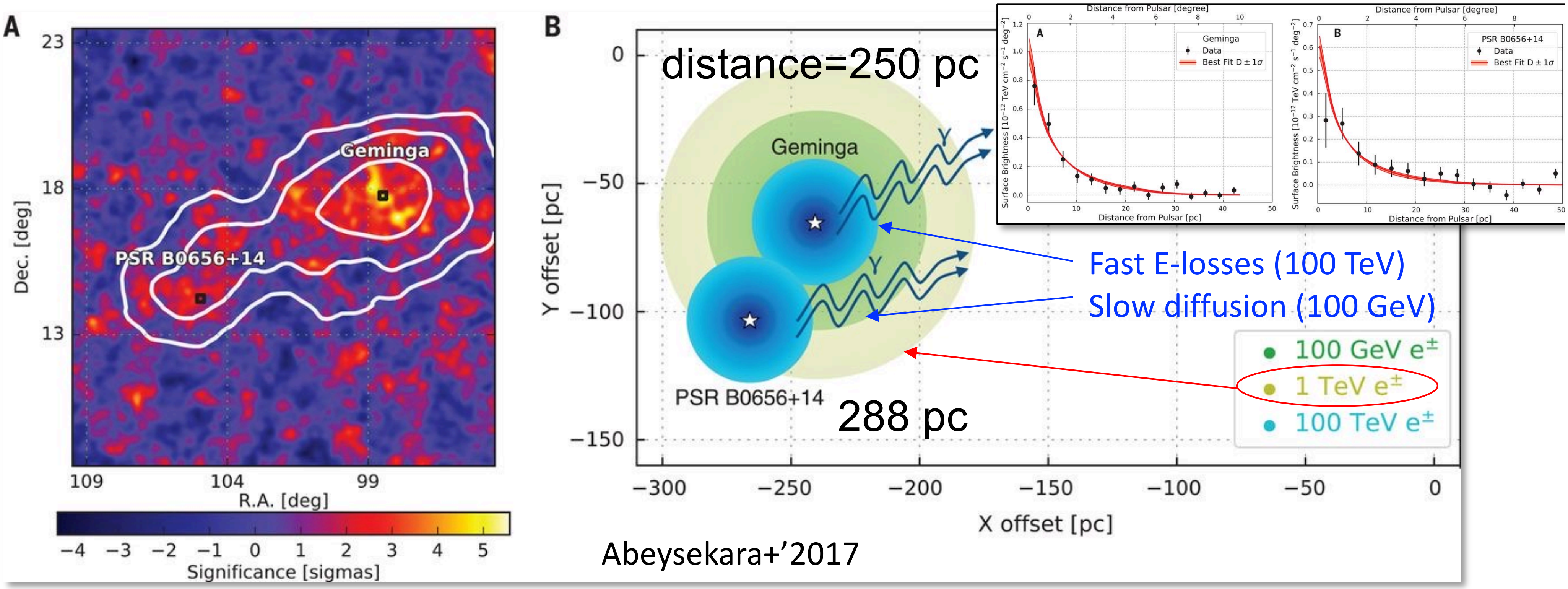

Abeysekara+’2017

- A non-uniform diffusion near the sources of CRs
- The local value ~4.5×10^{27} cm^2 s^{-1} @100 TeV is << the average from the B/C ratio
- Proper motion ~60 pc since SN (Geminga)
- Origin of the slow diffusion zone, the original SNR or pulsar? If the pulsar, how it depends on the age?

e^+ and γ from Geminga (2-zone model)

Predicted: Johannesson+'19
Detected: Di Mauro+'19

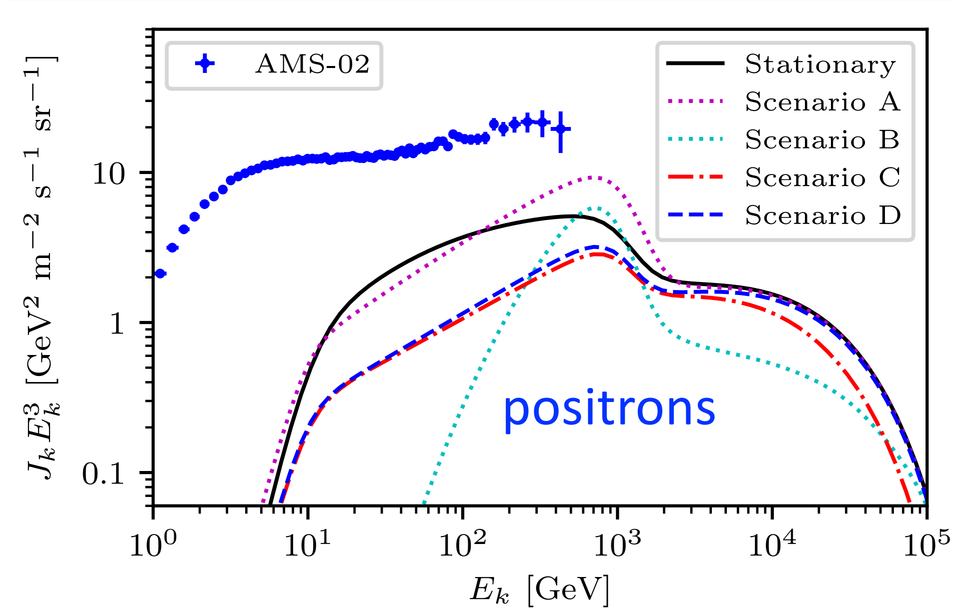

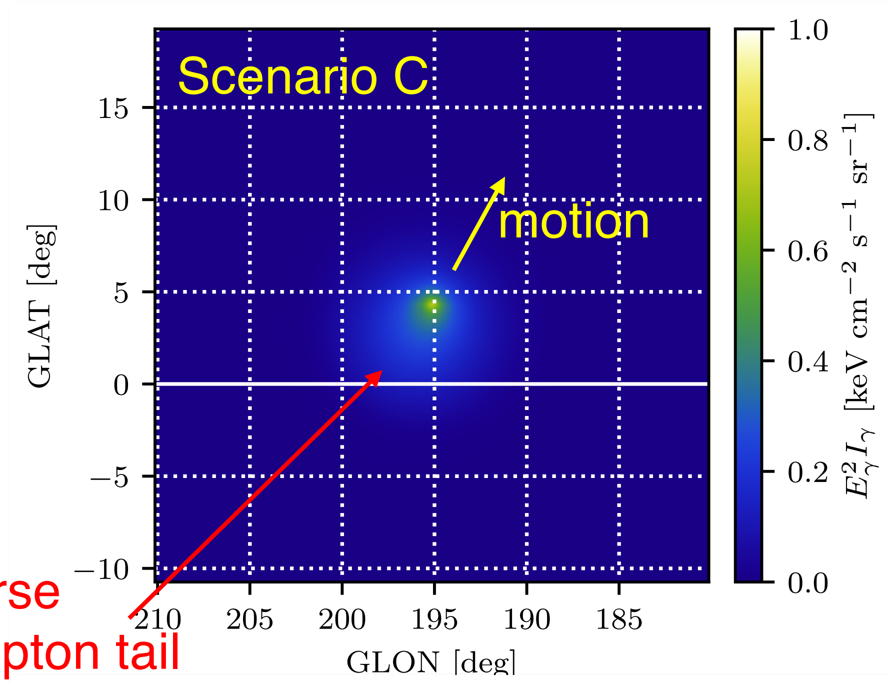

Inverse Compton tail (10 GeV)

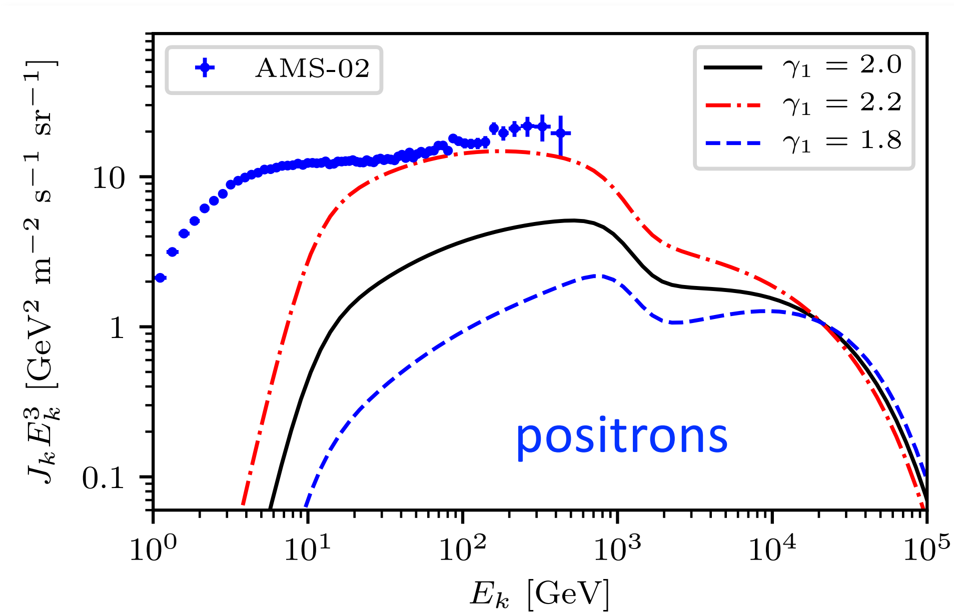

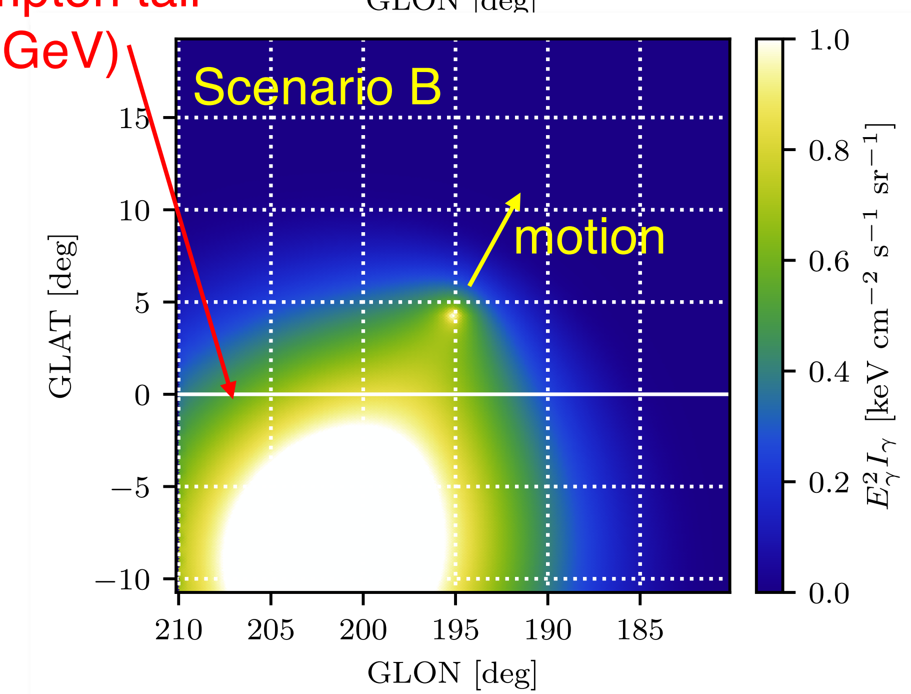

(also Profumo+,Tang&Piran, Fang+, Evoli+'18)

Fermi-LAT detection of the Geminga tail

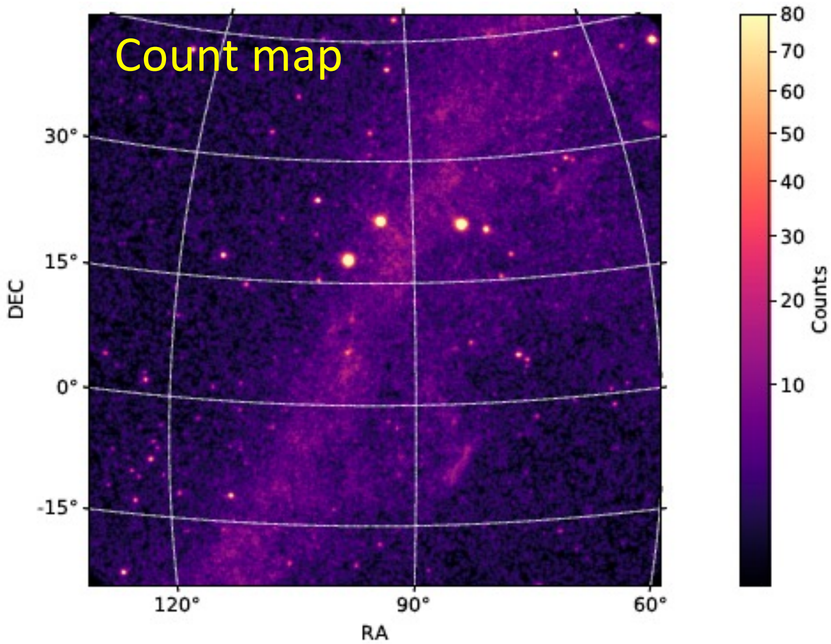

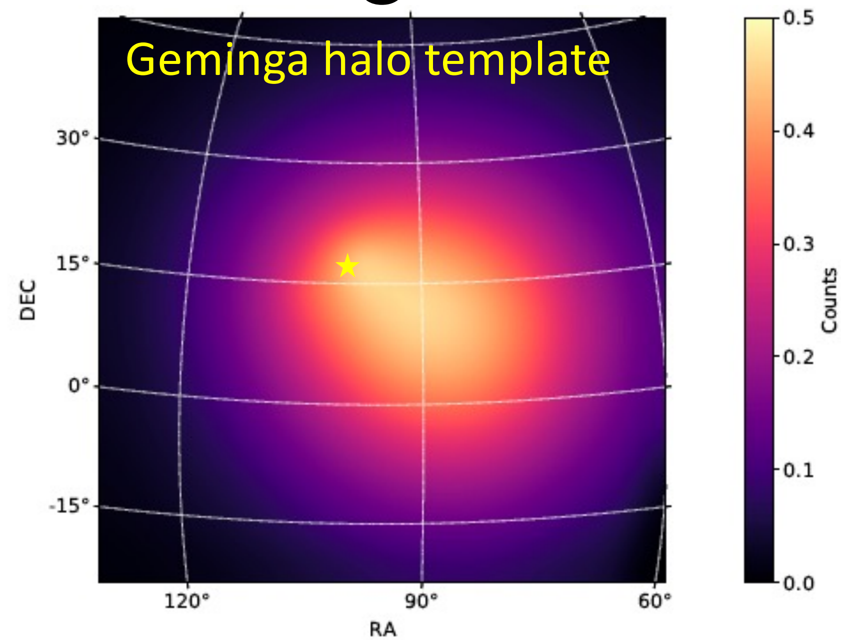

Residual map w. all components subtracted

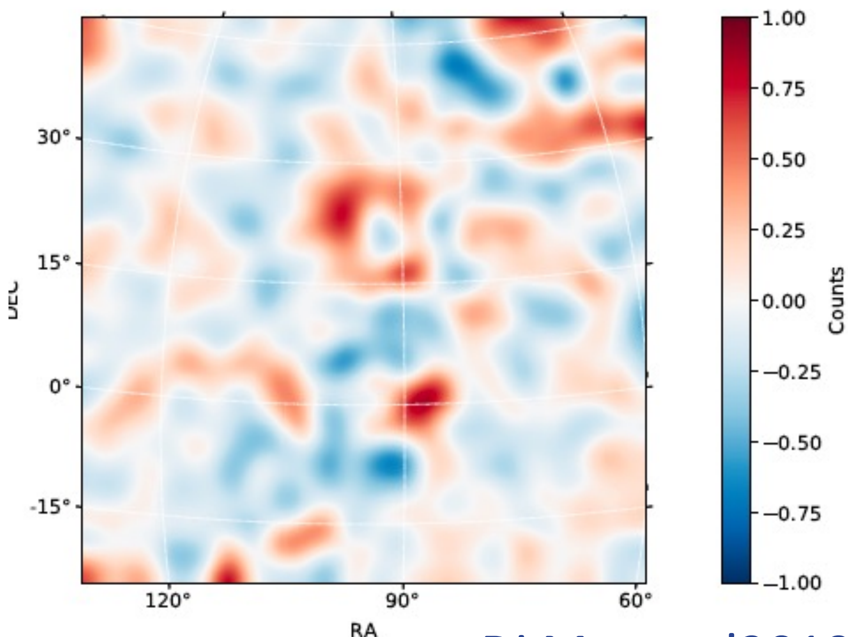

Residual map (halo template not subtracted)

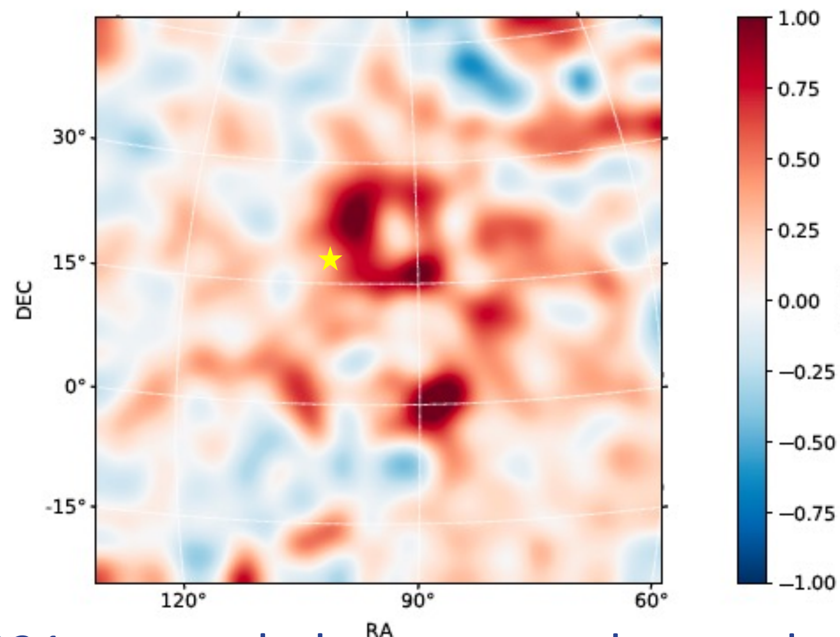

Di Mauro+’2019, 2021 – more halos are now detected

Generalization to the whole MW galaxy

Distribution of the effective diffusion coefficient in 2D and 3D model

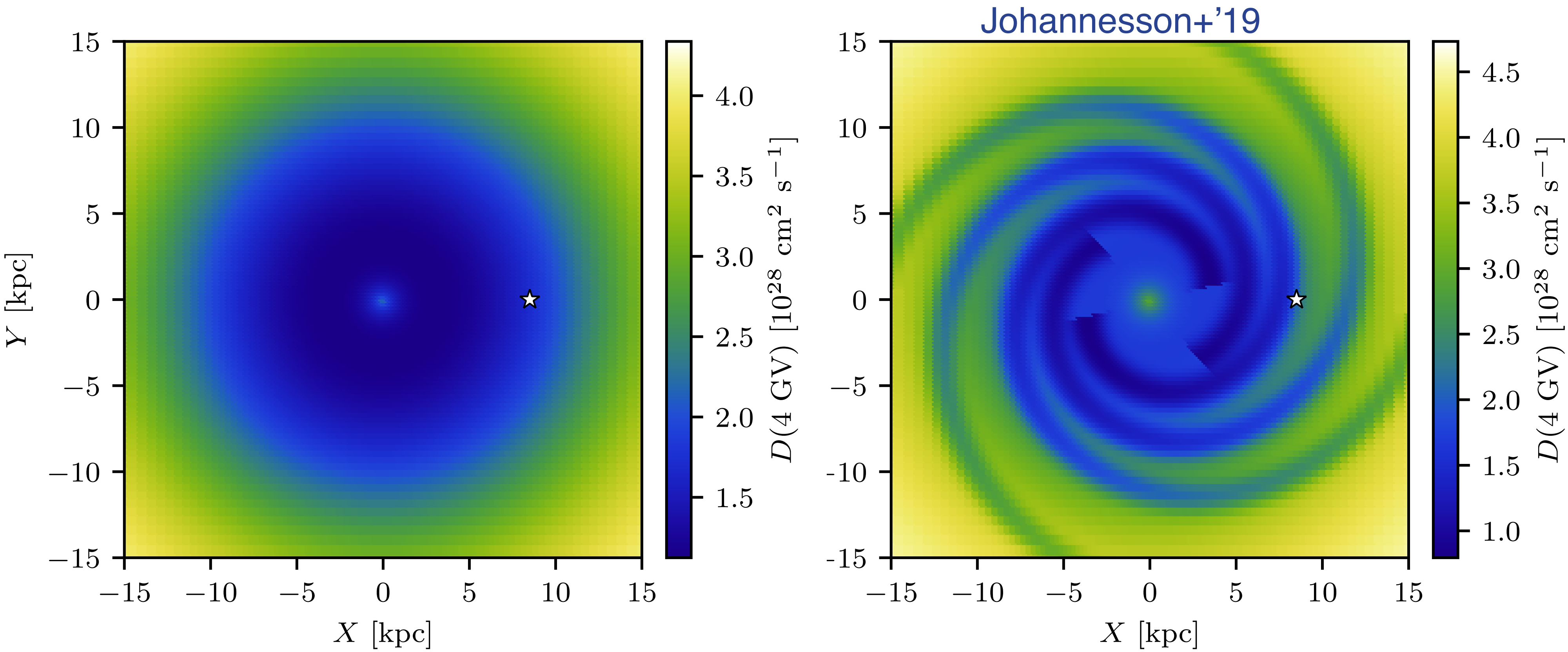

- ✧ Assuming the slow diffusion zone around each CR source, the effective diffusion coefficient in the plane may vary by a factor of 2-3
- ✧ Produces relatively small effect on CR spectra – diffusion coefficient in the halo remains unaltered
- ✧ Effect on the diffuse emission is still being evaluated

Andromeda galaxy M31 – a closest spiral

- Similar to the Milky Way at 778 kpc
- Provides an external view on our own Galaxy
- Large size on the sky 3°×1° – easy to resolve
- The rotation curve remains constant over large distances – large content of DM
- Virial radius ~300 kpc

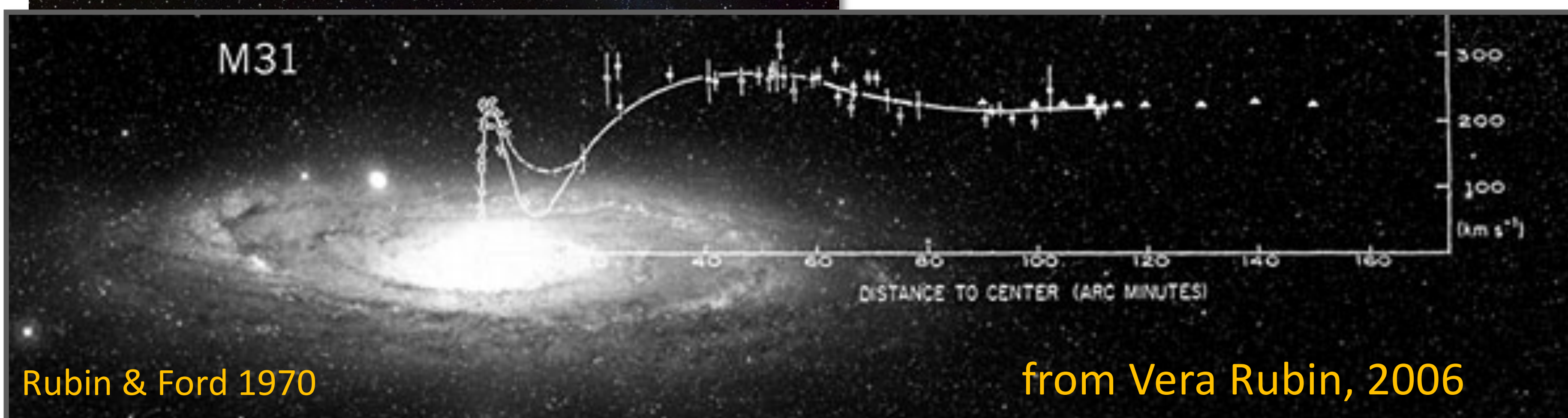

Test region and M31 field

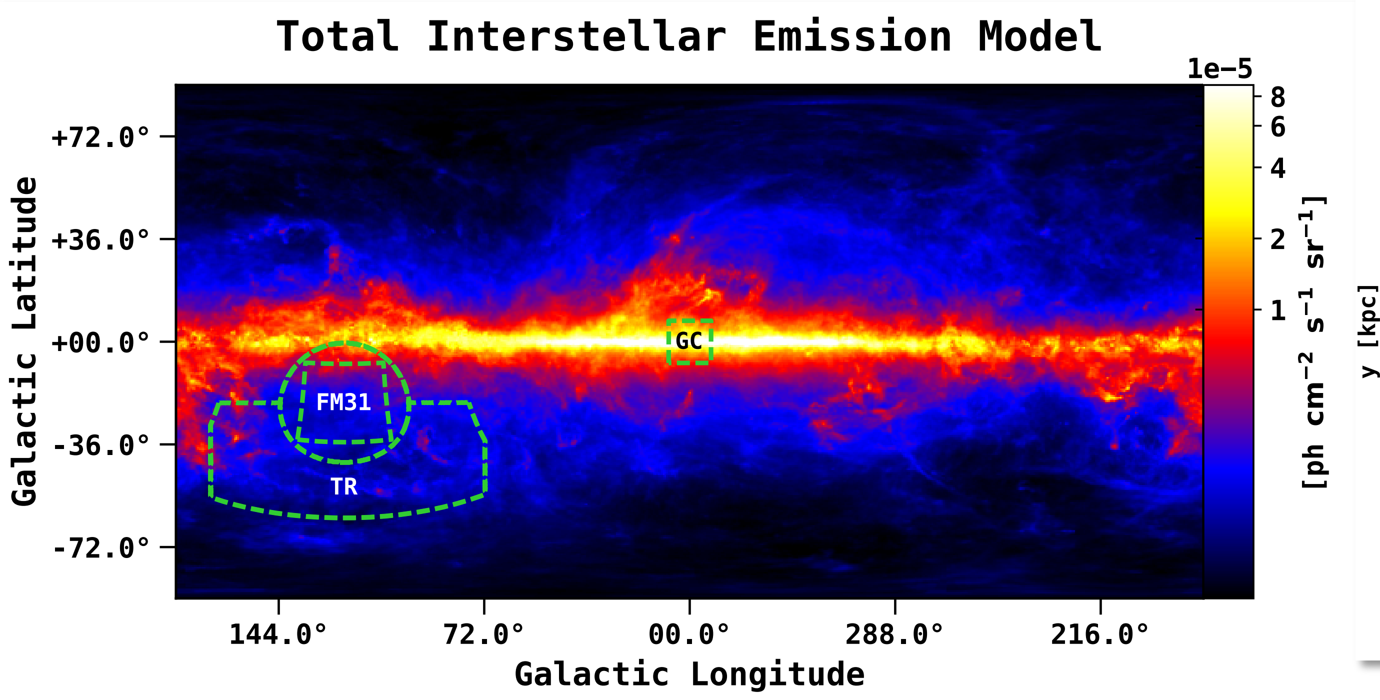

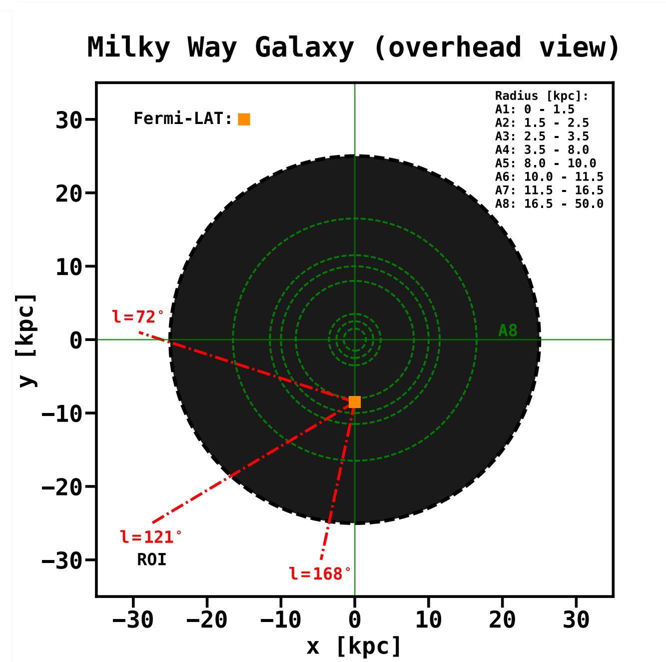

- The interstellar emission model for the MW (1-100 GeV):
  π^0-decay + (anisotropic) inverse Compton + Bremsstrahlung
- "Square" region is M31 field (28°×28°)
- "TR" labels the test region
- Schematic of the eight concentric circles which define the annuli (A1-A8) in the MW foreground model. Only A5-A8 contribute to the Galactic foreground emission for the field used in this analysis.

Karwin+'2019

γ-ray maps for π^0-decay for different rings (GALPROP) – 1

H I gas

H II, H_2 gas

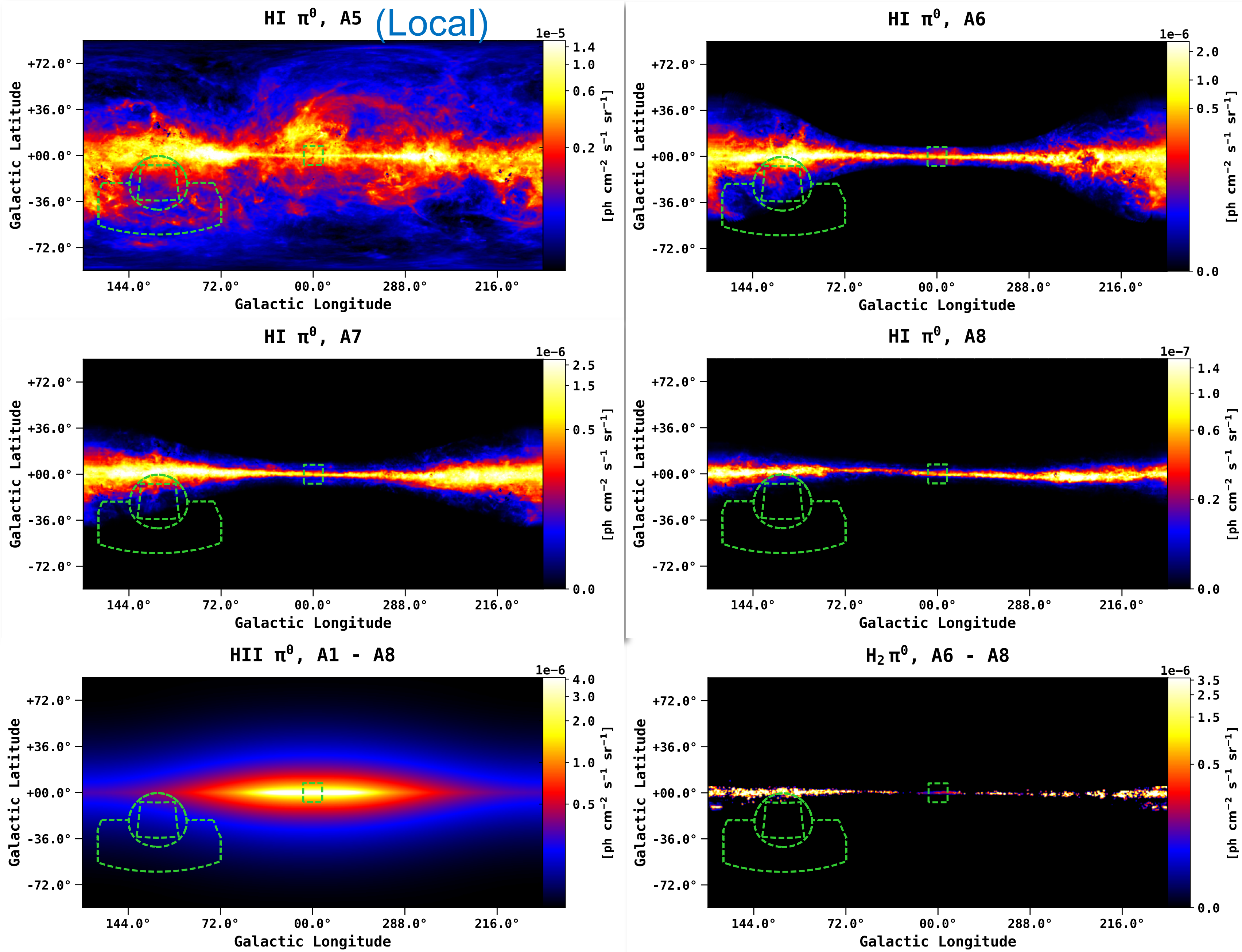

γ-ray maps for anisotropic IC for different rings (GALPROP) –2

(Local)

Anisotropic Inverse Compton Emission, A5

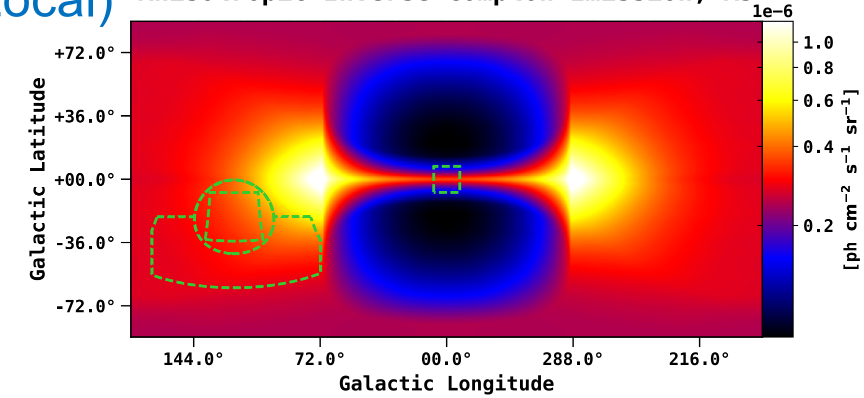

AIC/IC Flux Ratio

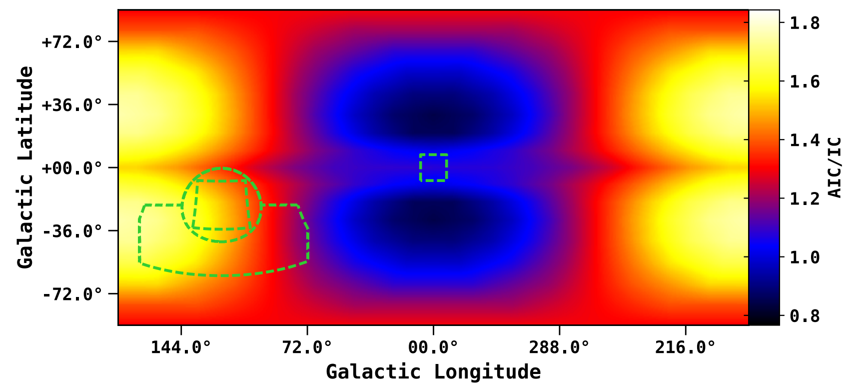

Anisotropic Inverse Compton Emission, A6-A7

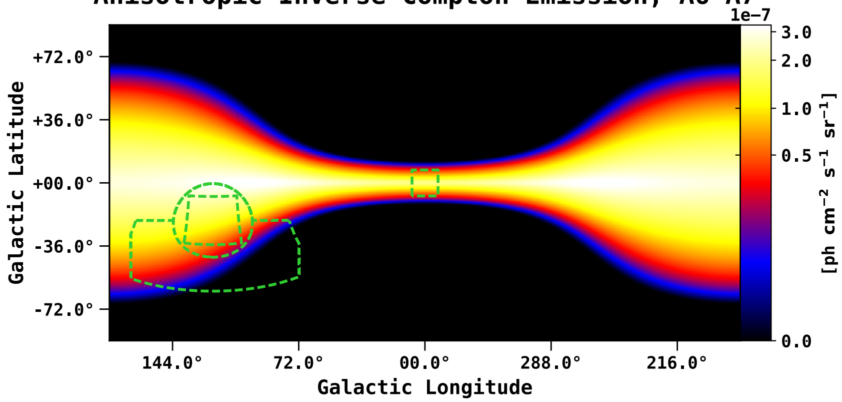

AIC/IC Flux Ratio

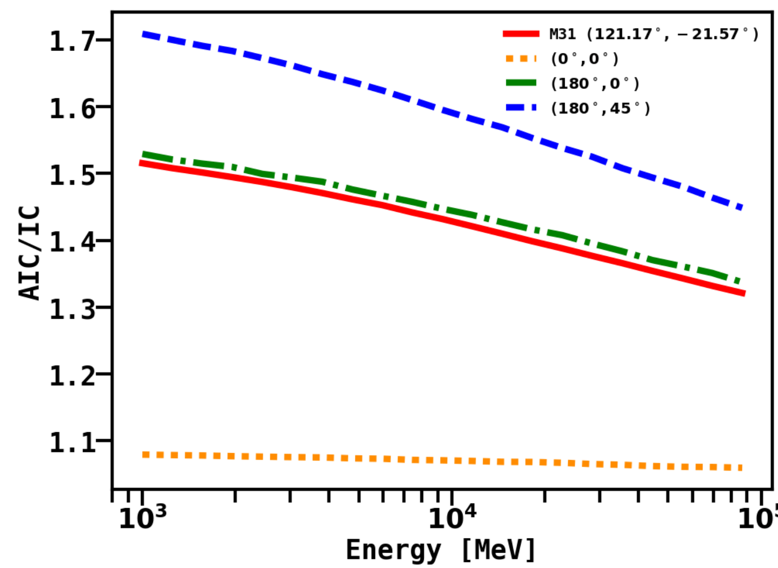

Anisotropic Inverse Compton Emission, A8

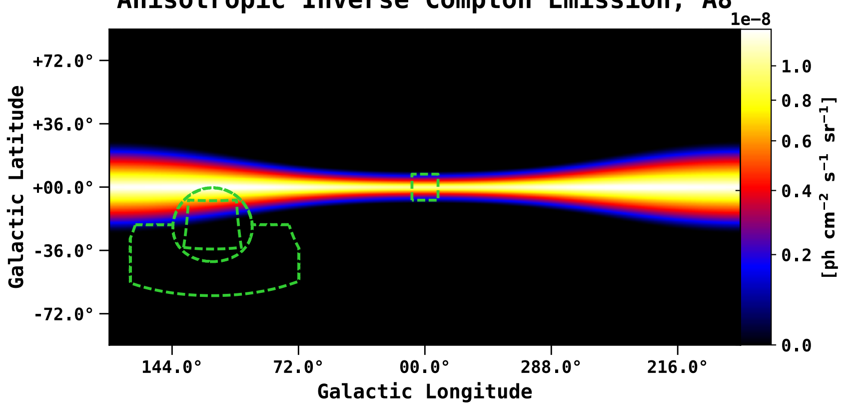

✧ Anisotropic/isotropic ratio illustrates the importance of the effect that reaches a factor of 1.7 for certain directions and is non-uniform on the sky

FM31: Spatial residuals

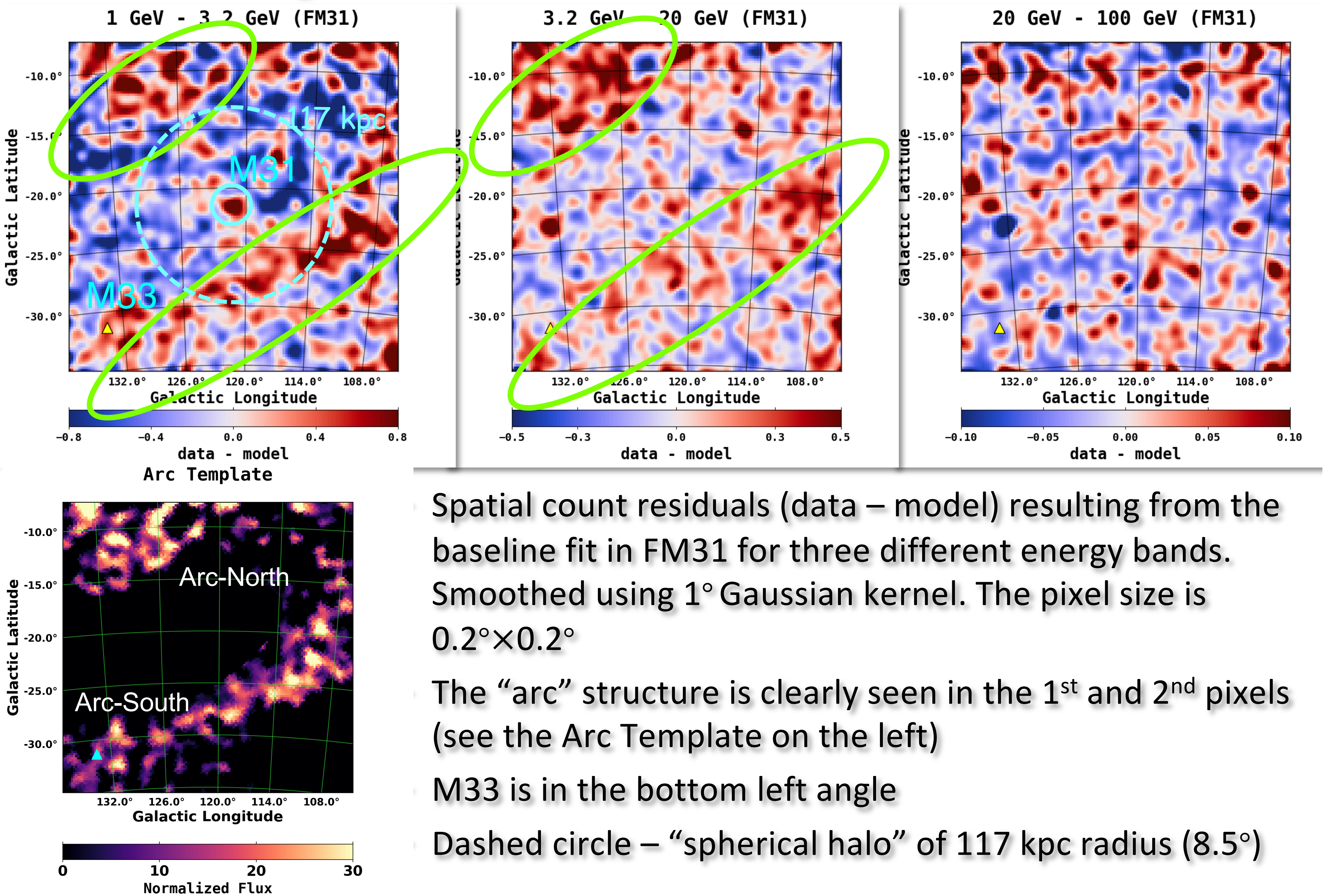

- Spatial count residuals (data – model) resulting from the baseline fit in FM31 for three different energy bands. Smoothed using 1° Gaussian kernel. The pixel size is 0.2°×0.2°
- The "arc" structure is clearly seen in the 1st and 2nd pixels (see the Arc Template on the left)
- M33 is in the bottom left angle
- Dashed circle – "spherical halo" of 117 kpc radius (8.5°)

What is the arc? Loops, loops, loops…

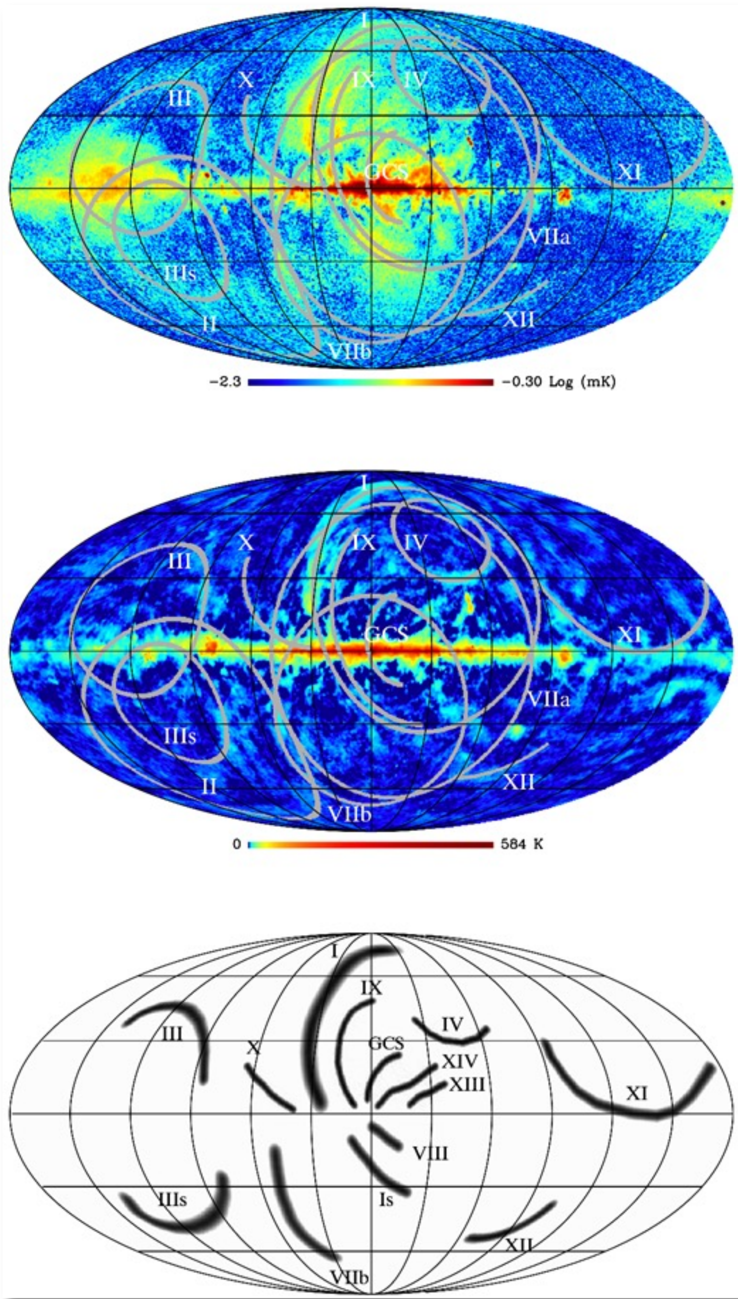

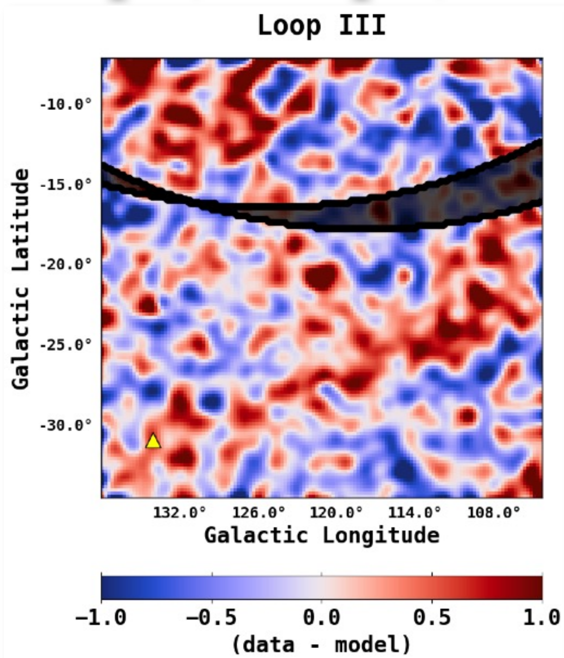

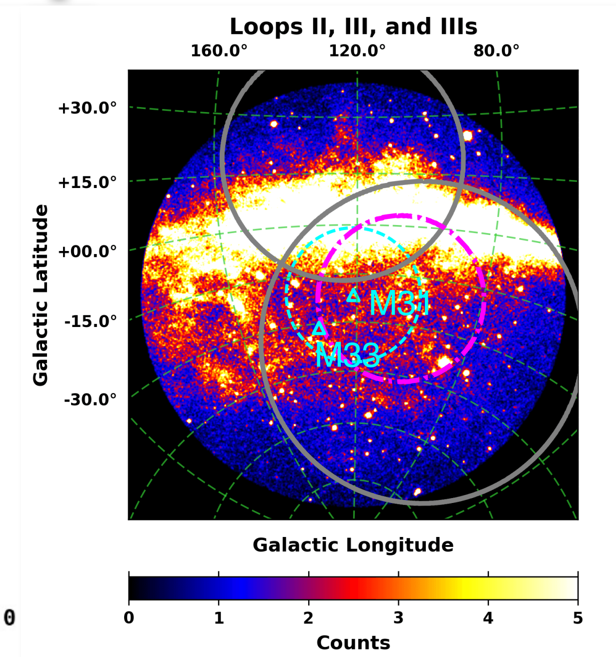

- ✧ There are ~17 so-called Loops found on the sky in radio and polarized radio emission; some of them are seen in γ-rays (e.g., famous Loop I)
- ✧ Loops or Spurs are large structures covering a significant part of the sky – their origin is unknown
- ✧ A part of the shell of Loop III seems to be associated with the north part of the arc, and Loops II and IIIs are covering the entire ROI
- ✧ The Arc could be a part of the old Loop III or other Loops; hard spectrum – particle acceleration

Adding M31 components: all-component fit

Karwin+'2019

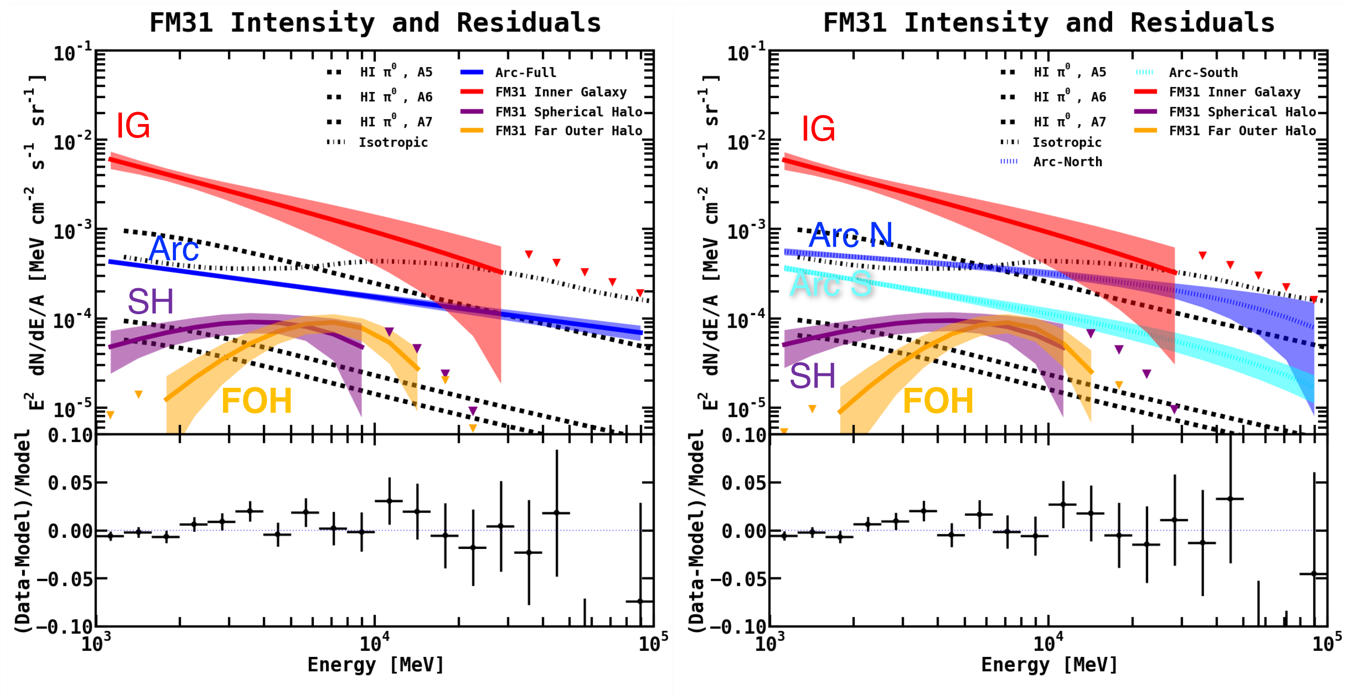

- Inner Galaxy (IG):
  - $0^{\circ} < r \leq 0.4^{\circ}$ (5.5 kpc)
- Spherical Halo (SH):
  - $0.4^{\circ} < r \leq 8.5^{\circ}$ (117 kpc)
- Far Outer Halo (FOH):
  - $r > 8.5^{\circ}$ (~200 kpc)

M31-related geometry: Uniform intensity templates centered at M31

- Three spherically symmetric templates centered at M31 are added to the model: inner galaxy (IG), spherical halo (SH), and far outer halo (FOH).
- Templates are given PLEXP spectral models and fit simultaneously with other components of the IEM, including the arc template. Two fit variations are performed, amounting to two different variations in the arc template: full arc with PL, arc north and south with PLEXP
- IG, SH, and FOH are detected at the significance levels of 7σ, 7σ, and 5σ, respectively. Results for the two fit variations are similar
- Spectral shapes (SH, FOH) are noticeably different from other components

Excess in different foreground models

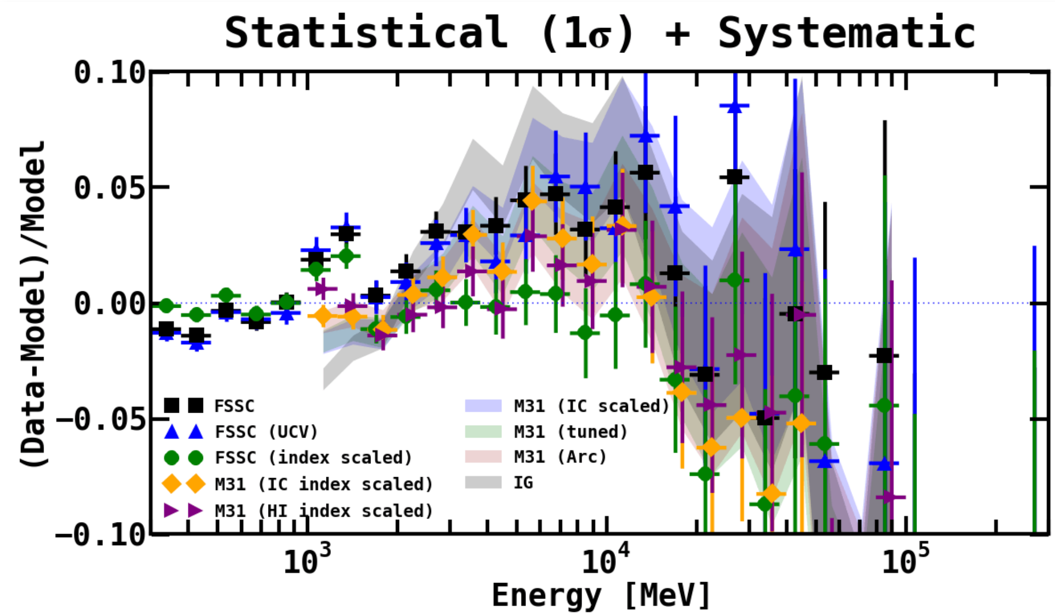

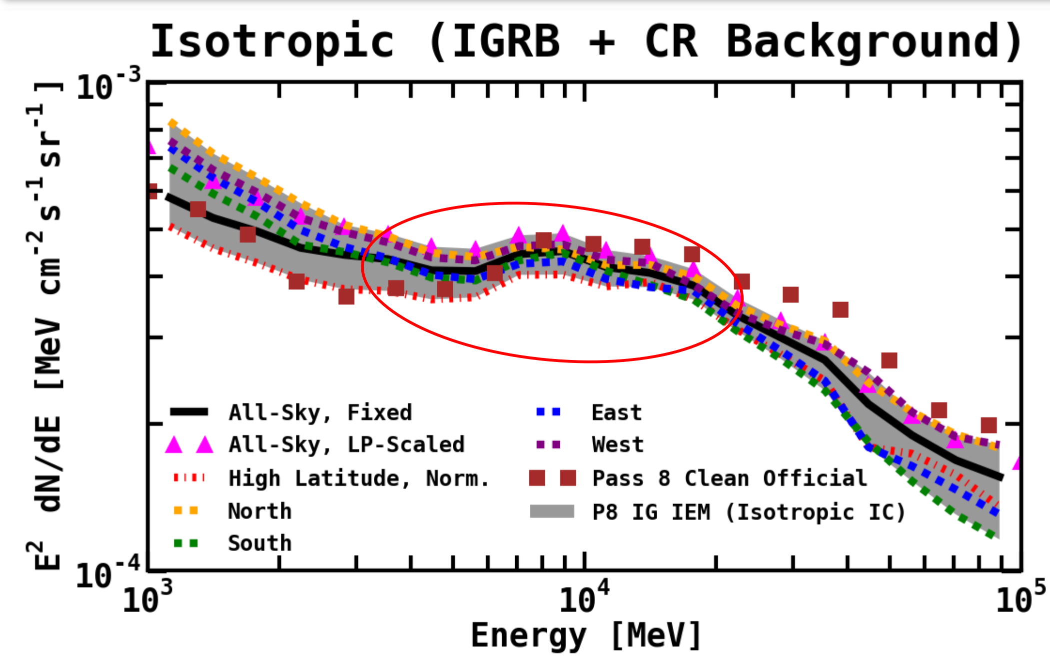

- A systematic excess is observed between 3–20 GeV at the level of 3–5% independently on the background (foreground) model used
- Absent only in case of the foreground model that is built using the LAT data itself, yet with free index (FSSC index scaled)
- Interestingly, isotropic component has a “bump” in the same energy range as the observed excess
- Dark Matter halo around the Milky Way?

Indirect detection of DM

DM limits from γ-ray emission of the M31 halo appears to be consistent with limits derived from the Galactic Center and antiprotons

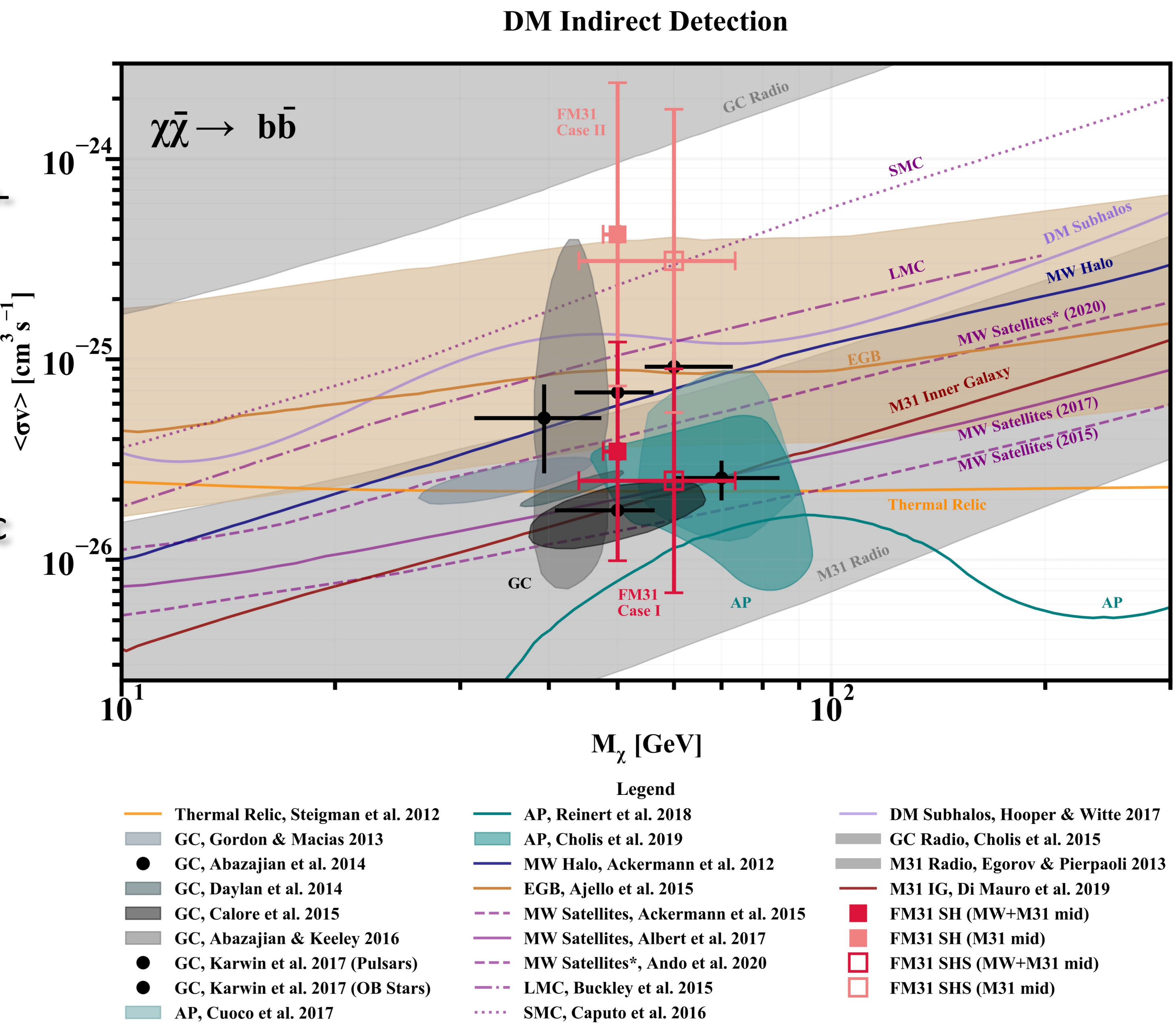

Karwin+'2021


Спасибо за внимание!